CHEMICAL MODIFICATION OF BOVINE MILK EXOSOMES, THE BIOLOGICAL NANOPARTICLES OF THE FUTURE, AS A CONTRAST AGENT AND DRUG DELIVERY VEHICLE

A Dissertation
Submitted to the Graduate Faculty
of the
North Dakota State University
of Agriculture and Applied Science

By

Jessica Elaine Pullan

In Partial Fulfillment of the Requirements
for the Degree of
DOCTOR OF PHILOSOPHY

Major Program:
Pharmaceutical Sciences

April 2021

Fargo, North Dakota

North Dakota State University
Graduate School

Title

CHEMICAL MODIFICATION OF BOVINE MILK EXOSOMES, THE BIOLOGICAL NANOPARTICLES OF THE FUTURE, AS A CONTRAST AGENT AND DRUG DELIVERY VEHICLE

By

Jessica Elaine Pullan

The Supervisory Committee certifies that this ***disquisition*** complies with North Dakota State University's regulations and meets the accepted standards for the degree of

DOCTOR OF PHILOSOPHY

SUPERVISORY COMMITTEE:

Sanku Mallik
Chair

Yagna Jarajapu

Kristine Steffen

Jiha Kim

Approved:

04/14/21
Date

Jagdish Singh
Department Chair

ABSTRACT

Chemically derived nanoparticles are widely used across many applications. While they showed great promise when first discovered, the main hurdles, such as clearance and targeting, have yet to be overcome. A recently discovered class of biological nanoparticles have the potential to circumvent these disadvantages. Exosomes are biological nanoparticles (30 – 150 nm) excreted from most mammalian cells. While exosomes are typically involved in cellular signaling and traditionally removed from the body to be examined for biomarkers, this work combines chemical modifications and a biological particle for diagnostics and treatment of solid tumor cancer. Exosome involvement in cancer treatment has grown over the past ten years with the encapsulation of RNA, proteins and traditional chemotherapeutics. However, this work takes these ideas and drives them into the future by using bovine milk derived exosomes as (1) an ultrasound contrasting agent and (2) a targeted and triggered chemotherapeutic drug delivery vehicle. As an ultrasound contrast agent, raw and pasteurized bovine milk exosomes were tested and found to be capable of echogenicity without altering the ability to identify key features of the exosome, including the presence of CD63 and miRNA. In the second part of this work a chemically synthesized, hypoxia responsive lipid and a tumor penetrating and targeting peptide, iRGD were integrated into the lipid bilayer of the exosome for chemotherapeutic drug delivery. These modified exosomes were characterized using a variety of techniques, including a novel adhesion assay, atomic force microscopy, and high-resolution transmission electron microscopy. The functional capacity of the modified exosomes to deliver doxorubicin to Triple Negative Breast Cancer (TNBC) cells was also evaluated using a combination of cellular internalization and cytotoxicity assays in both monolayer and 3D spheroid cultures. Overall exosomes have the

ability to be chemically modified in a variety of ways, opening a door to a new approach to nanoparticle drug delivery and targeted imaging.

ACKNOWLEDGMENTS

I will be forever grateful for my village, which extends far and wide. This degree has taken its toll on the people of my life more than I'll ever know. My first acknowledgement is to my husband who I dragged half-way across the country in order to pursue this degree. He has been my number one cheerleader throughout everything. I could not have earned this degree without him, the title is just as much his as it is mine. Next, my mom who I spent countless hours talking to, problem solving and venting about this roller coaster ride. She made this easier and provided more advice and insight into this project than anyone else. To my dad and my sister who continued to support me and encourage me in every possible way. To my sons who were born during this journey, part of me did this for you. You boys will never remember the days that were spent in the lab or in Fargo but despite the struggles that becoming a mother during graduate school caused it brought more focus and determination than I thought was possible.

Academically I'd like to thank my advisor, Dr. Sanku Mallik who brought me to his lab and let me struggle but never fail. He was always pushing me to do my best but giving me the space and support that I always needed. To Kaitlin and Jacob who helped me from start to finish, you will always be a part of my "Work-a-holics Anonymous" tribe, thank you for everything you've done for me. You two have truly become my family.

DEDICATION

To my family whole never stopped believing in me, even when I didn't believe in myself.

PREFACE

"Success is stumbling from failure to failure with no loss of enthusiasm."

-Winston Churchill

TABLE OF CONTENTS

LIST OF TABLES

LIST OF FIGURES

LIST OF ABBREVIATIONS

% mol ..... Molecular fraction

$\%O_2$ ..... Percent oxygenation

°C ..... Degrees Celsius

2D ..... Two-dimensional

3D ..... Three-dimensional

A-172 ..... Glioblastoma cells

AA-PEG ..... Aminoethylanisamide-polyethylene glycol

ABS ..... Acrylonitrile butadiene styrene

ACS ..... American Chemical Society

AdV_{HER2} ..... Adenoviral vector

AFM ..... Atomic Force Microscopy

ANOVA ..... Analysis of Variance

BBB ..... Blood Brain Barrier

BSA ..... Bovine Serum Albumin

CD63 ..... Human tetraspanin protein CD63

CD9 ..... Human tetraspanin protein CD9

cDNA ..... Complementary DNA

CO_2 ..... Carbon dioxide

CTCF ..... Corrected total cell fluorescence

DAPI ..... 4′,6-diamidino-2-phenylindole

dB ..... Decibel

DExo ..... Doxorubicin encapsulated exosome

DLS ..... Dynamic light scattering

DMEM ..... Dulbecco's Modified Minimum Media

DNA	Deoxyribonucleic acid
DR	Dynamic Range
DSPE	1,2-Distearoyl-sn-glycero-3-phosphorylethanolamine
e.g.	"For example"
ECL	Electrochemiluminescence
ECM	Extra cellular matrix
EDC HCl	N-(3-Dimethylaminopropyl)-N′-ethylcarbodiimide hydrochloride
EDTA	Ethylenediaminetetraacetic acid
EFGR	Epidermal growth factor receptor
ELISA	Enzyme Linked Immunoabsorbant Assay
EMEM	Essential Modified Minimum Media
EPR	Enhanced permeability and retention
Eq	Equation
Et al	Et alia, "and others"
Etc	Et cetera, "and so on"
EV	Extracellular Vesicle
Exo	Exosome
FBS	Fetal bovine serum
FDA	Federal Drug Administration
FFT	Fast Fourier Transform
Fig	Figure
FITC	Fluorescein isothiocyanate
g	Gram
GBM	Glioblastoma multiforme

GNPs	Gold nanoparticle
GSH	Glutathione
H	High
HBTU	(2-(1H-benzotriazol-1-yl)-1,1,3,3-tetramethyluronium hexafluorophosphate
HCC	Triple negative breast cancer cells from primary tumor site
HEK	Human embryonic kidney cells
HEPES	4-(2-hydroxyethyl)-1-piperazineethanesulfonic acid
HOBt	Hydroxybenzotriazole
Hr	Hours
HR-TEM	High-Resolution Transmission Electron Microscopy
HRX	Hypoxia responsive exosome
Hz	Hertz
i.e.	Id est, “in other words”
iDHRX	iRGD-doxorubicin encapsulated-hypoxia responsive exosomes
iExo	bone marrow derived mesenchymal stem cell exosomes encapsulating siRNA
iHRX	iRGD-hypoxia responsive exosomes
imDCs	Mouse immature dendritic cells
In vitro	Performed in a test tube
In vivo	Performed in a biological system
iRGD	Cyclized- Arginine-Glycine-Aspartic Acid Peptide
kHz	Kilohertz
kPa	Kilopascal
L	Liter

Lamp2b	Lysosome-associated membrane glycoprotein 2b
LNCaP	Androgen-sensitive human protstate adenocarcinoma
M	Molar
MCF	Human breast cancer cells
MDA-MB	Human triple negative breast cancer cells from pleural effusion metastasis sites
MHz	Megahertz
Min	Minute
miRNA/miR	Micro RNA
mL	Milliliter
mM	Milimolar
Mm	Millimeter
MW	Molecular weight
MWCO	Molecular weight cut off
NHS	N-Hydroxysuccinimide
nm	Nanometer
NMR	Nuclear magnetic resonance spectroscopy
NP	Nanoparticle
NRP1	Neuropilin-1
NSG	NOD skid gamma
p	p-Value, observed results of a statistical hypothesis test
PBS	Phosphate buffered saline
PC3	Prostate adenocarcinoma
PDI	Polydispersity index

PEG ..... Polyethylene glycol

PFSK-1 ..... Neuroectodermal tumor

pH ..... A measure of the acidity or alkalinity of a solution

PSF ..... Penicillin Streptomycin Fugisome

RC ..... Regenerated cellulose

RIPA ..... Radio immunoprecipitation assay buffer

RNA ..... Ribonucleic acid

rpm ..... Revolutions per minute

RPMI ..... Roswell Park Memorial Institute Media

s ..... Seconds

siRNA ..... Silencing RNA

U87-MG ..... Glioblastoma-astrocytoma

UCA ..... Ultrasound Contrast Agents

ug ..... Microgram

uL ..... Microliter

uM ..... Micromolar

V ..... Volts

Vs ..... Versus

w/v ..... Weight per volume

xg ..... G Forces

αvβ3 ..... Alpha five Beta three integrin

LIST OF SYMBOLS

/ .....Per, division

#.....Number

% .....Percent

° .....Degree

< .....Less than

= .....Equal

> .....Greater than

$.....Dollar

C.....Celsius

V.....Five

α .....Alpha

β .....Beta

LIST OF APPENDIX FIGURES

CHAPTER 1: EXOSOMES AS DRUG CARRIERS FOR CANCER THERAPY[1]

Abstract

Exosomes, biological extracellular vesicles, have recently begun to find use in targeted drug delivery in solid tumor research. Ranging from 30 -120 nm in size, exosomes are excreted from cells and isolated from bodily fluids. Exosomes provide a unique material platform due to their characteristics, including physical properties such as stability, biocompatibility, permeability, low toxicity, and low immunogenicity – all critical to the success of any nanoparticle drug delivery system. In addition to traditional chemotherapeutics, natural products and RNA have been encapsulated for the treatment of breast, pancreatic, lung, prostate cancers, and glioblastoma. This review discusses current research on exosomes for drug delivery to solid tumors.

Introduction

As a result of late diagnosis and limited treatment options, many malignant solid tumors have a poor prognosis and require more innovative approaches to cure such deadly disease. Targeted nanocarriers for drug delivery is a very promising avenue for treatment of solid cancerous tumors but have thus far been proven insufficient. With high clearance rates, toxicity to normal tissues, limited loading capacity, and shallow penetration depths, nanoparticles have proven difficult to use.[1,2] The common drug carriers, such as micelles, polymersomes, and liposomes have failed to address these issues adequately. [1,2]

---

[1] Reprinted with permission from Pullan, J. E.; Confeld, M. I.; Osborn, J. K.; Kim, J.; Sarkar, K.; Mallik, S., Exosomes as Drug Carriers for Cancer Therapy. Molecular Pharmaceutics 2019, 16 (5), 1789-1798. Copyright 2019 American Chemical Society. This work was co-authored by Jessica E Pullan, Matthew I Confeld, Jenna K Osborn, Jiha Kim, Kausik Sarkar, Sanku Mallik. Jessica Pullan outlined, contributed and edited the manuscript. Matthew Confeld and Jenna Osborn contributed to the manuscript. Jiha Kim, Kausik Sarkar, and Sanku Mallik edited the manuscript.

Although survival rates have increased in recent years, current treatments for many cancers remain ineffective and require the development of improved delivery methods. Amongst the cancers of breast, pancreas, lungs, prostate, and brain, the five-year survival rate is less than 22%, with glioblastoma being drastically lower (1%).[3,4] Solid tumor cancers are difficult to treat in all stages due to their unique characteristics in cell cycle and vasculature which limit the delivery of drugs.[5,6] Current treatment methods include chemotherapy, radiation, and surgical resection when possible Some adjuvant therapy options in experimental stages and clinical trials currently include natural compounds, such as curcumin, and anthocyanidins.[7–13] Common chemotherapeutic drugs such as paclitaxel and doxorubicin suffer from low aqueous solubility and off-site toxic side effects and as a result new methods for targeted drug delivery of chemotherapeutic drugs are desired.[14,15]

Many clinical trials and research in recent years have utilized nanoparticles, specifically polymersomes, liposomes, and micelles as drug carriers. Exosomes are cell-derived nanoparticles with more advantages over these nanocarriers.[1] Exosomes are extracellular vesicles secreted by cells into bodily fluids, ranging in size from 30 to 120 nm, and carry a variety of biomacromolecules such as, RNA, DNA, proteins, etc.[16,17] The Minimal Information for Studies of Extracellular Vesicles 2018 guidelines clearly state that many of the extracellular vesicles isolated need to contain at least three positive protein markers of EVs, including at least one transmembrane/lipid-bound protein or cytosolic protein as well as at least one negative protein marker, to ensure isolated vesicles are indeed exosomes.[17] Due to the need to characterize the extracellular vesicles that have been isolated, those same surface proteins and lipids can specify exosome origin and destination (**Figure 1.1**). These biomarkers and are indicative of the cell type the secreting the exosomes. The ability to differentiate surface proteins on the exosomes renders

them as tools for early diagnosis of diseases.[18] Surface proteins may also be used in targeting and decreasing clearance rates, both features that polymersomes and liposomes frequently lack.[19]

Mediating cell-cell signaling, transportation of bioactive molecules, and assisting in immune response are some of the exosomes' known functions.[16] Inherent stability, biocompatibility, biological barrier permeability, low toxicity, and low immunogenicity are critical for the natural function of these lipid-based vesicles.[16] These characteristics address issues associated with other nanoparticle delivery vehicles, such as toxicity and high rate of clearance.[20] Even unmodified exosomes can decrease proliferative effects in cancer cells and do not elicit harmful immune response in the bloodstream like other nanoparticle formulations. [11,20] However, when combined with other therapeutic strategies, such as traditional chemotherapeutics, exosomes decrease tumor proliferation with greater effectiveness.[11] When the correct biological markers are within the exosome bilayer, an anti-tumor immune response may occur, assisting in the fight against cancer.[21] Exosome drug delivery for diseases such as cancer can overcome the limitations of the current anticancer drug carriers. Synthetic chemotherapeutic drugs, silencing RNA, microRNA, and natural anti-cancer products are encapsulated and delivered through the exosomes of which all of these will be discussed in detail in this review.

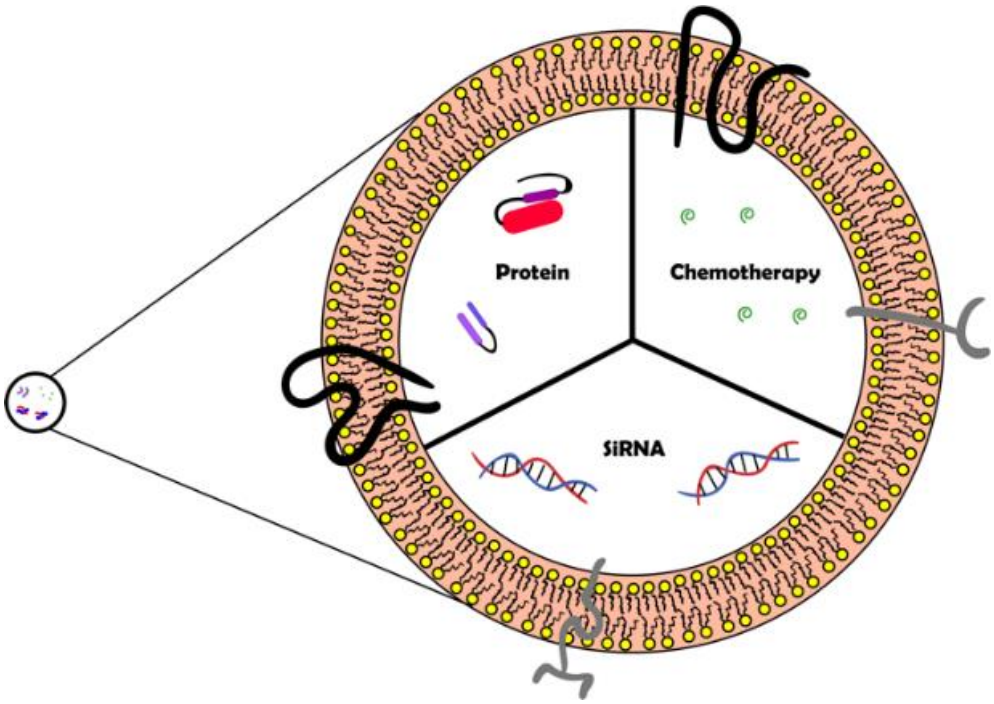

Figure 1.1. Exosomes are formed within the cell with specific proteins and lipids carrying cargo such as RNA and proteins. [22]

Exosomes for Drug Delivery to Breast Cancer

Breast cancer is the most prevalent form of malignancy and the leading cause of cancer-related death in women in the western world.[11,12] Despite the decreased mortality rate with advancements in early detection and improvements to systematic adjuvant therapies, recurrence is seen up to 20 years after surgical interventions with increased metastasis and drug resistance.[23–25] Currently, the treatment options for patients suffering from breast cancer are surgical resection, chemotherapy, radiotherapy, and hormone therapy.[24] All current treatments have challenges, including drug resistance and toxicity to healthy tissues.[24] Targeted, non-toxic, and non-immunogenic delivery technologies are needed to overcome the current challenges.[26] Exosomes have gained momentum as a potential targeted delivery vehicle for breast cancer.

Doxorubicin, a widely used chemotherapeutic drug for breast cancer, reduces the risk of recurrence up to 8% and mortality by 6.5%.[27,28] For patients taking doxorubicin, the side effects

of congestive heart failure and drug resistance require a shift to less-effective therapy options.[27] Tian et al. loaded exosomes with doxorubicin for targeted delivery to triple-negative (MDA-MB-231) and estrogen receptor positive (MCF-7) human breast cancer cells.[26] Exosomes were isolated from mouse immature dendritic cells (imDCs) to minimize immunogenicity and further modified to express tumor targeting motif on the surface (iRGD) to maximize specificity. These cells were engineered to create exosomes that express lysosome-associated membrane glycoprotein 2b (Lamp2b) on the membrane. The Lamp2b was fused to the tumor-penetrating iRGD peptide to target the αv integrin, critical for the proliferation, migration, survival, and invasion of cancer cells.[26] Functionalized exosomes were loaded with doxorubicin using electroporation.[26] In an *in vivo* study, the drug-encapsulated, iRGD functionalized exosomes improved the effects of doxorubicin with no observable toxicity.[26] Hadla and colleagues also demonstrated that doxorubicin-encapsulated exosomes decreased cardiac toxicity and adverse effects on other tissues compared to the free drug.[17,18] Thus, the dose of doxorubicin can be increased, leading to a targeted cytotoxic effect on the breast cancer cells.[29]

Exosomes' natural ability to carry biologically-relevant molecules is the main advantage over other nanoparticles. This characteristic has led to research in treatment options including use of nucleic acid drugs [31–33] or activation of the immune system.[7,23] Current research in miRNA delivery is focused on breast cancer and other solid tumors. The miRNA-134, a tumor suppressant, is down-regulated in breast cancer.[32] O'Brien used exosomes to deliver miR-134 to Hs578Ts(i)$_8$ triple-negative breast cancer cells and observed that migration and invasion were reduced by 1.2 fold and the sensitivity to anti-Hsp90 drugs was enhanced by 2.1 fold.[32] Ohno and colleagues modified exosomes with the GE11 peptide, which specifically binds EGFR, and were loaded with let-7a miRNA, a regulator for the reduction of cell division and alteration of

cell cycles. The epidermal growth factor receptor (EGFR)-expressing breast cancer cell lines (HCC70, HCC1954, and MCF-7) were used to test the exosomes' effectiveness.[33] The targeted and drug-loaded exosomes were delivered to EGFR-expressing xenograft breast cancer tissue in $RAG2^{-/-}$ mice.[33] These studies resulted in suppressed tumor growth (**Figure 1.2**) and provided another promising strategy for the delivery of nucleic acid drugs.[33]

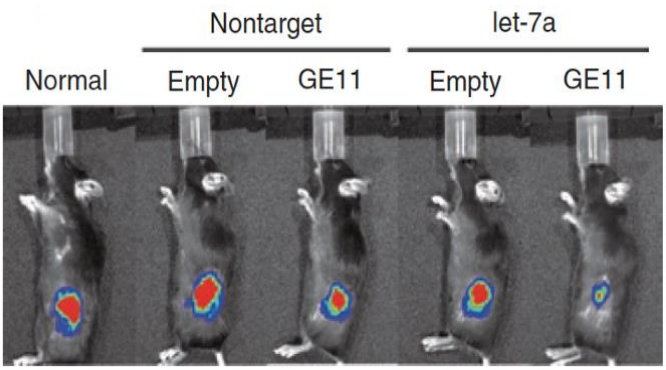

Figure 1.2. Reproduced with permission from Molecular Therapy. Human embryonic kidney cells (HEK293) expressing GE11 were transfected with synthetic let-7a. Exosomes containing let-7a were purified from culture supernatants and intravenously injected (1 μg of purified exosomes, once per week for four weeks) into mice bearing luciferase-expressing breast cancer cells HCC70.[33]

Due to tumor avoidance of the immune system, activating immune response using an exosome-based vaccine is a promising strategy for cancer.[7] Patients treated with trastuzumab, a chemotherapeutic monoclonal antibody, commonly develop resistance, making a delivery method an urgent necessity.[23] Exosomes from dendritic cells were transfected with adenoviral vector (AdV_{HER2}), creating a vaccine.[23] The vaccine was used for treatment in mice with trastuzumab-resistant BT474 and trastuzumab-sensitive MCF-7 tumors.[23] The vaccine stimulated the cytotoxic T lymphocyte response and was observed to kill cancer cells and eradicate tumors, providing a promising new strategy for drug-resistant tumors.[23] Despite in the *in vitro* and *in vivo* stages, the exosome delivery strategies are promising methods for new breast cancer therapy.

The exosomes provide solutions to many challenges that are faced by clinicians in the treatment of breast cancer, such as off-site toxicity and drug resistance. Clinical trials of exosome-based delivery methods are expected to occur due to the positive published results.

Exosomes for Drug Delivery to Pancreatic Cancer

With a single digit five-year survival rate, pancreatic cancer is deadly due to the inability to detect early and treat metastatic tumors. [34,35] Most conventional and targeted therapies fail to provide substantial response largely due to the limited delivery efficacy of cytotoxic agents.[36] One way to combat this problem is to utilize a targeted nanosized drug delivery vehicle. Recently, the FDA approved a nanoparticle delivery strategy for paclitaxel, Abraxane. [37] This monumental leap in the treatment of pancreatic cancer has accelerated the development of nanoparticle-based drug delivery methods. Abraxane, originally approved for metastatic breast and non-small cell lung cancers, utilizes albumin-bound paclitaxel.[34] Abraxane in conjunction with gentamicin leads to increased effectiveness for pancreatic cancer patients, making this plan first line treatment.[34]

One of the biggest challenges of nanoparticle-mediated drug delivery is the high rate of clearance. Due to exosomes' natural characteristics, they have longer retention in the circulation compared polymersomes or liposomes.[38] The increased retention time results from a transmembrane protein (CD47-SIRPα), which prevents exosomes from being phagocytosed and therefore increase the delivery efficacy of its content to the target sites.[38] Increased retention time leads to higher concentrations of exosomal cargo to pancreatic cancer cells and enhanced treatment effectiveness.[38] In addition, exosomes also enhance macropinocytosis of cancer cells, one mechanism of uptake.[38] While Abraxane has made significant advances in the treatment of pancreatic cancer, it is still not enough, and exosomes have the potential to a better option.

Due to exosomes' ability to effectively carry macromolecules, a silencing RNA can be encapsulated, turning off specific genes within the cancer cells. [38] Kamerkar employed exosomes to carry a siRNA against the oncogenic protein Kras ($Kras^{G12D}$). [38,39] Oncogenic Kras is a signaling protein that drives the mutation of pancreatic cancer formation. Silencing oncogenic Kras using this approach showed unprecedented tumor regression and potential to target pancreatic cancer.[38] In orthotopic and genetically engineered mouse model systems, siRNA encapsulated exosomes (iExosomes) showed superior antitumor efficacy (**Figure 1.3**), with decreased pancreas desmoplasia.[38] Anti-tumoral effect of iExosomes was accompanied by enhanced cancer cell apoptosis, suppressed proliferation, reduced phospho-ERK, phospho-AKT and oncogenic Kras levels in vivo experiments.[38] The engineered Kras encapsulated exosomes showed decreased clearance rates compared to plain exosomes.[38] Exosome research in pancreatic cancer is a rapidly advancing field as targeted drug delivery is the most viable solution to the treatment of pancreatic cancer.[40] siRNA is limited in use by the challenges of delivery to target organs during clinical trials.[41] The body's normal physiologic processes, such as renal filtration, breakdown by enzymes, and phagocytic cells have hampered the translation from in-vitro to *in-vivo* use. [41] Multiple research groups are optimizing the use of these small RNA molecules with successful early studies queuing interest from the field. The new ideas bring great promise to pancreatic cancer and the ability to decrease patient suffering while increasing effective treatment options.

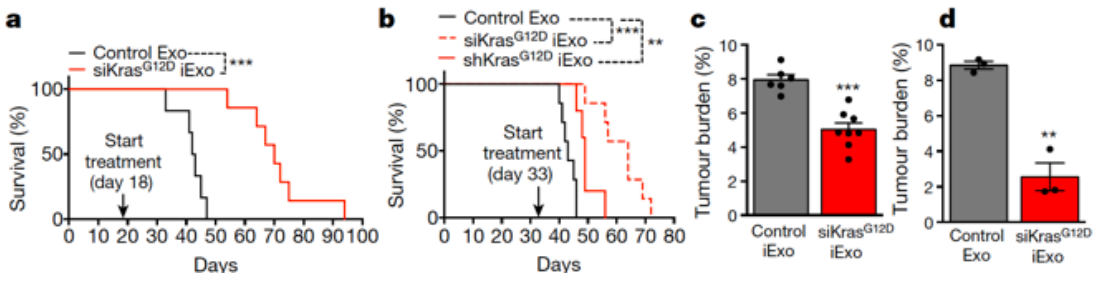

Figure 1.3. Reproduced with permission from Nature. Kras iExsomes suppress pancreatic cancer progression in genetically engineered mouse models for pancreatic cancer. Kaplan–Meier survival curve of tumor-bearing mice with early (a) or late (b) treatment of iExosomes. c. Tumor burden (early treatment) at the experimental endpoint. d. Tumor burden at 44 days of age.[38]

The study by Kamerkar et al. was further investigated by Mendt et. al showing effective upscaling on Kamerkar's idea.[42] One of the biggest obstacles with the use of an exosomes delivery system is the ability to upscale operations and maintain functionality and efficacy of exosomes. Mendt group demonstrated the effectiveness of bone marrow derived mesenchymal stem cell exosomes encapsulating siRNA (iExo) with up to six months in frozen conditions.[42] While ensuring stability in storage conditions and upscale potential, the group tested the iExo on patient-derived xenograft mice with positive results.[42] During in vivo studies Mendt et al. saw significant increases in life expectancies of mice treated with a combination of iExo and gemcitabine in both early and late stage progression.[42] Late stage pancreatic tumor treatment, mice surviving more than 90 total days in the study.[42] In early stage pancreatic tumor, mice had greater than 50 percent survival at day 89 when the study was terminated.[42] iExo are now making their way into phase I clinical trials but have not begun recruiting patients yet. The new idea of iExo brings great promise to pancreatic cancer and the ability to decrease patient suffering while increasing effective treatment options.

Exosomes for Drug Delivery to Lung Cancer

Lung cancer accounts for one out of four cancer-related deaths, making it the leading cause of mortality worldwide.[43] However, current therapeutic interventions are not efficient, and most are palliative.[43] Researchers are investigating natural products or synthetic drugs for use as a chemotherapeutic. Despite the development of substances for preventing progression and inhibiting malignancy of lung cancer, clinicians have been struggling with successful targeted delivery. The use of naturally occurring compounds is desired for their cost-effectiveness and feasibility for oral administration. However, many suffer from bioavailability and toxicity issues, making their use difficult due to lack of delivery methods.[43] Exosomes have been explored as a potential delivery method to overcome bioavailability, toxicity, and clearance. [43]

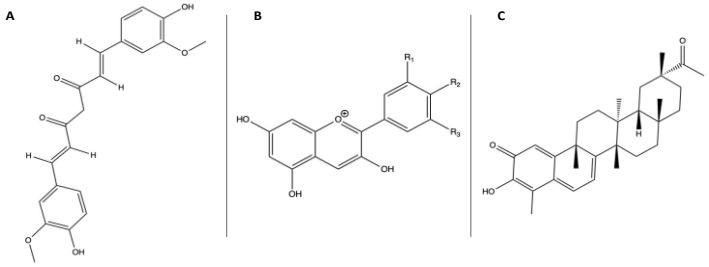

Figure 1.4. Chemical structures of natural substances used to treat lung cancer. (**A**) Curcumin (**B**) Anthocyanidins (**C**) Celastrol.

Three different naturally occurring substances that have been explored as possible treatments of lung cancer are celastrol, curcumin, and anthocyanidins (**Figure 1.4**). Celastrol is an herb shown to have antiproliferative and antitumor properties but has limited therapeutic use due to low bioavailability and off-site toxicity.[43] Aqil and colleagues studied the possibility of milk-derived exosomes delivering celastrol in an *in vitro* and *in vivo* lung cancer model.[43] In the *in vitro* assessment, human lung cancer H1299 cells were treated with free celastrol and celastrol-loaded exosomes.[43] The *in vivo* model used within this study was nude mice with a

subcutaneous injection of H1299 lung cancer xenografts.[43] The anti-proliferative effect of celastrol was further enhanced when encapsulated in exosomes in both the *in vitro* and *in vivo* setting.[43] The use of encapsulated celastrol in exosomes can reduce the toxicity while increasing the efficacy and has the potential to be a novel treatment of lung cancer.[43]

Curcumin, a naturally occurring substance, has been studied extensively as a potential chemopreventative for cancer.[7–9] Curcumin has poor water solubility due to hydrophobicity, reducing its clinical efficacy.[44] To enhance delivery of the compound, bovine milk-derived exosomes were loaded with curcumin and tested *in vitro* lung cancer models.[9] With the addition of curcumin-loaded exosomes, growth inhibition increased in the lung cancer cells without any toxic side effects to healthy cells.[9]

Aglycones (anthocyanidins) are naturally occurring substances found in berries possessing anti-proliferative, apoptotic, anti-inflammatory, and anti-oxidant properties, but suffer from low permeability and oral bioavailability.[11] Munagala et al. developed a method for loading milk-derived exosomes with anthocyanidins for oral delivery to mice with lung cancer xenografts. [11] The group initially tested the novel delivery method of plain exosomes and exosomes containing anthocyanidins *in vitro* using A549 and H1299 human lung cancer cells and observed a 66% and 76% reduction in cell number respectively (**Figure 1.5**).[11] When the exosomes were loaded with the anthocyanidins, up to a 30 fold decrease in cell survival was observed as compared to free compounds in lung cancer cell lines (**Figure 1.4**).[11] When tested *in vivo,* anthocyanidine-loaded exosomes also increased therapeutic response compared to free compounds without any toxicity.[11] The use of exosomes for the delivery of naturally occurring substances provides a promising method to overcome the challenges of bioavailability and toxicity.

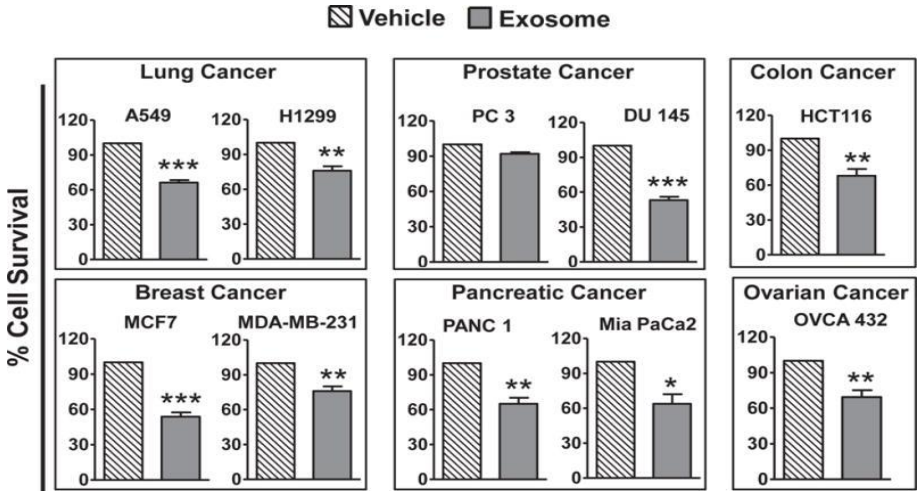

Figure 1.5. Reproduced with permission from Cancer Letters. Exosomes (vehicle) and exosomes containing Anthos were tested for cytotoxic effects on various cancer cell lines. Cancer cell lines of lung, breast, ovarian, colon, pancreas and prostate were treated with 50 μg/ml exosomes for 72 h and effect on cell growth inhibition was assessed by MTT assay and compared with untreated cells. Statistical analysis was performed using Student t-test to compare exosomes alone with vehicle treatment. *$p \leq 0.05$; **$p \leq 0.01$ and ***$p \leq 0.001$. [11]

In addition to the natural products, researchers have explored loading exosomes with synthetic pharmaceuticals. Kim et al. developed another method for loading paclitaxel via sonication into exosomes released by macrophages.[14] Exosome loaded with paclitaxel were shown to be a promising strategy for drug delivery to multi-drug resistant pulmonary cancers.[14] In a later study, the group modified the exosomes with the aminoethylanisamide-polyethylene glycol (AA-PEG) vector for targeting the sigma receptor, a commonly overexpressed receptor in non-small cell lung cancer.[45] The exosomes were biocompatible, long-circulating, and targeted drug delivery vehicles with innate features of macrophages.[45] The targeted exosomes increased the survival of the mouse model while decreasing toxic side effects.[45] Agarwal et al. developed paclitaxel-loaded exosomes for use as an oral delivery method.[15] The exosomes were isolated from raw cow milk and loaded with paclitaxel by mixing.[15] The group found the orally administered paclitaxel-loaded exosomes decreased the toxicity and increased the therapeutic efficiency of the drug to A549 xenograft lung tumor in mice.[15]

Other groups are working on loading exosomes with doxorubicin for possible lung cancer therapy.[46] Srivastava et al. investigated the efficacy of exosomes encapsulating doxorubicin conjugated to gold nanoparticles (GNPs) as a drug carrier.[46] In a separate study, Srivastava et al. explored exosomes for delivery of doxorubicin-GNPs by a pH-sensitive hydrazine linker, which they called nanosomes (**Figure 1.6**).[46] The efficacy of the exosomes were evaluated in an *in vitro* setting using two non-small cell lung cancer cell lines, H1299, and A549, and one lung fibroblast cell line MRC9.[46] The exosomes showed preferential cytotoxicity to lung cancer cells compared to healthy cells as evidenced by the reduced viability of the H1299 and A549 cells compared to MRC9 cells.[46]

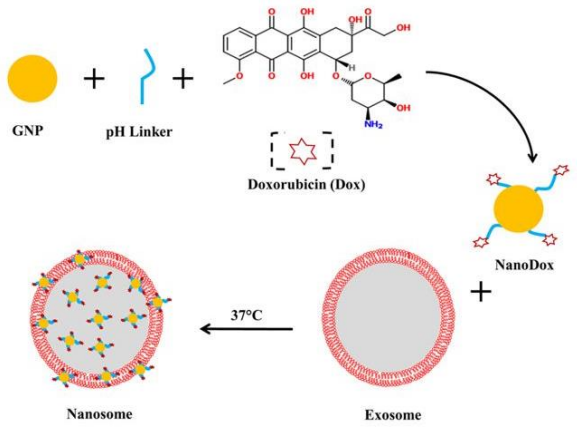

Figure 1.6. Reproduced with permission from Scientific Reports. Schematic of nanosome synthesis.[46]

In addition to the promising *in vitro* and *in vivo* results, Morse et al. conducted a Phase I clinical trial using exosomes encapsulating tumor antigens for advanced non-small cell lung cancer.[47] Exosomes derived from dendritic cells from the patient and loaded with MAGE tumor antigens were given four times weekly to study participants.[47] The therapy was well tolerated, and some of the participates experienced long term disease stability.[47] To investigate further, Phase II clinical trials are planned to expand the number of patients.[47] The use of exosomes as a

drug carrier for lung cancer shows considerable translational potential to overcome the current challenges faced by clinicians.

Exosomes for Drug Delivery to Prostate Cancer

Prostate cancer is the most frequently diagnosed malignancy in the United States, being the third most common type of cancer death in men.[48] Successful treatment of prostate cancer is difficult due to the rate of metastasis and late detection.[49,50] If treated early with surgical intervention, radiation or hormone therapy, moderate success has been observed but can become devastating with tumor metastasis.[50] Specific biomarkers are required for determining the type of prostate cancer, and exosomal surface proteins can be used for early detection of the malignancy.[51–54]

In addition to early detection, exosomes show promise as a chemotherapeutic carrier by increasing the cytotoxic effect and toxicity of chemotherapeutic on cancer cells.[45] Saari et al. isolated exosomes from the conditioned culture media of LNCaP (androgen-sensitive human prostate adenocarcinoma) and PC-3 (prostate adenocarcinoma) cells using ultracentrifugation. Subsequently, the exosomes were loaded with paclitaxel and assays showed decreased prostate cancer cell viability.[55] To determine the importance of exosomal surface proteins, all surface proteins were removed from paclitaxel loaded exosomes.[55] Although there were no indications of formation problems, the delivery efficiency for paclitaxel decreased.[55] This is likely due to the decreased entry of the in the cancer cells. Endocytosis of the exosomes is partially mediated by the surface proteins.[55] The surface proteins are vital in the drug delivery properties of exosomes due to their specific mechanisms of entering cells.[55]

In addition to chemotherapeutic drug delivery, exosomes have been researched as a vaccine for prostate cancer and a delivery method for the anti-inflammatory agent, curcumin

(previously discussed in lung cancer section of this article).[56–58] With these potential applications of exosomes for the treatment of prostate cancer, there is hope that the most frequently diagnosed cancer will begin to have higher survival rates in the near future.

Exosomes for Drug Delivery to Glioblastoma

Even with a multimodal treatment plan, often consisting of surgery, radiation, and chemotherapy, the median survival remains under 15 months for glioma.[59] The most prevalent form of glioma, tumors arising from glial precursor cells, is glioblastoma multiforme (GBM).[60] Frontline therapy for GBM is termed the Stupp protocol, involving concurrent radiotherapy along with temozolomide-based chemotherapy.[61] Heterogeneity among glioblastoma leading to both inter and intratumor variation results in altering responses to therapy, warranting novel therapeutic strategies. The blood-brain barrier (BBB) remains near impenetrable, blocking the penetration of more than 98% of all small molecule drugs.[62] Exosomes with limitless variation in loading capacity and homing abilities showcase a possible treatment modality for GBM,[61] allowing for new and old classes of drugs to be effectively delivered to their target sites.

Yang et al., showcased the ability of drug-loaded exosomes to cross the BBB *in vivo*, using a zebrafish model.[62,63] The propensity of zebrafish as a reliable *in-vivo* BBB model was shown by Jeong et al., by confirmation of specific characteristics seen in higher order vertebrates.[64] Exosomes were isolated from cell culture media from various cell lines including GBM U-87 MG, brain endothelial cells bEND.3, neuroectodermal tumor PFSK-1, and glioblastoma A-172. Paclitaxel and doxorubicin were incorporated into the exosomes using electroporation along with a fluorescent dye (rhodamine 123) and then tested for CD9, CD63, and CD81. No significant differences were found between cell lines except bEND.3 cells. These cells had a near 2000 times greater expression of CD63, possibly eluting to a unique receptor-

mediated transport mechanism for crossing the BBB.[62] This theory was partially confirmed by incubating bEND.3 cells with rhodamine 123 exosomes. This resulted in a significantly higher cellular uptake, showing the involvement of active transport mechanisms. Exosome delivery across the zebrafish BBB was tested using all four cell types (**Figure 1.7)**. While the exosomes from glioblastoma-astrocytoma (U87-MG), neuroectodermal tumor (PFSK-1), and glioblastoma (A-172) cells failed to cross the BBB, the bEND.3 exosomes were successful. The crossing of the BBB by drug encapsulated bEND.3 exosomes resulted in reduced tumor size compared to free drug and control treatments.

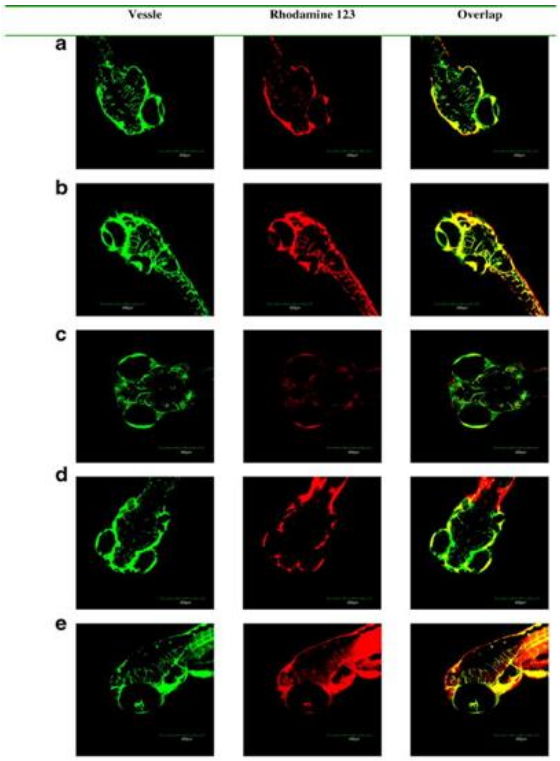

Figure 1.7. Reproduced with permission from Pharmaceutical Research In vivo brain imaging of exosome delivered rhodamine 123 in Tg (fli1: GFP) embryonic zebrafish. Rhodamine 123 (red) retained within vessels (green) after the injected formulations without exosome (a) and with exosomes isolated from (b) neuroectodermal tumor PFSK-1, (c) glioblastoma A-172, and (d) glioblastoma- astrocytoma U-87 MG. Rhodamine 123 (red) dispersed out of vessels (green) after the injected formulation with exosomes isolated from (e) brain endothelial bEND.3 cells. [62]

Yang et al. attempted to further their zebrafish studies by loading siRNA in the exosomes.[62] After finding the significant uptake by bEND.3 exosomes, [62] the group loaded VEGF siRNA into the isolated exosomes. siRNA alone was unable to effectively cross the zebrafish BBB. However, the bEND.3 siRNA loaded exosomes again showed utility (**Figure 1.8**).[62,63] The siRNA loaded exosome decreased the cellular fluorescence signal of the in-vivo DiD-labeled cells by a factor of 4. This decrease in cellular fluorescence and supporting results from the paper indicated siRNA loaded exosomes can cross the blood-brain barrier while inhibiting VEGF in this xenographic mouse model.[63]

A second type of RNA related therapeutic, miRNAs also show anticancer characteristics by their ability to alter the posttranscriptional gene expression.[65–67] Expression levels of specific miRNAs have been implicated in GBM showing downregulation relative to non-neoplastic brain tissues.[68] Lang et al. screened eight miRNAs found to have implications in GBM against five glioma stem cell lines representing all GBM subtypes.[69] miRNA-124a was selected based on effectiveness in decreasing cellular viability across all five cell lines.

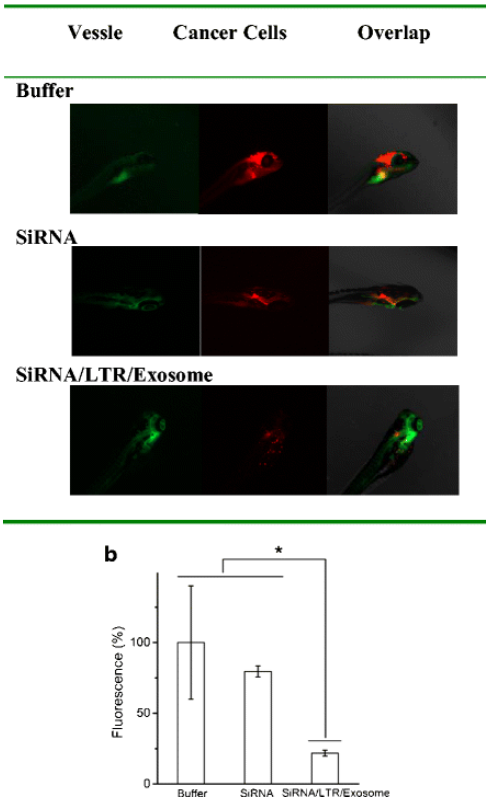

Figure 1.8. Reproduced with permission from Pharmaceutical Research. Efficacy of exosome-delivered VEGF siRNA in a zebrafish cancer model. Images (a) and statistical analysis (b) of quantified DiD-labeled (red) cancer cells in the zebrafish brain. *Results are significantly different ($p < 0.05$). Data represent the mean ± SD, n = 12(5)[63]

Using a lentivirus, the group was able to overexpress miRNA-124a in cultured mesenchymal stem cells (MSCs). Exosomes were harvested from MSC cultures that are transfected with the cDNA for miRNA-124a, a nonsense control cDNA (miRControl), or medium only (Exo-empty). The exosomes were lysed, and RNA was collected for qRT-PCR analysis. Exosomes from miRNA-124a transfected MSCs had a 60 fold increase vs. miRControl or medium only exosomes.[69] Lang et al., lastly tested their exosomes *in-vivo* using surgically implanted GBM cells in mice. Exo- miR control, and Exo-empty treated animals died within 48 days with a median survival of 41 days, while Exo-miRNA124 animals showed a median survival of 104 days (**Figure 1.9**).[69]

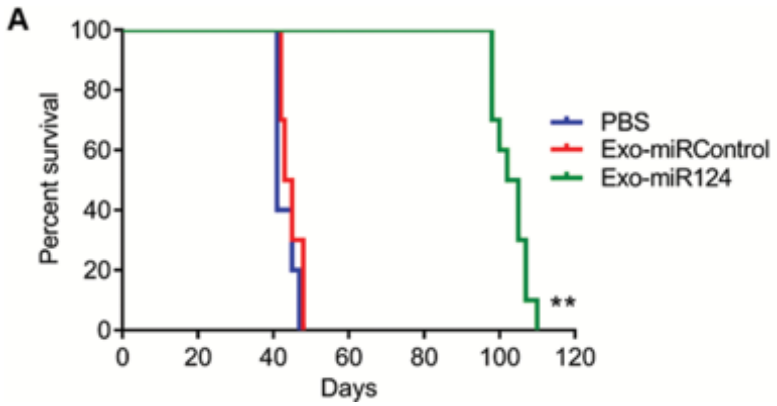

Figure 1.9. Reproduced with permission from Neuro Oncology. Percent survival of mice treated ex vivo Exo-miR124 after being implanted with GSCs. **P < 0.01 [69]

The BBB provides a necessary protection system; however, it also provides a barricade against treatment. Practically all large molecule pharmaceutics including monoclonal antibodies, recombinant proteins, and RNA-like molecules are unable to pass through the BBB on their own.[70] Exosomes appear as a viable option for a delivery vehicle capable of carrying both large and small molecules across the blood-brain barrier.

Challenges

Although there are numerous advantages to the use of exosomes there are a couple of global challenges with the use of exosomes. One of the major ones is the composition of exosomes and their function. Exosomes been shown to be involved in cellular communication through the transport of biomacromolecules from the host cell. However, it is unclear exactly what is being transported and the purpose behind this communication leading to a lack of homogeneity.[21] As such, it is necessary to choose an appropriate donor cell to prevent problems such as triggering an immune response or promoting metastasis. [71] Many researchers are struggling to find an adequate source of exosomes with the desired features for the intended treatment and more methods for obtaining exosomes in a cost efficient manner is in high demand. [24] Many have turned to cell culture exosome derivation, which has significant flaws due

to cargo that is being carried. Studies have implicated exosomes in signaling tumor metastases when exosomes are derived from cancer cells.[72–76] As a result of that information they should not be used in the treatment of cancer, however many continue to do so (**Table 1.1**), which could lead to significant problems *in vivo*. Bovine milk exosomes may provide a solution to these challenges due to the ease of access and lack of human diseases.[77,78] Further research will be required into the composition of these types of exosomes to determine efficacy as a human drug carrier.

Conclusion

Exosomes are potential drug carriers at the early stages of development and validation.[21,79] Recent studies show their capabilities and have the potential to rise to the most effective drug carrier. Exosomes possess the ability to communicate to cells with distinct biomarkers making them specific.[16] Their naturally derived properties are not easily replicated in liposomes or polymersomes leading to the increased success of exosomes over other nanocarriers. Exosomes' ability to fight solid tumor cancers comes at a much needed time, with many current nanoparticle delivery systems failing at a rate of 90 ± 5% in industry and government settings.[1] The problems being faced are clearance and specificity, which exosomes can address..

Table 1.1. Overview of cancer type, exosomal cargo and source of exosomes discussed in this review.

Cancer Type	Cargo	Source of Exosomes
Breast	Curcumin	TS/A, 4T.1 and B16 Cell Derived [7]
		Raw bovine milk[9]
	Anythocyanidins	Raw bovine milk [40]
	Paclitaxel	Macrophage Cell Derived [14]
		Raw bovine milk[15]
	Soluble proteins	HEK293, HT1080 and HeLa Cell Derived [19]
	Berry Anthos	Raw bovine milk [40]
	Doxorubicin	MDA-MB-231 and MCF7 Cell Derived [26]
	siRNA	HEK 293 and MCF7 Cell Derived [31,33]
	miRNA	HEK 293 and MCF7 Cell Derived [31,33]
	ssDNA	HEK293 and MCF7 Cell Derived [31]
	miR-134	Hs578T Cell Derived [32]
	Trastuzumab	Modified Dendritic Cell Derived [23]
Pancreatic	Oncogenic Kras	Human Foreskin Fibroblast Derived [38]
		Bone Marrow Derived Mesenchymal Stem Cell Derived [42]
Lung	Celastrol	Raw bovine milk [43]
	Paclitaxel	Macrophage Cell Derived [45]
	Doxorubicin-Gold Nanoparticle Conjugate	H1299 and YRC9 Cell Derived [46]
	Peptide	Peripheral Blood Mononuclear Cell Derived [47]
Prostate	Paclitaxel	LNCaP and PC3 Cell Derived [55]
	Curcumin	GL26 Cell Derived [58]
	STAT3 Inhibitor	Gl26 Cell Derived [58]
Glioblastoma	Rhodamine 123 with Paclitaxel or Doxorubicin	Brain neuronal glioblastoma-astrocytoma U-87 MG, endothelial bEND.3, neuroectodermal tumor PFSK-1, and glioblastoma A-172 cell Derived [62]
	MiR-124a	Mesenchymal Stem Cell Derived [69]
	siRNA	bEND.3 Cell Derived [80]

Lung, pancreatic, glioblastoma, prostate, and breast cancers are deadly malignancies and require more specialized treatment methods. Current approaches do not treat many of these cancers successfully. The biological origin has given exosomes a unique ability to address current issues with nanoparticle-based drug delivery.[21,79] With decreased clearance and increased specificity due to surface proteins and artificial targeting methods, exosomes are very promising

drug carriers to target and deliver chemotherapeutics, RNA, and natural products. Versatility of exosomes is a great strength and is demonstrated throughout the wide variety in cargo and sources of exosomes discussed within this review (**Table 1.1**). Clinical trials are still on the horizon for the use of exosomes as a drug carrier for solid tumors and great strides in this area will be made in the upcoming years.

Author Contributions

The manuscript was written through the contributions of all authors.

Funding

This research was supported by NIH grant 1 R01GM 114080 to SM and KS. SM also acknowledges support from the Grand Challenge Initiative and the Office of the Dean, College of Health Profession, North Dakota State University.

References

1 Maeda H, Khatami M. Analyses of repeated failures in cancer therapy for solid tumors: poor tumor-selective drug delivery, low therapeutic efficacy and unsustainable costs. Clin Transl Med 2018;7:. https://doi.org/10.1186/s40169-018-0185-6.

2 Butcher L. Solid Tumors: Prevalence, Economics, And Implications for Payers and Purchasers. Biotechnol Healthc 2008;5:20–1.

3 Alves TR, Lima FRS, Kahn SA, Lobo D, Dubois LGF, Soletti R, et al. Glioblastoma cells: A heterogeneous and fatal tumor interacting with the parenchyma. Life Sciences 2011;89:532–9. https://doi.org/10.1016/j.lfs.2011.04.022.

4 Siegel RL, Miller KD, Jemal A. Cancer statistics, 2016. CA: A Cancer Journal for Clinicians n.d.;66:7–30. https://doi.org/10.3322/caac.21332.

5 Schito L. Bridging angiogenesis and immune evasion in the hypoxic tumor microenvironment. Am J Physiol Regul Integr Comp Physiol 2018. https://doi.org/10.1152/ajpregu.00209.2018.

6 Young RC, DeVita VT. Cell Cycle Characteristics of Human Solid Tumors in Vivo. Cell Proliferation 1970;3:285–90. https://doi.org/10.1111/j.1365-2184.1970.tb00273.x.

7 Zhang H-G, Kim H, Liu C, Yu S, Wang J, Grizzle WE, et al. Curcumin reverses breast tumor exosomes mediated immune suppression of NK cell tumor cytotoxicity. Biochimica et Biophysica Acta (BBA) - Molecular Cell Research 2007;1773:1116–23. https://doi.org/10.1016/j.bbamcr.2007.04.015.

8 Cheng AL, Hsu CH, Lin JK, Hsu MM, Ho YF, Shen TS, et al. Phase I clinical trial of curcumin, a chemopreventive agent, in patients with high-risk or pre-malignant lesions. Anticancer Res 2001;21:2895–900.

9 Aqil F, Munagala R, Jeyabalan J, Agrawal AK, Gupta R. Exosomes for the Enhanced Tissue Bioavailability and Efficacy of Curcumin. AAPS J 2017;19:1691–702. https://doi.org/10.1208/s12248-017-0154-9.
10 Earle CC, Evans WK. A comparison of the costs of paclitaxel and best supportive care in stage IV non-small-cell lung cancer. Cancer Prev Control 1997;1:282–8.
11 Munagala R, Aqil F, Jeyabalan J, Agrawal AK, Mudd AM, Kyakulaga AH, et al. Exosomal formulation of anthocyanidins against multiple cancer types. Cancer Lett 2017;393:94–102. https://doi.org/10.1016/j.canlet.2017.02.004.
12 Panahi Y, Saadat A, Beiraghdar F, Sahebkar A. Adjuvant Therapy with Bioavailability-Boosted Curcuminoids Suppresses Systemic Inflammation and Improves Quality of Life in Patients with Solid Tumors: A Randomized Double-Blind Placebo-Controlled Trial. Phytotherapy Research 2014;28:1461–7. https://doi.org/10.1002/ptr.5149.
13 Teixeira LL, Costa GR, Dörr FA, Ong TP, Pinto E, Lajolo FM, et al. Potential antiproliferative activity of polyphenol metabolites against human breast cancer cells and their urine excretion pattern in healthy subjects following acute intake of a polyphenol-rich juice of grumixama (Eugenia brasiliensis Lam.). Food Funct 2017;8:2266–74. https://doi.org/10.1039/C7FO00076F.
14 Kim MS, Haney MJ, Zhao Y, Mahajan V, Deygen I, Klyachko NL, et al. Development of Exosome-encapsulated Paclitaxel to Overcome MDR in Cancer cells. Nanomedicine 2016;12:655–64. https://doi.org/10.1016/j.nano.2015.10.012.
15 Agrawal AK, Aqil F, Jeyabalan J, Spencer WA, Beck J, Gachuki BW, et al. Milk-derived exosomes for oral delivery of paclitaxel. Nanomedicine: Nanotechnology, Biology and Medicine 2017;13:1627–36. https://doi.org/10.1016/j.nano.2017.03.001.
16 Rashed MH, Bayraktar E, Helal GK, Abd-Ellah MF, Amero P, Chavez-Reyes A, et al. Exosomes: From Garbage Bins to Promising Therapeutic Targets. International Journal of Molecular Sciences 2017;18:. https://doi.org/10.3390/ijms18030538.
17 Théry C, Witwer KW, Aikawa E, Alcaraz MJ, Anderson JD, Andriantsitohaina R, et al. Minimal information for studies of extracellular vesicles 2018 (MISEV2018): a position statement of the International Society for Extracellular Vesicles and update of the MISEV2014 guidelines. Journal of Extracellular Vesicles 2018;7:1535750. https://doi.org/10.1080/20013078.2018.1535750.
18 Schorey JS, Bhatnagar S. Exosome Function: From Tumor Immunology to Pathogen Biology. Traffic 2008;9:871–81. https://doi.org/10.1111/j.1600-0854.2008.00734.x.
19 Yim N, Ryu S-W, Choi K, Lee KR, Lee S, Choi H, et al. Exosome engineering for efficient intracellular delivery of soluble proteins using optically reversible protein–protein interaction module. Nature Communications 2016;7:12277. https://doi.org/10.1038/ncomms12277.
20 Batrakova EV, Kim MS. Using exosomes, naturally-equipped nanocarriers, for drug delivery. J Control Release 2015;219:396–405. https://doi.org/10.1016/j.jconrel.2015.07.030.
21 Munagala R, Aqil F, Jeyabalan J, Agrawal AK, Mudd AM, Kyakulaga AH, et al. Exosomal formulation of anthocyanidins against multiple cancer types. Cancer Lett 2017;393:94–102. https://doi.org/10.1016/j.canlet.2017.02.004.
22 Lener T, Gimona M, Aigner L, Börger V, Buzas E, Camussi G, et al. Applying extracellular vesicles based therapeutics in clinical trials – an ISEV position paper. J Extracell Vesicles 2015;4:. https://doi.org/10.3402/jev.v4.30087.

23 Zha QB, Yao YF, Ren ZJ, Li XJ, Tang JH. Extracellular vesicles: An overview of biogenesis, function, and role in breast cancer, Extracellular vesicles: An overview of biogenesis, function, and role in breast cancer. Tumour Biol 2017;39:1010428317691182. https://doi.org/10.1177/1010428317691182.
24 Wang L, Xie Y, Ahmed KA, Ahmed S, Sami A, Chibbar R, et al. Exosomal pMHC-I complex targets T cell-based vaccine to directly stimulate CTL responses leading to antitumor immunity in transgenic FVBneuN and HLA-A2/HER2 mice and eradicating trastuzumab-resistant tumor in athymic nude mice. Breast Cancer Res Treat 2013;140:273–84. https://doi.org/10.1007/s10549-013-2626-7.
25 Yu D, Wu Y, Shen H, Lv M, Chen W, Zhang X, et al. Exosomes in development, metastasis and drug resistance of breast cancer. Cancer Sci 2015;106:959–64. https://doi.org/10.1111/cas.12715.
26 Ono M, Kosaka N, Tominaga N, Yoshioka Y, Takeshita F, Takahashi R, et al. Exosomes from bone marrow mesenchymal stem cells contain a microRNA that promotes dormancy in metastatic breast cancer cells. Sci Signal 2014;7:ra63. https://doi.org/10.1126/scisignal.2005231.
27 Tian Y, Li S, Song J, Ji T, Zhu M, Anderson GJ, et al. A doxorubicin delivery platform using engineered natural membrane vesicle exosomes for targeted tumor therapy. Biomaterials 2014;35:2383–90. https://doi.org/10.1016/j.biomaterials.2013.11.083.
28 Swain SM, Whaley FS, Ewer MS. Congestive heart failure in patients treated with doxorubicin. Cancer n.d.;97:2869–79. https://doi.org/10.1002/cncr.11407.
29 Crozier JA, Swaika A, Moreno-Aspitia A. Adjuvant chemotherapy in breast cancer: To use or not to use, the anthracyclines. World Journal of Clinical Oncology 2014;5:529–38. https://doi.org/10.5306/wjco.v5.i3.529.
30 Hadla M, Palazzolo S, Corona G, Caligiuri I, Canzonieri V, Toffoli G, et al. Exosomes increase the therapeutic index of doxorubicin in breast and ovarian cancer mouse models. Nanomedicine (Lond) 2016;11:2431–41. https://doi.org/10.2217/nnm-2016-0154.
31 Toffoli G, Hadla M, Corona G, Caligiuri I, Palazzolo S, Semeraro S, et al. Exosomal doxorubicin reduces the cardiac toxicity of doxorubicin. Nanomedicine (Lond) 2015;10:2963–71. https://doi.org/10.2217/nnm.15.118.
32 Bayet-Robert M, Kwiatowski F, Leheurteur M, Gachon F, Planchat E, Abrial C, et al. Phase I dose escalation trial of docetaxel plus curcumin in patients with advanced and metastatic breast cancer. Cancer Biology & Therapy 2010;9:8–14. https://doi.org/10.4161/cbt.9.1.10392.
33 Lamichhane TN, Jeyaram A, Patel DB, Parajuli B, Livingston NK, Arumugasaamy N, et al. Oncogene Knockdown via Active Loading of Small RNAs into Extracellular Vesicles by Sonication. Cell Mol Bioeng 2016;9:315–24. https://doi.org/10.1007/s12195-016-0457-4.
34 O'Brien K, Lowry MC, Corcoran C, Martinez VG, Daly M, Rani S, et al. miR-134 in extracellular vesicles reduces triple-negative breast cancer aggression and increases drug sensitivity. Oncotarget 2015;6:32774–89. https://doi.org/10.18632/oncotarget.5192.
35 Ohno S, Takanashi M, Sudo K, Ueda S, Ishikawa A, Matsuyama N, et al. Systemically Injected Exosomes Targeted to EGFR Deliver Antitumor MicroRNA to Breast Cancer Cells. Mol Ther 2013;21:185–91. https://doi.org/10.1038/mt.2012.180.
36 Mohammed S, Van Buren II G, Fisher WE. Pancreatic cancer: Advances in treatment. World J Gastroenterol 2014;20:9354–60. https://doi.org/10.3748/wjg.v20.i28.9354.

37 Pancreatic Cancer - Cancer Stat Facts. n.d. URL: https://seer.cancer.gov/statfacts/html/pancreas.html (Accessed 18 January 2018).
38 PDQ Adult Treatment Editorial Board. Pancreatic Cancer Treatment (PDQ®): Patient Version. PDQ Cancer Information Summaries. Bethesda (MD): National Cancer Institute (US); 2002.
39 Von Hoff DD, Ervin T, Arena FP, Chiorean EG, Infante J, Moore M, et al. Increased Survival in Pancreatic Cancer with nab-Paclitaxel plus Gemcitabine. N Engl J Med 2013;369:1691–703. https://doi.org/10.1056/NEJMoa1304369.
40 Kamerkar S, LeBleu VS, Sugimoto H, Yang S, Ruivo CF, Melo SA, et al. Exosomes facilitate therapeutic targeting of oncogenic KRAS in pancreatic cancer. Nature 2017;546:498. https://doi.org/10.1038/nature22341.
41 Zorde Khvalevsky E, Gabai R, Rachmut IH, Horwitz E, Brunschwig Z, Orbach A, et al. Mutant KRAS is a druggable target for pancreatic cancer. Proceedings of the National Academy of Sciences 2013;110:20723–8. https://doi.org/10.1073/pnas.1314307110.
42 Whitehead KA, Langer R, Anderson DG. Knocking down barriers: advances in siRNA delivery. Nature Reviews Drug Discovery 2009;8:129–38. https://doi.org/10.1038/nrd2742.
43 Mendt M, Kamerkar S, Sugimoto H, McAndrews KM, Wu C-C, Gagea M, et al. Generation and testing of clinical-grade exosomes for pancreatic cancer. JCI Insight n.d.;3:. https://doi.org/10.1172/jci.insight.99263.
44 Aqil F, Kausar H, Agrawal AK, Jeyabalan J, Kyakulaga A-H, Munagala R, et al. Exosomal formulation enhances therapeutic response of celastrol against lung cancer. Experimental and Molecular Pathology 2016;101:12–21. https://doi.org/10.1016/j.yexmp.2016.05.013.
45 Sun D, Zhuang X, Xiang X, Liu Y, Zhang S, Liu C, et al. A Novel Nanoparticle Drug Delivery System: The Anti-inflammatory Activity of Curcumin Is Enhanced When Encapsulated in Exosomes. Mol Ther 2010;18:1606–14. https://doi.org/10.1038/mt.2010.105.
46 Stoner GD, Wang L-S, Casto BC. Laboratory and clinical studies of cancer chemoprevention by antioxidants in berries. Carcinogenesis 2008;29:1665–74. https://doi.org/10.1093/carcin/bgn142.
47 Kim MS, Haney MJ, Zhao Y, Yuan D, Deygen I, Klyachko NL, et al. Engineering macrophage-derived exosomes for targeted paclitaxel delivery to pulmonary metastases: in vitro and in vivo evaluations. Nanomedicine: Nanotechnology, Biology and Medicine 2018;14:195–204. https://doi.org/10.1016/j.nano.2017.09.011.
48 Srivastava A, Amreddy N, Babu A, Panneerselvam J, Mehta M, Muralidharan R, et al. Nanosomes carrying doxorubicin exhibit potent anticancer activity against human lung cancer cells. Scientific Reports 2016;6:38541. https://doi.org/10.1038/srep38541.
49 Morse MA, Garst J, Osada T, Khan S, Hobeika A, Clay TM, et al. A phase I study of dexosome immunotherapy in patients with advanced non-small cell lung cancer. J Transl Med 2005;3:9. https://doi.org/10.1186/1479-5876-3-9.
50 Hotte SJ, Saad F. Current management of castrate-resistant prostate cancer. Curr Oncol 2010;17:S72–9.
51 Kim SJ, Kim SI. Current Treatment Strategies for Castration-Resistant Prostate Cancer. Korean J Urol 2011;52:157–65. https://doi.org/10.4111/kju.2011.52.3.157.

52 Lepor H. Challenging the Current Treatment Paradigm of Androgen-Independent Prostate Cancer. Rev Urol 2007;9:S1–2.
53 Perkins GL, Slater ED, Sanders GK, Prichard JG. Serum Tumor Markers. AFP 2003;68:1075–82.
54 Pan J, Ding M, Xu K, Yang C, Mao L-J. Exosomes in diagnosis and therapy of prostate cancer. Oncotarget 2017;8:97693–700. https://doi.org/10.18632/oncotarget.18532.
55 Nilsson J, Skog J, Nordstrand A, Baranov V, Mincheva-Nilsson L, Breakefield XO, et al. Prostate cancer-derived urine exosomes: a novel approach to biomarkers for prostate cancer. Br J Cancer 2009;100:1603–7. https://doi.org/10.1038/sj.bjc.6605058.
56 Logozzi M, Angelini DF, Iessi E, Mizzoni D, Di Raimo R, Federici C, et al. Increased PSA expression on prostate cancer exosomes in in vitro condition and in cancer patients. Cancer Letters 2017;403:318–29. https://doi.org/10.1016/j.canlet.2017.06.036.
57 Saari H, Lázaro-Ibáñez E, Viitala T, Vuorimaa-Laukkanen E, Siljander P, Yliperttula M. Microvesicle- and exosome-mediated drug delivery enhances the cytotoxicity of Paclitaxel in autologous prostate cancer cells. Journal of Controlled Release 2015;220:727–37. https://doi.org/10.1016/j.jconrel.2015.09.031.
58 Andre F, Schartz NE, Movassagh M, Flament C, Pautier P, Morice P, et al. Malignant effusions and immunogenic tumour-derived exosomes. The Lancet 2002;360:295–305. https://doi.org/10.1016/S0140-6736(02)09552-1.
59 Wolfers J, Lozier A, Raposo G, Regnault A, Théry C, Masurier C, et al. Tumor-derived exosomes are a source of shared tumor rejection antigens for CTL cross-priming. Nature Medicine 2001;7:297–303. https://doi.org/10.1038/85438.
60 Zhuang X, Xiang X, Grizzle W, Sun D, Zhang S, Axtell RC, et al. Treatment of Brain Inflammatory Diseases by Delivering Exosome Encapsulated Anti-inflammatory Drugs From the Nasal Region to the Brain. Mol Ther 2011;19:1769–79. https://doi.org/10.1038/mt.2011.164.
61 Ammirati M, Chotai S, Newton H, Lamki T, Wei L, Grecula J. Hypofractionated intensity modulated radiotherapy with temozolomide in newly diagnosed glioblastoma multiforme. J Clin Neurosci 2014;21:633–7. https://doi.org/10.1016/j.jocn.2013.09.005.
62 Davis ME. Glioblastoma: Overview of Disease and Treatment. Clin J Oncol Nurs 2016;20:S2-8. https://doi.org/10.1188/16.CJON.S1.2-8.
63 Gourlay J, Morokoff AP, Luwor RB, Zhu H-J, Kaye AH, Stylli SS. The emergent role of exosomes in glioma. J Clin Neurosci 2017;35:13–23. https://doi.org/10.1016/j.jocn.2016.09.021.
64 Yang T, Martin P, Fogarty B, Brown A, Schurman K, Phipps R, et al. Exosome Delivered Anticancer Drugs Across the Blood-Brain Barrier for Brain Cancer Therapy in Danio Rerio. Pharm Res 2015;32:2003–14. https://doi.org/10.1007/s11095-014-1593-y.
65 Yang T, Fogarty B, LaForge B, Aziz S, Pham T, Lai L, et al. Delivery of Small Interfering RNA to Inhibit Vascular Endothelial Growth Factor in Zebrafish Using Natural Brain Endothelia Cell-Secreted Exosome Nanovesicles for the Treatment of Brain Cancer. AAPS J 2017;19:475–86. https://doi.org/10.1208/s12248-016-0015-y.
66 Jeong J-Y, Kwon H-B, Ahn J-C, Kang D, Kwon S-H, Park JA, et al. Functional and developmental analysis of the blood–brain barrier in zebrafish. Brain Research Bulletin 2008;75:619–28. https://doi.org/10.1016/j.brainresbull.2007.10.043.

67 Chakraborty C, Sharma AR, Sharma G, Doss CGP, Lee S-S. Therapeutic miRNA and siRNA: Moving from Bench to Clinic as Next Generation Medicine. Mol Ther Nucleic Acids 2017;8:132–43. https://doi.org/10.1016/j.omtn.2017.06.005.
68 Huntzinger E, Izaurralde E. Gene silencing by microRNAs: contributions of translational repression and mRNA decay. Nat Rev Genet 2011;12:99–110. https://doi.org/10.1038/nrg2936.
69 Ambros V. The functions of animal microRNAs. Nature 2004;431:350–5. https://doi.org/10.1038/nature02871.
70 Silber J, Lim DA, Petritsch C, Persson AI, Maunakea AK, Yu M, et al. miR-124 and miR-137 inhibit proliferation of glioblastoma multiforme cells and induce differentiation of brain tumor stem cells. BMC Med 2008;6:14. https://doi.org/10.1186/1741-7015-6-14.
71 Lang FM, Hossain A, Gumin J, Momin EN, Shimizu Y, Ledbetter D, et al. Mesenchymal stem cells as natural biofactories for exosomes carrying miR-124a in the treatment of gliomas. Neuro Oncol 2018;20:380–90. https://doi.org/10.1093/neuonc/nox152.
72 Pardridge WM. Blood-brain barrier delivery. Drug Discov Today 2007;12:54–61. https://doi.org/10.1016/j.drudis.2006.10.013.
73 Ohno S, Takanashi M, Sudo K, Ueda S, Ishikawa A, Matsuyama N, et al. Systemically Injected Exosomes Targeted to EGFR Deliver Antitumor MicroRNA to Breast Cancer Cells. Mol Ther 2013;21:185–91. https://doi.org/10.1038/mt.2012.180.
74 Azmi AS, Bao B, Sarkar FH. Exosomes in Cancer Development, Metastasis and Drug Resistance: A Comprehensive Review. Cancer Metastasis Rev 2013;32:. https://doi.org/10.1007/s10555-013-9441-9.
75 Becker A, Thakur BK, Weiss JM, Kim HS, Peinado H, Lyden D. Extracellular Vesicles in Cancer: Cell-to-Cell Mediators of Metastasis. Cancer Cell 2016;30:836–48. https://doi.org/10.1016/j.ccell.2016.10.009.
76 Fu Q, Zhang Q, Lou Y, Yang J, Nie G, Chen Q, et al. Primary tumor-derived exosomes facilitate metastasis by regulating adhesion of circulating tumor cells via SMAD3 in liver cancer. Oncogene 2018;37:6105. https://doi.org/10.1038/s41388-018-0391-0.
77 Weidle HU, Birzele F, Kollmorgen G, Rüger R. The Multiple Roles of Exosomes in Metastasis. Cancer Genomics Proteomics 2016;14:1–16.
78 Zocco D, Ferruzzi P, Cappello F, Kuo WP, Fais S. Extracellular Vesicles as Shuttles of Tumor Biomarkers and Anti-Tumor Drugs. Front Oncol 2014;4:. https://doi.org/10.3389/fonc.2014.00267.
79 Munagala R, Aqil F, Jeyabalan J, Gupta RC. Bovine milk-derived exosomes for drug delivery. Cancer Lett 2016;371:48–61. https://doi.org/10.1016/j.canlet.2015.10.020.
80 Aqil F, Munagala R, Jeyabalan J, Agrawal AK, Kyakulaga A-H, Wilcher SA, et al. Milk exosomes - Natural nanoparticles for siRNA delivery. Cancer Letters 2019;449:186–95. https://doi.org/10.1016/j.canlet.2019.02.011.
81 Fais S, O'Driscoll L, Borras FE, Buzas E, Camussi G, Cappello F, et al. Evidence-Based Clinical Use of Nanoscale Extracellular Vesicles in Nanomedicine. ACS Nano 2016;10:3886–99. https://doi.org/10.1021/acsnano.5b08015.
82 Yang T, Fogarty B, LaForge B, Aziz S, Pham T, Lai L, et al. Delivery of Small Interfering RNA to Inhibit Vascular Endothelial Growth Factor in Zebrafish Using Natural Brain Endothelia Cell-Secreted Exosome Nanovesicles for the Treatment of Brain Cancer. AAPS J 2017;19:475–86. https://doi.org/10.1208/s12248-016-0015-y.

CHAPTER 2: ECHOGENIC EXOSOMES AS ULTRASOUND CONTRAST AGENTS[2]

Abstract

Exosomes are naturally secreted extracellular bilayer vesicles (diameter 40-130 nm), which have recently been found to play a critical role in cell-to-cell communication and biomolecule delivery. Their unique characteristics—stability, permeability, biocompatibility and low immunogenicity—have made them a prime candidate for use in delivering cancer therapeutics and other natural products. Here we present the first ever report of echogenic exosomes, which combine the benefits of the acoustic responsiveness of traditional microbubbles with the non-immunogenic and small-size morphology of exosomes. Microbubbles, although effective as ultrasound contrast agents, are restricted to intravascular usage due to their large size. In the current study, we have rendered bovine milk-derived exosomes echogenic by freeze drying them in presence of mannitol. Ultrasound imaging and direct measurement of linear and nonlinear scattered responses were used to investigate the echogenicity and stability of the prepared exosomes. A commercial scanner registered enhancement (28.9% at 40 MHz) in the brightness of ultrasound images in presence of echogenic exosomes at 5 mg/mL. The exosomes also showed a significant linear and nonlinear scattered responses—11 dB enhancement in fundamental, 8.5 dB in subharmonic and 3.5 dB in second harmonic all at 40 μg/mL concentration. Echogenic exosomes injected into the tail vein of mice and the synovial fluid of rats resulted in significantly higher brightness—as much as 300%—of the ultrasound images,

---

[2] Published by The Royal Society of Chemistry. The material in this chapter was co-authored by Jenna Osborn, Jessica E Pullan, James Froberg, Jacob Shreffler, Kara N Gange, Todd Molden, Yongki Choi, Amanda Brooks, Sanku Mallik, Kausik Sarkar. Jenna Osborn and Jessica Pullan contributed to experimental design, performed experiments, and wrote the manuscript. Sanku Mallik and Kausik Sarkar contributed to experimental design and writing the manuscript. James Froberg, Jacob Shreffler, Kara Gange, Todd Molden, Yongki Choi, and Amanda Brooks assisted in performing experiments.

showing their promise in a variety of *in vivo* applications. The echogenic exosomes, with their large-scale extractability from bovine milk, lack of toxicity and minimal immunogenic response, successfully served as ultrasound contrast agents in this study and offers an exciting possibility to act as an effective ultrasound responsive drug delivery system.

Introduction

The role of exosomes as a tool in research and clinical applications continues to grow. An increasing number of new research articles are being published using exosomes in various unique facets of biomedical research, including drug delivery and diagnostics. Exosomes are ubiquitous, secreted, membrane-derived vesicles that play a critical role in cellular communication through the transportation of biological macromolecules, such as RNA and proteins.[1] Ranging from 40 to 130 nm in diameter, exosomes have the same lipid bilayer composition as the excreting cell, including the extracellular proteins and polysaccharides.[1-2] Internal contents of exosomes also vary depending on secreting host cell signals. Unfortunately, much remains unknown about the cellular mechanisms prompting and determining the exosome's encapsulation contents. Recently, exosomes have gained attention not only for their small size and natural, cell-like morphology but also for being universally present in bodily fluids regardless of species.[1] Although it is tempting to equate exosomes with nanoparticles due to their small size and ability to transport contents, the ability of exosomes to interact with cell membranes without eliciting an immune response is a distinct advantage.[1] The innate ability of exosomes to circumvent many of the natural immune system clearance pathways, due to their cell-like properties, may overcome one of the greatest barriers to the clinical translation of nanoparticles.

Due to their unique physical features, exosomes are becoming prevalent as a drug delivery tool in preclinical research and clinical trials for both cancer and arthritis. The ability for exosomes to transport hydrophobic, hydrophilic and large biomolecules allows a broad spectrum of treatment (e.g., genetic materials, proteins or small molecules) to quickly reach a desired tissue.[3] While most previous efforts have focused on the utility of exosomes in drug delivery, they also hold great potential for diagnostics as well.[3] The ability to treat complex pathologies is rapidly expanding and revealing not only the importance of early disease diagnosis but also a gap in the available tools to do so. Exosomes may fill that gap, having the ability to detect either through molecular and/or visual recognition. While patient derived exosomes are no longer thought to be a viable delivery strategy due to incomplete characterization of their transported cargo, which may potentially confer pathology, bovine and healthy cell culture derived exosomes are becoming more popular. The same reasons that argue against using patient derived exosomes for drug delivery, make them excellent for diagnostics. Exosome cargo can be analyzed to examine specific markers for disease states leading to faster and earlier diagnosis. [4-6] Identification of disease state biomarkers combined with the exosomes ability to carry a defined cargo, may bridge the gap between delivery and diagnostics.

Despite intense efforts in nanoparticle enabled biomedical research [7-8], clinical translation of nanoparticles has lagged behind, leaving their promise largely unfulfilled. [9] Nevertheless, many lessons can be learned from both their successes and failures. Nanoparticles – particles with diameters less than 200 nm – have gained attention for their ability to enhance the delivery of drugs with active or passive targeting mechanisms.[1, 10] The nanoparticles' ability to target tissues and effectively deliver drugs has been successful in preclinical trials, specifically those in cancer therapy. [3, 11-14] While surprisingly few of these nanoparticle drug delivery studies have

transitioned to broad clinical adoptions, nanoparticles have been more successful as a diagnostic/visualization tool, with their prevalence continuing to increase.[15-16] Previously, we have performed detailed acoustic characterizations of echogenic nanoparticles (i.e., liposomes and polymersomes) by varying their properties and shell chemistry.[17-21] Tracing diagnostic nanoparticles has revealed rapid nanoparticle clearance rates and adverse immune responses as the point of failure for many clinical trials.[22] However, unlike synthetic nanoparticles, many exosomes do not face these same issues potentially making them a more viable option for clinical drug delivery and diagnostics.[3, 23] Combining the advantages of naturally derived exosomes to make the particle echogenic is a particularly exciting approach to demonstrate the utility of exosomes in biomedical research. [17-18, 24-27]

Ultrasound is known as a safe, inexpensive, and real-time imaging modality. However, it suffers from low contrast.[28-29] The low contrast is alleviated with the addition of intravenously injectable microbubble-based ultrasound contrast agents (UCA).[30] The Food and Drug Administration (FDA) approved their use in echocardiography as a diagnostic tool for myocardial microperfusion in 2001 and in liver imaging in 2016.[31-33] The UCAs range between 1-5 μm in diameter and have a lipid, polymer, or protein shell with a perfluorocarbon gas core for enhanced stability.[34-36] Due to the compressible nature of the gas core, UCAs oscillate under ultrasound excitation generating linear and nonlinear (sub- and higher harmonic) responses that can improve the enhancement of ultrasound image contrast.[37-41] UCA oscillations also cause acoustic microstreaming flows surrounding the microbubble leading to enhanced mixing and shear stress experienced by nearby cell membranes.[31, 42] The shear stress is believed to increase membrane permeability or excite mechanosensitive ion channels, potentially allowing for therapeutic drug delivery to the cells.[43-44] However, UCAs are restricted to the vascular system as

they are too large to permeate outside of the blood vessels. For extravascular imaging and ultrasound medicated therapeutic applications, researchers have sought smaller, nanosized echogenic particles.[45-46] Here, we report a first ever study of exosomes, made echogenic, for imaging applications.

To quantify and understand the acoustic behaviors of the engineered, echogenic exosomes, their echogenicity was investigated by directly measuring their linear and nonlinear scatter responses in a customized *in vitro* setup and by imaging with a commercial scanner *in vivo*. Overall, the ability to make exosomes ultrasound responsive shows excellent promise for contrast enhanced ultrasound imaging and concurrent drug delivery. In the current study, bovine milk derived exosomes, which offer the added advantages of large-scale production along with strong biocompatibility and minimal immunogenic response, were made echogenic. Our development of echogenic exosomes has potentials as a diagnostic and drug delivery separately and in combination. [47] [48]

Materials and Methods

Exosome Isolation

Raw bovine milk was collected from the North Dakota State University Dairy Farm in 1 L quantities. If the raw bovine milk was not used the same day of pickup, it was stored at 4°C for up to 4 days. Due to the fat content of the milk, serial centrifugation was used to isolate exosomes. Raw bovine milk was placed in six 50 mL centrifuge tubes with 45 mL in each and spun for 20 min a 3,500g in a VWR Clinical 200 Centrifuge. Following the initial 20-minute spin, white fat deposits formed on the wall of the centrifuge tubes and the milk was passed through a cheesecloth to remove fat. A Beckman Coulter Optima LE-80K Ultracentrifuge was used with a 28W rotor for the remainder of centrifugation steps. After being passed through the

cheesecloth, the milk was collected and placed with equal weight into six 38.5 mL thin wall, Ultra-Clear tubes (Beckman Coulter, CA, USA.). Tubes were spun at 12,950g at 4°C for 30 minutes. The milk was removed from the tubes and was filtered through cheesecloth to remove more fat. Once the milk was filtered, it was placed in 4 new ultracentrifuge tubes and spun at 98,500g for 70 minutes at 4°C. Three layers then formed in each tube and the middle layer was collected. The middle layer was then placed in two fresh ultracentrifuge tubes and spun at 135,030g for 1 hour and 45 min at 4°C. Subsequently, the liquid was removed from the ultracentrifuge tubes, taking care not to disturb the pellet. The pellet was then resuspended in 400 μL of phosphate buffer solution (1X Dulbecco's PBS, VWR). Both tubes of PBS suspended exosomes were combined leaving a clear film at the bottom of the tube. A 0.45 μm filter was pre-wet using PBS. Then the exosomes were passed through the filter into an Eppendorf tube. The first three drops of PBS in the syringe filter were discarded after the exosomes were filtered through using a 1 mL syringe using two separate filters. To ensure all exosomes were retrieved from the filter, more PBS was passed through the filter until the first three drops come out and the remainder was discarded. Dynamic light scattering was performed to hydrodynamic diameters of the exosomes. Parafilm was placed around the outside of the Eppendorf tube and was kept at -80°C until used.

Echogenic Exosomes Preparation

Exosomes were thawed at room temperature. [49] Once the exosomes reached room temperature, 210 μL of exosomes were added dropwise to 1.5 mL of 320 mM mannitol-HEPES buffer (pH 7.4) while stirring. After 10 minutes of stirring, pressurized filtered ambient air was bubbled in for 45 minutes. Following evaporation, the solution was sonicated for 60 minutes ensuring that the temperature does not exceed 30°C. Sonication (Symphony Sonicator, 117V, 60

Hz, VWR, USA) is a variable that was tested to determine its necessity in the protocol. Next, the sample was frozen in -80°C for 1 day after which the sample was thawed in a 65°C water bath. Three freeze-thaw cycles occurred each separated by 1 day. Following the freeze-thaw cycles, the sample was lyophilized for four days to prepare a powder.

Ultrasound Imaging and Processing

Echogenic exosomes were reconstituted in BSA-HEPES solution. The BSA-HEPES solution was made using 2.5 g of BSA in 500 mL of 10 mM HEPES buffer at pH 7.4. *In vitro* studies used a concentration of 5 mg/mL echogenic exosomes in BSA-HEPES. *In vivo* studies used 58 mg/mL and 150 mg/mL of echogenic exosomes. Vevo 3100 Imaging System (Fujifilm Visual Sonics, Toronto, ON, Canada) was used. Transducer heads with frequencies of 40 and 21 MHz were utilized for *in vitro,* and only 40 MHz was utilized for *in vivo* imaging. For frequencies 4-15 MHz, the ultrasound scan properties were set at high (H) frequency, level 51 2D Gain, level 60 Dynamic Range (DR), 3 cm scan depth, and 22 Hz frame rate using a 15L4 transducer head.

Atomic Force Microscopy (AFM)

The samples of echogenic exosomes were prepared by incubating 10 µL of each solution on silicon substrates (University Wafer) for 10 minutes in a sealed compartment to prevent evaporation at room temperature. The samples were then washed with de-ionized water (Millipore) and dried under purified nitrogen flow. The imaging measurements were performed using a commercial atomic force microscope (NT-MDT NTEGRA AFM). The samples were imaged under ambient conditions in semi-contact mode using an AFM tip with a resonant frequency of 190 kHz (Budget sensors).

Size and Concentration

The dry powder of echogenic exosomes was reconstituted as 1 mg/mL for size distribution and concentration determination. All measurements were performed using qNano Gold with nanopore size NP150 (Izon Science™, Medford, MA). The sample size and concentration were calibrated during each measurement using the manufacturer's calibrations particles of carboxylated polystyrene beads (CPC100, average diameter: 110 nm, concentration: 1.1 x 10^{13} particles/mL). The samples were repeated at least 3 times on 3 different batches. Dynamic light scattering (DLS) was also performed on exosomes. The exosomes were isolated freshly for DLS. The samples were repeated at least 3 times on 3 different batches.

Western Blot of Exosomes

Exosomes were freshly isolated with storage at -80^{o} C for three days prior to lysing for analysis of exosomal membrane protein markers. These markers were assessed using ExoAb Antibody's CD63 and CD9 with their respective secondary antibodies (SBI System Biosciences, Palo Alto, CA) according to the manufacturer's protocol. Immuno-positive bands were detected using an ECL Plus kit (Invitrogen).

Linear and Nonlinear Acoustic Characterization

A setup similar to what was used previously [17, 24, 50] was employed to characterize the acoustic scattering behavior of the echogenic exosomes (**Figure 2.1**). Briefly, two spherically focused transducers positioned perpendicular to each other were confocally aligned in a 125 mL polycarbonate tank. The transmitting transducer had a center frequency of 5 MHz (Olympus, Waltham, MA, -6 dB bandwidth: 2.95-6.77 MHz, focal distance 1.2 in) with a pressure amplitude of 500 kPa, and receiving frequency of either 2.25 MHz (Olympus, Waltham, MA, -6 dB bandwidth 1.48-2.90 MHz, focal distance 1.2 in), 5 MHz (Olympus, Waltham, MA, -6 dB

bandwidth: 2.95-6.77 MHz,, focal distance 1.2 in), or 10 MHz (Olympus, Waltham, MA, -6 dB bandwidth 6.96-13.16 MHz, focal distance 1.2 in). All transducers were calibrated with a needle hydrophone (PZT-Z44-0400, Onda Corporation, CA, USA). A smaller, triangular 3D printed chamber of acrylonitrile butadiene styrene (ABS) with acoustically transparent windows was placed in the chamber, so the focus of the two transducers overlaps at the center of the chamber. The dry powder of the echogenic exosomes at a concentration of 40 μg/mL was reconstituted into either 10 mM HEPES buffer with or without 0.5% (w/v) BSA or only 0.5% (w/v) BSA. Then, 8 mL of the reconstituted exosomes in respective solutions were placed inside the triangular chamber, and the surrounding volume was filled with deionized water. A function generator (Model AFG 3251, Tektronix, Beaverton, OR, USA) amplified by a 55-dB power amplifier (Model A-300; ENI, Rochester, NY, USA) excited the transmitting transducer to produce a 32-cycle sinusoidal pulse at 500 kPa amplitude, 5 MHz frequency and pulse repetition frequency of 100 Hz. The scattered response was obtained by a pulsar/receiver (Panametrics 5800, Waltham, MA, 6qUSA) with 20 dB gain through a receiving transducer. Signals Signals were averaged over 64 sequences to improve the signal to noise ratio.

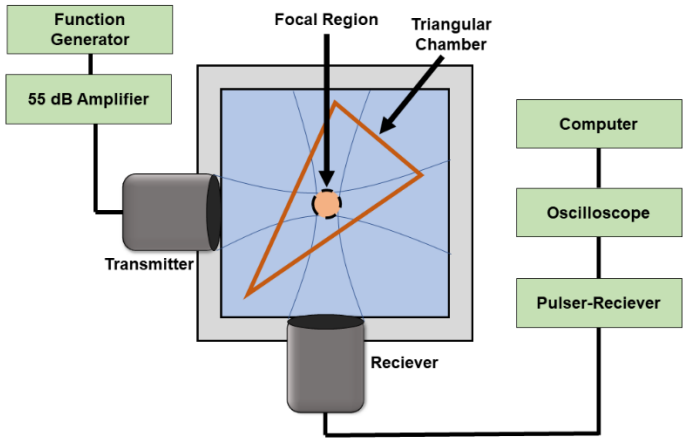

Figure 2.1. The experimental setup for measuring the linear and nonlinear scattering response of the echogenic exosomes.

The data was acquired for 50 replicates using a custom MATLAB program (Mathworks, Natick, MA). A Fast Fourier Transform (FFT) was performed on the signals after the acquisition. The signal intensity was evaluated as an enhancement over control (signal without exosomes) to eliminate the effect of the scattering from the chamber. The linear scattering of the exosomes was assessed at fundamental (5 MHz) component. For nonlinear behavior, the subharmonic (2.25 MHz) and second harmonic (10 MHz) signal enhancements were investigated. The acoustic response of the exosomes was evaluated across four batches of exosomes for ensuring repeatability across batches. To assess the stability of the exosomes under constant ultrasound exposure, the enhancement was monitored for 180 seconds. The experiment was run and compared in sequence with polymersomes of the same concentration for comparison.

Mannitol Concentration Variation in Preparation Protocol

To investigate the role of mannitol [51] in the echogenicity, exosomes were prepared following the same protocol but with varying amounts of mannitol in the HEPES buffer 50, 100, 150, 200, 250, 300, 320, 350 and 400 mM. Evaporation, sonication, and freeze-thaw cycles and freeze-drying were performed as before.

Injection into the Synovial Fluid in Sprague Dawley Rats

Echogenic exosomes were injected into the synovial fluid of euthanized Sprague Dawley Rats. The exosomes were resuspended from powder in BSA-HEPES buffer for a concentration of 58 mg/mL. Then 100 uL of the solutions was injected into the synovial space. The injections were completed on 4 different knees in 2 different rats. The Vevo 3100 imaging system was used with 40 MHz frequency transducer head. Since the synovial space in rats is small, the area of interested was easy to locate in before and after injection of the exosomes.

Tail Vein Injection into NOD Scid Gamma Mouse (NSG) Mice

Echogenic exosomes were injected into the tail vein of an NSG mouse (IACUC Protocol Number #A18037). The exosomes were resuspended from powder in BSA-HEPES buffer for a concentration of 150 mg/mL. A 100 uL bolus was injected into the tail vein 3 different times. The Vevo 3100 imaging system was used with a 40 MHz pixel quantification. The transducer head was fixed throughout the protocol to insure the area being imaged remained constant. In an ultrasound image obtained by the scanner, areas of interest were selected, maintaining approximately the same area throughout the images. Histograms were created of the pixel counts in the images. Counts were compared to control images and normalized by the area. Analysis of ultrasound images was done using the Fuji image processing package[52].

Results

Echogenicity

In this article, we assessed the echogenicity of the specially prepared exosomes using three different imaging techniques. Using the Vevo 3100 Imaging System, we imaged the echogenic exosomes in a BSA-HEPES buffer and compared it to the control image of only the BSA-HEPES buffer (**Figure 2.2**). The average brightness of the image was used to evaluate the echogenicity of the particles. In the 4-15 MHz image, the average brightness was 23.1% brighter with exosomes (**Figure 2.2B**) compared to the control (**Figure 2.2A**). The corresponding increase at 21 MHz (**Figure 2.2C-D**) and 40 MHz (**Figures 2.2E-F**) were more than 800% and 28.9% respectively.

Table 2.1. The average size of exosomes with and without sonication as measured by DLS, AFM, and qNano. PDI is polydispersity index of exosomes.

	DLS	PDI of DLS	AFM	qNano
With sonication	101 ± 14 nm	0.43 ± 0.143	60 ± 20 nm	95 ± 26 nm
Without sonication	126 ± 14 nm	0.50 ± 0.13	55 ± 15 nm	107 ± 17 nm

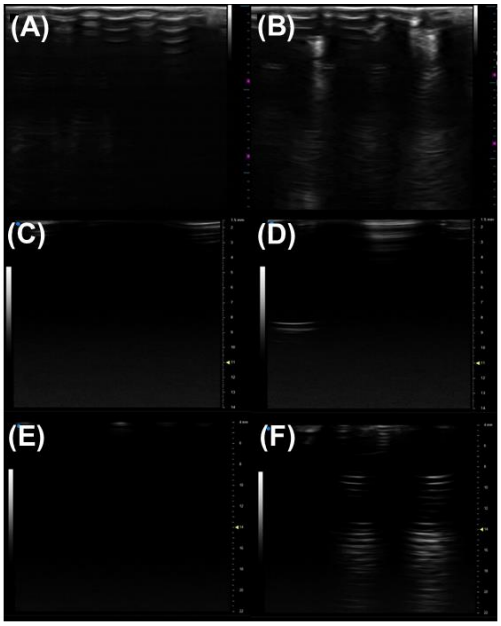

Figure 2.2. Ultrasound images of echogenic exosomes in a black 96 well plate, with 250 µL of 5 mg/mL echogenic exosomes placed in the plate and read with different transducer heads. Images with 4-15 MHz transducer (100% Power, 22 fps, 51 dB gain, 60 dB dynamic range) at a depth of 3 cm: (A) BSA-HEPES control and (B) echogenic exosomes. Images with 40 MHz transducers (100% power, 65 fps frame rate, 24 dB gain, depth 10 mm and width 12 mm, 70 dB dynamic range): (C) BSA-HEPES control and (D) echogenic exosomes. Images with 21 MHz transducers (100% power, 34 fps frame rate, 21 dB gain, depth 22 mm and width 21 mm, 60 dB dynamic range for both images): (E) BSA- HEPES Control and (F) echogenic exosomes. Brightness and contrast for all images were at 50.

Size Morphology and Concentration

The size distribution was measured by qNano using a tunable resistive pulse sensing principle (**Figure 2.3A**). AFM images of the echogenic exosomes can be seen in **Figures 2.3(B-D**) indicating as expected an approximately spherical morphology. A summary of the average

sizes measured by different methods can be seen in **Table 1**. The average size of the exosomes was found to be 101 ± 14 nm (DLS) and 96 ± 26 nm (qNano) when the solution was sonicated during the preparation. In absence of sonication, the exosomes were slightly larger, with an average diameter of 126 ± 14 nm (DLS) and 107 ± 17 nm (qNano). The concentration of the dry powder was measured to be 4.1 ± 1.8 x 10^9 particles/mg when reconstituted at a concentration of 1 mg/mL.

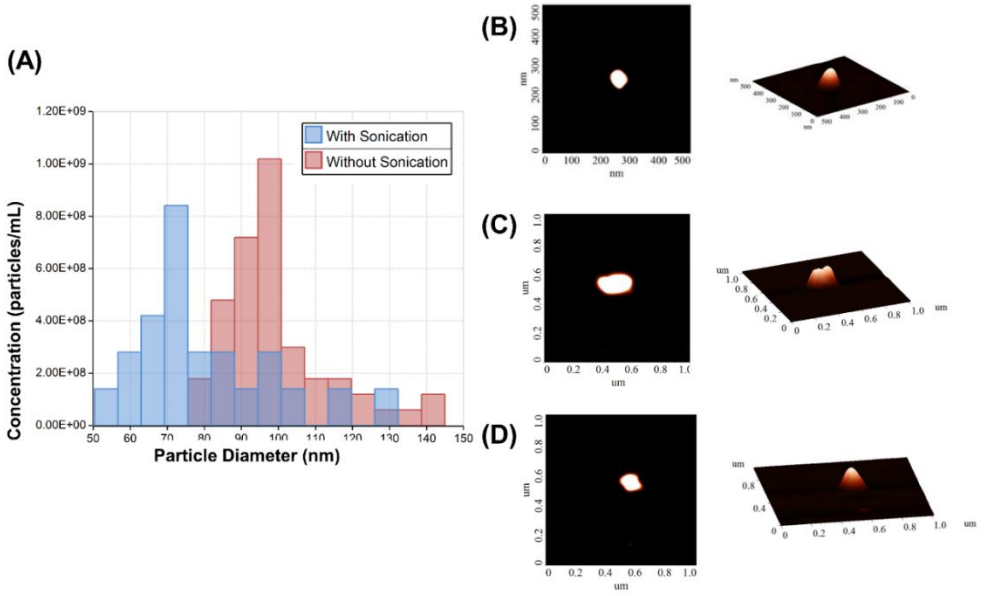

Figure 2.3. (A) The size distribution of the echogenic exosomes as measured by the qNano (with and without sonication). Atomic force microscopy images (B-D) of echogenic exosomes. These exosomes range between 60 to 90 nm in diameter after they undergo the protocol to make them echogenic

Western Blot of Exosomes

Western blot analysis of exosomes indicated positive for markers for CD63 and CD9 (**Figure 2.4**) ascertaining that the nanovesicles isolated from bovine milk are indeed exosomes.

Figure 2.4. Western blot analysis of CD63 and CD9.

Preparation and Reconstitution Protocol Optimization

The echogenicity of specially prepared echogenic exosomes reconstituted in four different media—PBS, HEPES, BSA, and HEPES-BSA—and with and without sonication during preparation was investigated. In the presence of BSA, we found noticeable effects of echogenic exosomes. We investigated effects of different media and sonication during preparation on exosome echogenicity by directly measuring scattered response in a customized *in vitro* setup. Both linear and nonlinear scattered signals were recorded when exosomes were exposed to a 5 MHz ultrasound excitation. The enhancement of the scattered fundamental response was highest when the exosomes were reconstituted in 10 mM HEPES + 0.5% BSA —11.4 ± 6.3 dB with sonication during preparation and 11.04 ± 6.6 dB without sonication (**Figure 2.5A**). The signals were significantly higher than when the powder was reconstituted in either 10 mM HEPES or 0.5% BSA by themselves ($p < 0.0001$). When the powder was reconstituted in only 0.5% BSA, the enhancement was also statistically higher than in 10 mM HEPES alone ($p < 0.001$) reaching 8.6 ± 4.4 dB with sonication and 6.8 ± 4.1 dB without sonication. For all solutions, and as we will see below for both linear and nonlinear scattering, there was no significant difference in enhancement with and without sonication during preparation.

Similar to the fundamental response, the enhancement in subharmonic response shown in **Figure 2.5B** was also the highest when the exosomes were reconstituted with 10 mM HEPES + 0.5% BSA ($p < 0.001$). The subharmonic enhancement reached 8.6 ± 6.6 dB with sonication and 8.3 ± 5.8 dB without sonication when reconstituted with 10 mM HEPES + 0.5% BSA. There was no statistical difference between the scattered subharmonic responses when the powder was reconstituted in 10 mM HEPES or 0.5% BSA by themselves.

The second harmonic signal enhancement is shown in **Figure 2.5C**. The scattered signal was similar ($p=0.9959$) when the powder was reconstituted in 10 mM HEPES + 0.5% BSA and 0.5% BSA when the exosomes were reconstituted with 10 mM HEPES + 0.5% BSA, the enhancement of the second harmonic scattered signal was 3.4 ± 2.9 dB with sonication and 3.7 ± 3.0 dB without sonication. The second harmonic scattered signal was 3.3 ± 2.1 dB with sonication and 3.9 ± 2.6 dB without sonication when reconstituted with 0.5% BSA. However, the signal enhancement reduced in the absence of BSA ($p < 0.001$).

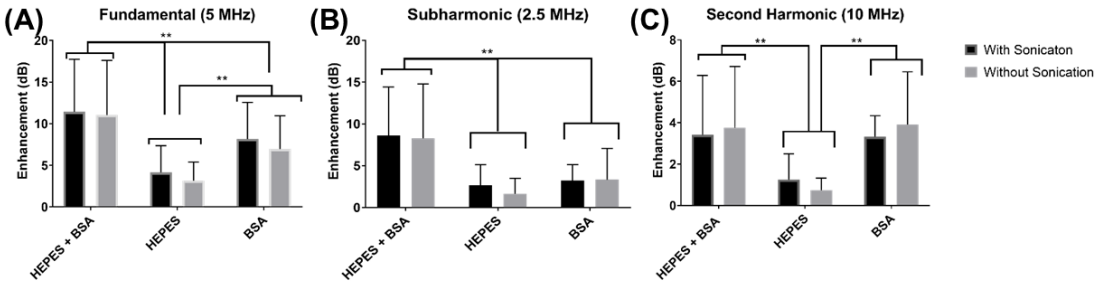

Figure 2.5. Scattered enhancements of the echogenic exosome (prepared with and without sonication) solutions for 3 different reconstitution solutions (HEPES + BSA, HEPES, BSA) when exposed to 5 MHz excitation frequencies. Enhancements when compared to control (DI Water) in (A) fundamental, (B) subharmonic and (C) second harmonic. (** $p<0.001$) (500 kPa pressure amplitude, PRF 100 Hz, 32 cycles)

Varying Concentration of Mannitol

To understand the role that the presence of mannitol during preparation plays in the echogenicity of the exosomes, mannitol concentration was varied. Different batches prepared

with different concentrations of mannitol were imaged with the Vevo 3100 Imaging System at 40 MHz (**Figure 2.6A**). There is significant echo when the mannitol concentration rose above 300mM. We also measure the scattered fundamental response from these batches at 5 MHz (**Figure 2.6B**) using our customized scattering setup. Here also the scattered signal increased as the mannitol concentration increased. Strong backscattered signal was seen only above 150 mM of mannitol.

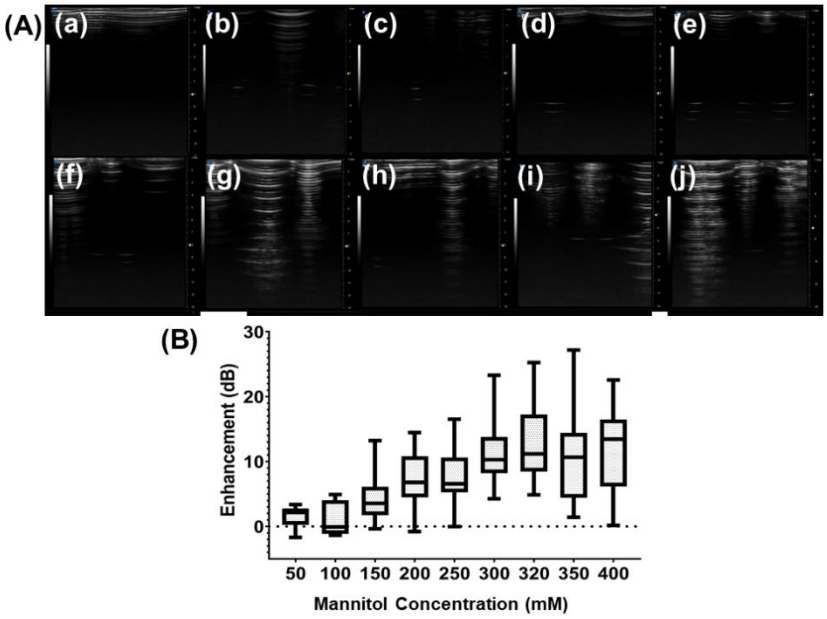

Figure 2.6. (A) 40 MHz ultrasound images of echogenic exosomes varying concentrations of Mannitol during preparation. (a) Only BSA-HEPES (control), (b) 50 mM, (c) 100 mM, (d) 150 mM, (e) 200 mM, (f) 250 mM, (g) 300 mM, (h) 320 mM, (i) 350 mM, and (j) 400 mM of mannitol. Ultrasound setting is the same for all images taken with Vevo 3100 Imaging System (transmitter frequency 40 MHz, power 100%, frame rate 68 fps, 24 bD, 14 mm depth, 12.08 mm width, 65 dB dynamic range, brightness 50 and contrast 50). (B) Enhancement in fundamental response from echogenic exosomes prepared with varying concentration of mannitol during freeze-dry cycles when exposed to 5 MHz excitation (500 kPa pressure amplitude, PRF 100 Hz, 32 cycles)

Stability Under Ultrasound

The fundamental signal enhancement due to the echogenic exosomes prepared with or without sonication as well as polymersomes are investigated as a function of time while being

exposed to ultrasound excitation (**Figure 2.7**). The enhancement decreased with time. However, the enhancement remains significant even after 3 minutes of exposure similar to what was observed for polymersomes by Xia et al.[17] Presence of sonication during preparation didn't change the dynamics.

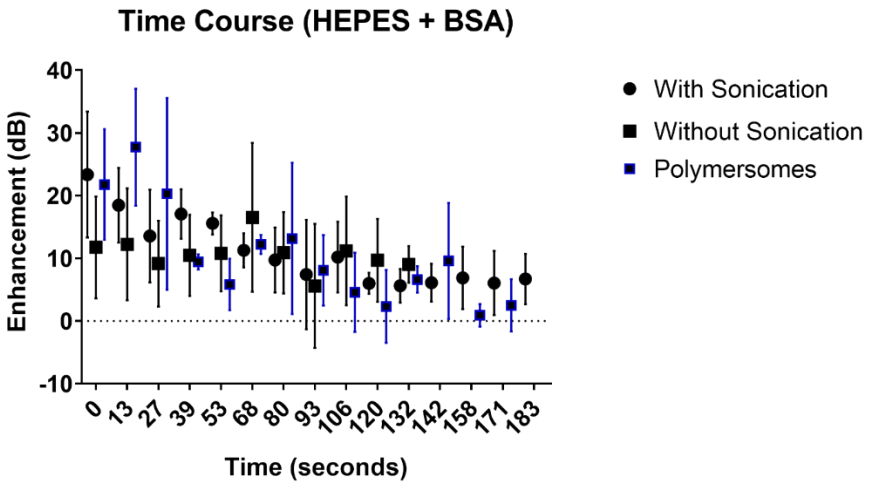

Figure 2.7. The fundamental enhancement of the echogenic exosomes (with and without sonication) reconstituted with 10 mM HEPES with 0.5% BSA as compared to echogenic polymersomes of the same concentration over 3 minutes of ultrasound exposure (excitation frequency 5 MHz, 500 kPa pressure amplitude, PRF 100 Hz, 32 cycles)

In vivo Imaging of Echogenic Exosomes

Echogenic exosomes were injected into the synovial space of a Sprague Dawley rat (**Figure 2.8**). Injecting echogenic exosomes (**Figure 2.8B**) results in a brighter image when compared to control (**Figure 2.8A**). It is further validated by the quantification of pixel brightness (**Figure 2.8C**) showing a 37.2% increase in brightness of the images upon the injection of the exosomes. The exosomes were also injected into the tail vein of an NSG mouse (**Figure 2.9**). The images of the mouse kidney were found to be enhanced by the addition of exosomes (**Figure 2.9B**) when compared to before the exosomes were injected (**Figure 2.9A**) as

also shown by pixel histogram (**Figure 2.9C**). There was more than 3-fold increase in brightness when the echogenic exosomes were injected into the vein.

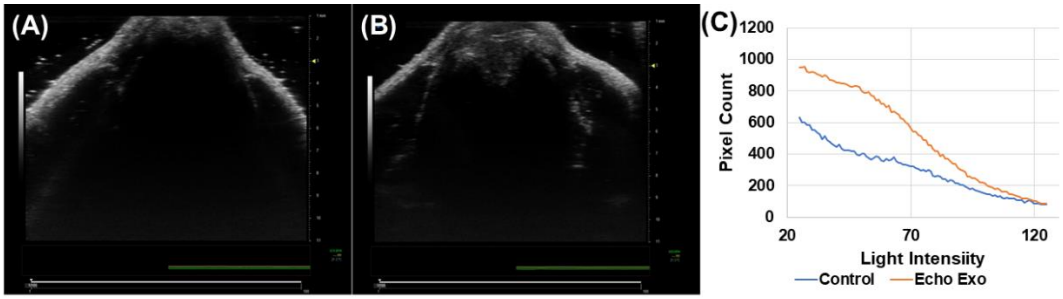

Figure 2.8. Ultrasound images (A) before and (B) after injection of echogenic exosomes into the synovial space of a Sprague Dawley rat. Images were taken with a Vevo 3100 Imaging System and 40 MHz transducer head (at 100% power, 76 fps frame rate, 25 dB gain, depth 11.00 mm and width 14.08 mm, 70 dB dynamic range, brightness 50 and contrast 50 for both images). (C) Pixel counts from (A) and (B) echogenic exosomes before (blue) and after (orange) injection into synovial space. Pixel count was normalized by the area for all graphs.

Figure 2.9. Ultrasound images of mouse kidney (A) before and (B) after injection of echogenic exosomes (100 uL of 58 mg/mL) into the tail vein of NSG mouse using Vevo 3100 Imaging System and 40 MHz transducer head (at 100% power, 70 fps frame rate, 25 dB gain, depth 10 mm and width 18 mm, 70 dB dynamic range, brightness 50 and contrast 50 for both images). (C) Pixel count differences of light intensity between echogenic exosomes before (blue) and after (red) tail vein injection. Pixel count was normalized by the area for the graph.

Discussion

Exosomes are naturally secreted bilayer vesicles known to play critical roles in inter-cellular communications and transport. Utilizing bovine milk exosomes provides unique advantages and has been shown to be effective and non-toxic within *in vitro* and *in vivo* environments. Here they have been isolated from bovine milk and then made to undergo a

specialized protocol of repeated freeze-thaw cycles followed by a freeze-drying process in the presence of mannitol that made them echogenic. The procedure was motivated by our as well as others' studies that indicated that mannitol plays a crucial role during the preparation of echogenic liposomes and polymersomes encapsulating gaseous cores that render such vesicles echogenic. [24, 51, 53] The echogenicity of the specially prepared exosomes were investigated using commercial ultrasound scanner both *in vitro* and *in vivo*. We also measure their scattered responses in a customized setup. This is the first ever report of echogenicity of exosomes offering potentials for their concurrent ultrasound imaging and drug delivery capabilities.

There was a noticeable difference in brightness between the ultrasound scanner images of echogenic exosomes and the control images at three different frequencies (**Figure 2.2**). The average brightness in all three imaging environments demonstrate that the exosomes became responsive to ultrasound after undergoing the specialized protocol of repeated freeze-thaw and freeze-drying in presence of mannitol.

After the exosomes underwent the preparation protocol, the size and the concentration of exosomes in the resulting powder were quantified using DLS, AFM, and qNano. The measured sizes lie within the expected range of 40-130 nm. The exosomes did not appear to be destroyed through the freeze-drying procedure, and $4.1 \pm 1.8 \times 10^9$ particles/mg were present in the freeze-dried powder. When the particles were measured by AFM, the shapes appeared to have remained roughly spherical with a slightly smaller diameter of roughly 60 nm (**Figure 2.3**). The smaller diameter in AFM observation could have resulted from drying of the sample for AFM imaging. **Figure 2.3A** indicates that with sonication, the size distribution shifts to the left resulting is slightly reduced average size in **Table 2.1**. But the similarity in average size with and without sonication indicates very little destruction of exosomes due to sonication. Echogenic exosomes

are slightly smaller than echogenic liposomes (125-185 nm) [24] and much smaller than echogenic polymersomes (400-450 nm).[17] The smaller size and natural morphology make echogenic exosomes an ideal candidate for drug delivery without immune responses but with added capabilities due to its responsiveness to ultrasound.[1]

Ultrasound contrast agents are known to generate both linear and nonlinear response to ultrasound excitation.[17, 24, 37-38, 45, 54] We investigated the ability of the echogenic exosomes reconstituted in three different media—HEPES, BSA, HEPES+BSA—to generate the linear and nonlinear responses (**Figure 2.5**). Echogenic exosomes show strong sub- and second-harmonic scattered responses. The strong nonlinear responses offer possibilities for their applications in nonlinear imaging modalities with better signal-to-tissue ratios [55-56]. For all reconstitution parameters and at all receiving frequencies, there was no statistical difference between the signal enhancement of exosomes prepared with and without sonication. This could be due to the similarity in size between these echogenic exosomes.

Echogenicity of the exosomes varied with variation in reconstitution media. The linear and nonlinear signal enhancements were statistically higher in cases where BSA was added to the solution compared to being reconstituted in HEPES alone (**Figure 2.5**). This was also borne out by ultrasound scanner images (40 MHz transducer) of exosomes prepared in these three different media (data not shown). The addition of BSA appears to be critical to the scattering behavior of the exosomes. Kumar et al. while exploring the role of freeze-dried mannitol on the echogenicity of liposomes and polymersomes also found strong echogenicity of freeze-dried mannitol powder by itself in DI water, which is further enhanced by addition of BSA.[57] It was hypothesized that BSA acts like a surfactant to the microbubbles stabilizing them and allowing

them to remain in the solution longer. The present study seems to indicate a similar stabilizing role of BSA for the air pockets created in association with exosomes.

As noted before, mannitol has been assumed to play a critical role in ensuring echogenicity in specially prepared liposomes and polymersomes [24, 53, 58-61]. We investigated the echogenicity of specially modified exosomes varying amount of mannitol during the freeze-dry process, ranging from 50 to 400 mM. Previously, we have demonstrated that the crystalline nature of mannitol facilitates bubble generation during dissolution, [57] and we believe that mannitol is the key to the echogenicity of the echogenic liposomes, polymersomes, and exosomes. Similar to the findings of Paul et al. [24] for echogenic liposomes, ultrasound images of echogenic exosomes freeze dried in the presence of different concentrations of mannitol (**Figures 2.6A**) and their enhancement (**Figure 2.6B**) showed echogenicity when freeze-drying was performed with mannitol at a concentration above 150 mM.

We chose freeze drying in the presence of 320 mM of mannitol and reconstitution in BSA-HEPES with sonication as our preparation protocol of choice. Exosomes thus prepared were investigated for their stability and *in vivo* imaging potential (**Figure 2.7**). The stability of the echogenic exosomes appears to be similar to echogenic polymersomes[13] —echogenic even after 3 minutes of constant ultrasound exposure at a 5 MHz excitation frequency.

To explore their *in vivo* imaging potential, echogenic exosomes were injected in the synovial fluid of Sprague Dawley rats and into the tail vein of NSG mice and imaged at 40 MHz. In both cases, the image pixel brightness clearly showed enhancements after echogenic exosome injection (**Figures 2.8 and 2.9**). The enhancements were 37.2% in case of the synovial fluid of the rats and 300% for mice.

Exosomes - specially modified here by a freeze-drying process in presence of mannitol - have demonstrated significant echogenicity in ultrasound scanner as well as in customized *in vitro* scattering setup. Liposomes and polymersomes have previously been shown to be echogenic when prepared by freeze-drying in presence of mannitol. Small air-pockets were hypothesized to be situated in the bilayer, outside or inside such echogenic vesicles. [24, 53, 58] Recently, Shekhar et al. evaluated the nature of the echogenic behaviors of liposomes using differential interference contrast microcopy (DIC).[62] Their DIC images showed micrometer sized bubbles encapsulated inside liposome, but the typical size of the observable liposomes in the DIC images were far larger; the number weighted and volume-weighted diameters of these vesicles were 1.35 μm and 8.23 μm respectively. [62] The exosomes studied here, unlike previously studied echogenic liposomes and the polymersomes, are preformed vesicles, but they underwent the same the freeze-drying procedure in presence of mannitol that was also part of the preparation protocol for echogenic liposomes and polymersomes. [18, 24, 28, 53, 58, 63-65] However, unlike echogenic liposomes carrying encapsulated microbubble inside studied by Shekhar et al [62] the echogenic exosomes are much smaller in size—50-150nm. The smaller nanometer size of the exosomes indicates similarity to nanocups and other such nanoparticles investigated by Kwan et al.[66] which spontaneously grow surface trapped bubbles upon ultrasound excitation due to their geometry and surface properties. However, further investigation is needed for elucidating the origin of the echogenicity of these nanoparticles.

While the exact location of the bubble remains uncertain for the application of the exosomes, the results here also imply that the presence of mannitol during the freeze-drying process and reconstituting the freeze-dried powder in solutions containing BSA are critical for creating and maintaining echogenic behavior or the exosomes. [62, 66] These results indicate that

echogenic exosomes, when prepared following the specialized protocol described here, hold promising potential for use in contrast ultrasound imaging as well as drug delivery application when loaded with appropriate drugs.

Conclusion

Exosomes are naturally secreted nanoparticles—diameters 40-130 nm—that inherit the morphology and contain the biological information of the parent cell. Their structure and size make them ideal for potential drug delivery applications. Here for the first time, we proposed and demonstrated a procedure for rendering bovine milk-derived exosomes echogenic. The exosomes, that underwent the specialized protocol, were shown to be echogenic through an array of *in vitro* and *in vivo* investigation using a commercial ultrasound scanner as well as a customized setup. The acoustic behavior was found to be similar to that of echogenic liposomes or polymersomes. Previously, exosomes have shown success in being able to be functionalized and loaded with a variety of drugs.[2] The ability to make them echogenic, along with the large scale extractability from bovine milk, opens the possibility for their applications as ultrasound contrast agents or as ultrasound responsive drug delivery vehicles.

Acknowledgments

This research was supported by NIH grant 1 R01GM 114080 to S.M. and K.S. JO and KS would like to acknowledge the ARCS MWC Chapter, The McNichols Family Foundation, and The Myers family for their support.

Supporting Information

All mice were housed under standard housing conditions at the Animal Studies Core Facility of North Dakota State University (NDSU). All animal procedures were reviewed and

approved by the Institute of Animal Care and Use Committee at the NDSU, protocol number 17052.

Conflicts of Interest

The authors declare no conflicts of interest. The funders had no role in the design of this publication; in the collection, analyses, or interpretation of data; in the writing of the manuscript, or in the decision to publish the results.

References

1. Kim MS, Haney MJ, Zhao Y, Mahajan V, Deygen I, Klyachko NL, et al. Development of Exosome-encapsulated Paclitaxel to Overcome MDR in Cancer cells. Nanomedicine 2016;12:655–64. https://doi.org/10.1016/j.nano.2015.10.012.
2 Vlassov AV, Magdaleno S, Setterquist R, Conrad R. Exosomes: Current knowledge of their composition, biological functions, and diagnostic and therapeutic potentials. Biochimica et Biophysica Acta (BBA) - General Subjects 2012;1820:940–8. https://doi.org/10.1016/j.bbagen.2012.03.017.
3 Pullan, J. E.; Confeld, M. I.; Osborn, J. K.; Kim, J.; Sarkar, K.; Mallik, S., Exosomes as Drug Carriers for Cancer Therapy. Molecular Pharmaceutics 2019, 16 (5), 1789-1798.
4 Makler A, Asghar W. Exosomal biomarkers for cancer diagnosis and patient monitoring. Expert Review of Molecular Diagnostics 2020;0:1–14. https://doi.org/10.1080/14737159.2020.1731308.
5 Sun Z, Wang L, Wu S, Pan Y, Dong Y, Zhu S, et al. An Electrochemical Biosensor Designed by Using Zr-Based Metal–Organic Frameworks for the Detection of Glioblastoma-Derived Exosomes with Practical Application. Anal Chem 2020;92:3819–26. https://doi.org/10.1021/acs.analchem.9b05241.
6 Chiriacò MS, Bianco M, Nigro A, Primiceri E, Ferrara F, Romano A, et al. Lab-on-Chip for Exosomes and Microvesicles Detection and Characterization. Sensors (Basel) 2018;18:. https://doi.org/10.3390/s18103175.
7 Kumari A, Yadav SK, Yadav SC. Biodegradable polymeric nanoparticles based drug delivery systems. Colloids Surf B Biointerfaces 2010;75:1–18. https://doi.org/10.1016/j.colsurfb.2009.09.001.
8 Kundranda MN, Niu J. Albumin-bound paclitaxel in solid tumors: clinical development and future directions. Drug Des Devel Ther 2015;9:3767–77. https://doi.org/10.2147/DDDT.S88023.
9 Shreffler JW, Pullan JE, Dailey KM, Mallik S, Brooks AE. Overcoming Hurdles in Nanoparticle Clinical Translation: The Influence of Experimental Design and Surface Modification. Int J Mol Sci 2019;20:. https://doi.org/10.3390/ijms20236056.
10 Cho K, Wang X, Nie S, Chen Z (Georgia), Shin DM. Therapeutic Nanoparticles for Drug Delivery in Cancer. Clin Cancer Res 2008;14:1310–6. https://doi.org/10.1158/1078-0432.CCR-07-1441.

11 Tian Y, Li S, Song J, Ji T, Zhu M, Anderson GJ, et al. A doxorubicin delivery platform using engineered natural membrane vesicle exosomes for targeted tumor therapy. Biomaterials 2014;35:2383–90. https://doi.org/10.1016/j.biomaterials.2013.11.083.
12 di Magliano MP, Logsdon CD. Roles for KRAS in Pancreatic Tumor Development and Progression. Gastroenterology 2013;144:1220–9. https://doi.org/10.1053/j.gastro.2013.01.071.
13 Yang Y, Pan D, Luo K, Li L, Gu Z. Biodegradable and amphiphilic block copolymer-doxorubicin conjugate as polymeric nanoscale drug delivery vehicle for breast cancer therapy. Biomaterials 2013;34:8430–43. https://doi.org/10.1016/j.biomaterials.2013.07.037.
14 Aqil F, Munagala R, Jeyabalan J, Agrawal AK, Gupta R. Exosomes for the Enhanced Tissue Bioavailability and Efficacy of Curcumin. AAPS J 2017;19:1691–702. https://doi.org/10.1208/s12248-017-0154-9.
15 Théry C, Zitvogel L, Amigorena S. Exosomes: composition, biogenesis and function. Nature Reviews Immunology 2002;2:569–79. https://doi.org/10.1038/nri855.
16 Pan J, Ding M, Xu K, Yang C, Mao L-J. Exosomes in diagnosis and therapy of prostate cancer. Oncotarget 2017;8:97693–700. https://doi.org/10.18632/oncotarget.18532.
17 Xia L, Karandish F, Kumar KN, Froberg J, Kulkarni P, Gange KN, et al. Acoustic Characterization of Echogenic Polymersomes Prepared From Amphiphilic Block Copolymers. Ultrasound Med Biol 2018;44:447–57. https://doi.org/10.1016/j.ultrasmedbio.2017.10.011.
18 R N, Mk H, S P, A M, Ah A, Ks K, et al. Polymer-coated echogenic lipid nanoparticles with dual release triggers. Biomacromolecules 2013;14:841–53. https://doi.org/10.1021/bm301894z.
19 Kulkarni P, Haldar MK, Katti P, Dawes C, You S, Choi Y, et al. Hypoxia Responsive, Tumor Penetrating Lipid Nanoparticles for Delivery of Chemotherapeutics to Pancreatic Cancer Cell Spheroids. Bioconjug Chem 2016;27:1830–8. https://doi.org/10.1021/acs.bioconjchem.6b00241.
20 Anajafi T, Scott MD, You S, Yang X, Choi Y, Qian SY, et al. Acridine Orange Conjugated Polymersomes for Simultaneous Nuclear Delivery of Gemcitabine and Doxorubicin to Pancreatic Cancer Cells. Bioconjug Chem 2016;27:762–71. https://doi.org/10.1021/acs.bioconjchem.5b00694.
21 Anajafi T, Mallik S. Polymersome-based drug-delivery strategies for cancer therapeutics. Ther Deliv 2015;6:521–34. https://doi.org/10.4155/tde.14.125.
22 Kraft JC, Freeling JP, Wang Z, Ho RJY. Emerging research and clinical development trends of liposome and lipid nanoparticle drug delivery systems. J Pharm Sci 2014;103:29–52. https://doi.org/10.1002/jps.23773.
23 Bunggulawa EJ, Wang W, Yin T, Wang N, Durkan C, Wang Y, et al. Recent advancements in the use of exosomes as drug delivery systems. Journal of Nanobiotechnology 2018;16:81. https://doi.org/10.1186/s12951-018-0403-9.
24 Paul S, Russakow D, Nahire R, Nandy T, Ambre AH, Katti K, et al. In vitro measurement of attenuation and nonlinear scattering from Echogenic liposomes. Ultrasonics 2012;52:962–9. https://doi.org/10.1016/j.ultras.2012.03.007.
25 Kopechek JA, Abruzzo TM, Wang B, Chrzanowski SM, Smith DAB, Kee PH, et al. Ultrasound-mediated release of hydrophilic and lipophilic agents from echogenic

liposomes. J Ultrasound Med 2008;27:1597–606. https://doi.org/10.7863/jum.2008.27.11.1597.
26 Kopechek JA, Haworth KJ, Raymond JL, Douglas Mast T, Perrin SR, Klegerman ME, et al. Acoustic characterization of echogenic liposomes: Frequency-dependent attenuation and backscatter. The Journal of the Acoustical Society of America 2011;130:3472–81. https://doi.org/10.1121/1.3626124.
27 Alkan-Onyuksel, H.; Demos, S. M.; Lanza, G. M.; Vonesh, M. J.; Klegerman, M. E.; Kane, B. J.; Kuszak, J.; McPherson, D. D., Development of Inherently Echogenic Liposomes as an Ultrasonic Contrast Agent†. Journal of Pharmaceutical Sciences 1996, 85 (5), 486-490.
28 Paul S, Nahire R, Mallik S, Sarkar K. Encapsulated microbubbles and echogenic liposomes for contrast ultrasound imaging and targeted drug delivery. Comput Mech 2014;53:413–35. https://doi.org/10.1007/s00466-013-0962-4.
29 Goldberg BB, Raichlen JS, Forsberg F. Ultrasound Contrast Agents: Basic Principles and Clinical Applications. 1st edition. London: CRC Press; 2001.
30 de Jong N, Ten Cate FJ, Lancée CT, Roelandt JRTC, Bom N. Principles and recent developments in ultrasound contrast agents. Ultrasonics 1991;29:324–30. https://doi.org/10.1016/0041-624X(91)90030-C.
31 Bekeredjian R, Grayburn PA, Shohet RV. Use of ultrasound contrast agents for gene or drug delivery in cardiovascular medicine. J Am Coll Cardiol 2005;45:329–35. https://doi.org/10.1016/j.jacc.2004.08.067.
32 Paefgen V, Doleschel D, Kiessling F. Evolution of contrast agents for ultrasound imaging and ultrasound-mediated drug delivery. Front Pharmacol 2015;6:. https://doi.org/10.3389/fphar.2015.00197.
33 Durot I, Wilson SR, Willmann JK. Contrast-enhanced ultrasound of malignant liver lesions. Abdom Radiol (NY) 2018;43:819–47. https://doi.org/10.1007/s00261-017-1360-8.
34 Sarkar K, Katiyar A, Jain P. Growth and dissolution of an encapsulated contrast microbubble: effects of encapsulation permeability. Ultrasound Med Biol 2009;35:1385–96. https://doi.org/10.1016/j.ultrasmedbio.2009.04.010.
35 Katiyar A, Sarkar K, Jain P. Effects of encapsulation elasticity on the stability of an encapsulated microbubble. Journal of Colloid and Interface Science 2009;336:519–25. https://doi.org/10.1016/j.jcis.2009.05.019.
36 Katiyar A, Sarkar K. Stability Analysis of an Encapsulated Microbubble against Gas Diffusion. J Colloid Interface Sci 2010;343:42. https://doi.org/10.1016/j.jcis.2009.11.030.
37 Chatterjee D, Sarkar K. A Newtonian rheological model for the interface of microbubble contrast agents. Ultrasound Med Biol 2003;29:1749–57. https://doi.org/10.1016/s0301-5629(03)01051-2.
38 Sarkar K, Shi WT, Chatterjee D, Forsberg F. Characterization of ultrasound contrast microbubbles using in vitro experiments and viscous and viscoelastic interface models for encapsulation. The Journal of the Acoustical Society of America 2005;118:539–50. https://doi.org/10.1121/1.1923367.
39 Paul S, Katiyar A, Sarkar K, Chatterjee D, Shi WT, Forsberg F. Material characterization of the encapsulation of an ultrasound contrast microbubble and its subharmonic response: Strain-softening interfacial elasticity model. The Journal of the Acoustical Society of America 2010;127:3846–57. https://doi.org/10.1121/1.3418685.

40 Paul S, Russakow D, Rodgers T, Sarkar K, Cochran M, Wheatley M. Determination of the interfacial rheological properties of a PLA encapsulated contrast agent using in vitro attenuation and scattering. Ultrasound Med Biol 2013;39:1277–91. https://doi.org/10.1016/j.ultrasmedbio.2013.02.004.
41 Kumar KN, Sarkar K. Interfacial Rheological Properties of Contrast Microbubble Targestar P as a Function of Ambient Pressure. Ultrasound in Medicine and Biology 2016;42:1010–7. https://doi.org/10.1016/j.ultrasmedbio.2015.11.017.
42 Mobadersany N, Sarkar K. Acoustic microstreaming near a plane wall due to a pulsating free or coated bubble: velocity, vorticity and closed streamlines. Journal of Fluid Mechanics 2019;875:781–806. https://doi.org/10.1017/jfm.2019.478.
43 Stride E, Saffari N. Microbubble ultrasound contrast agents: A review. Proc Inst Mech Eng H 2003;217:429–47. https://doi.org/10.1243/09544110360729072.
44 Osborn J, Aliabouzar M, Zhou X, Rao R, Zhang LG, Sarkar K. Enhanced Osteogenic Differentiation of Human Mesenchymal Stem Cells Using Microbubbles and Low Intensity Pulsed Ultrasound on 3D Printed Scaffolds. Advanced Biosystems 2019;3:1800257. https://doi.org/10.1002/adbi.201800257.
45 Aliabouzar M, Kumar KN, Sarkar K. Acoustic vaporization threshold of lipid-coated perfluoropentane droplets. J Acoust Soc Am 2018;143:2001. https://doi.org/10.1121/1.5027817.
46 Aliabouzar M, Kumar KN, Sarkar K. Effects of droplet size and perfluorocarbon boiling point on the frequency dependence of acoustic vaporization threshold. J Acoust Soc Am 2019;145:1105–16. https://doi.org/10.1121/1.5091781.
47 Munagala R, Aqil F, Jeyabalan J, Gupta RC. Bovine milk-derived exosomes for drug delivery. Cancer Lett 2016;371:48–61. https://doi.org/10.1016/j.canlet.2015.10.020.
48 Somiya M, Yoshioka Y, Ochiya T. Biocompatibility of highly purified bovine milk-derived extracellular vesicles. Journal of Extracellular Vesicles 2018;7:1440132. https://doi.org/10.1080/20013078.2018.1440132.
49 Karandish F, Mamnoon B, Feng L, Haldar MK, Xia L, Gange KN, et al. Nucleus-Targeted, Echogenic Polymersomes for Delivering a Cancer Stemness Inhibitor to Pancreatic Cancer Cells. Biomacromolecules 2018;19:4122–32. https://doi.org/10.1021/acs.biomac.8b01133.
50 Paul S, Russakow D, Rodgers T, Sarkar K, Cochran M, Wheatley M. Determination of the interfacial rheological properties of a PLA encapsulated contrast agent using in vitro attenuation and scattering. Ultrasound Med Biol 2013;39:1277–91. https://doi.org/10.1016/j.ultrasmedbio.2013.02.004.
51 Kumar KN, Mallik S, Sarkar K. Role of freeze-drying in the presence of mannitol on the echogenicity of echogenic liposomes. J Acoust Soc Am 2017;142:3670–6. https://doi.org/10.1121/1.5017607.
52 Schindelin, J.; Arganda-Carreras, I.; Frise, E.; Kaynig, V.; Longair, M.; Pietzsch, T.; Preibisch, S.; Rueden, C.; Saalfeld, S.; Schmid, B.; Tinevez, J.-Y.; White, D. J.; Hartenstein, V.; Eliceiri, K.; Tomancak, P.; Cardona, A., Fiji: an open-source platform for biological-image analysis. Nature Methods 2012, 9, 676.
53 Xia, L.; Karandish, F.; Kumar, K. N.; Froberg, J.; Kulkarni, P.; Gange, K. N.; Choi, Y.; Mallik, S.; Sarkar, K., ACOUSTIC CHARACTERIZATION OF ECHOGENIC POLYMERSOMES PREPARED FROM AMPHIPHILIC BLOCK COPOLYMERS. Ultrasound Med. Biol. 2018, 44 (2), 447-457.

54 Kumar KN, Sarkar K. Effects of ambient hydrostatic pressure on the material properties of the encapsulation of an ultrasound contrast microbubble. J Acoust Soc Am 2015;138:624–34. https://doi.org/10.1121/1.4923364.
55 Katiyar A, Sarkar K, Forsberg F. Modeling subharmonic response from contrast microbubbles as a function of ambient static pressure. J Acoust Soc Am 2011;129:2325–35. https://doi.org/10.1121/1.3552884.
56 Forsberg, F.; Shi, W. T.; Goldberg, B. B., Subharmonic imaging of contrast agents. Ultrasonics 2000, 38 (1-8), 93-98.
57 Kumar KN, Mallik S, Sarkar K. Role of freeze-drying in the presence of mannitol on the echogenicity of echogenic liposomes. The Journal of the Acoustical Society of America 2017;142:3670–6. https://doi.org/10.1121/1.5017607.
58 Huang S-L, Hamilton AJ, Nagaraj A, Tiukinhoy SD, Klegerman ME, Mcpherson DD, et al. Improving ultrasound reflectivity and stability of echogenic liposomal dispersions for use as targeted ultrasound contrast agents. JPharmSci 2001;90:1917–26. https://doi.org/10.1002/jps.1142.
59 Huang S-L, Hamilton AJ, Pozharski E, Nagaraj A, Klegerman ME, McPherson DD, et al. Physical correlates of the ultrasonic reflectivity of lipid dispersions suitable as diagnostic contrast agents. Ultrasound in Medicine and Biology 2002;28:339–48. https://doi.org/10.1016/S0301-5629(01)00512-9.
60 Huang, S. L.; MacDonald, R. C., Acoustically active liposomes for drug encapsulation and ultrasound-triggered release. Biochimica Et Biophysica Acta-Biomembranes 2004, 1665 (1-2), 134-141.
61 Kopechek, J. A.; Haworth, K. J.; Raymond, J. L.; Douglas Mast, T.; Perrin Jr, S. R.; Klegerman, M. E.; Huang, S.; Porter, T. M.; McPherson, D. D.; Holland, C. K., Acoustic characterization of echogenic liposomes: Frequency-dependent attenuation and backscatter. The Journal of the Acoustical Society of America 2011, 130 (5), 3472-3481.
62 Shekhar H, Kleven RT, Peng T, Palaniappan A, Karani KB, Huang S, et al. In vitro characterization of sonothrombolysis and echocontrast agents to treat ischemic stroke. Sci Rep 2019;9:. https://doi.org/10.1038/s41598-019-46112-z.
63 Nahire R, Paul S, Scott MD, Singh RK, Muhonen WW, Shabb J, et al. Ultrasound Enhanced Matrix Metalloproteinase-9 Triggered Release of Contents from Echogenic Liposomes. Mol Pharm 2012;9:2554–64. https://doi.org/10.1021/mp300165s.
64 Nahire R, Hossain R, Patel R, Paul S, Meghnani V, Ambre AH, et al. pH-Triggered Echogenicity and Contents Release from Liposomes. Mol Pharm 2014;11:4059–68. https://doi.org/10.1021/mp500186a.
65 Nahire R, Haldar MK, Paul S, Ambre AH, Meghnani V, Layek B, et al. Multifunctional polymersomes for cytosolic delivery of gemcitabine and doxorubicin to cancer cells. Biomaterials 2014;35:6482–97. https://doi.org/10.1016/j.biomaterials.2014.04.026.
66 Kwan JJ, Myers R, Coviello CM, Graham SM, Shah AR, Stride E, et al. Ultrasound-Propelled Nanocups for Drug Delivery. Small 2015;11:5305–14. https://doi.org/10.1002/smll.201501322.

CHAPTER 3: FURTHER CHARACTERZATION OF ECHOGENIC EXOSOMES AS ULTRASOUND CONTRASTING AGENTS[3]

Abstract

Nanoparticle use as an ultrasound contrasting agent has been widely used, but experience rapid clearance. Exosomes have decreased clearance due to their biologically derived nature. Echogenic exosomes are a newly discovered characteristic of bovine milk exosomes. This work examines the properties of these modified exosomes in both raw and pasteurized bovine milk. The lipid bilayer, transmembrane protein CD63 and miRNA characteristically found within exosomes is intact indicating exosomes protect their cargo from harsh conditions. Pasteurized bovine milk echogenic exosomes also underwent scattering testing and did not show significant difference from our previously published work on raw bovine milk echogenic exosomes.

Introduction

Historically, the discovery and use of nanoparticles promised to usher in a new era of universal efficacy, holding promise in diverse areas such as drug delivery, biomarker discovery, diagnostics, and imaging. Unfortunately, synthetic nanoparticles have not made good on those promises. Clearance and ineffective targeted delivery have proven to be significant pitfalls that have limited their efficacy. Alternatively, biological nanoparticles, such as exosomes, have emerged on the scene with the potential to bypass both clearance and targeting problems in drug delivery and diagnostic applications. Exosomes are nanosized (30-150nm), biologically-derived particles that are heavily involved in cellular signaling.[1–3] These important molecular entities can

[3] The material in this chapter was co-authored by Jessica Pullan, Kaitlin Dailey, Lina Alhalhooly, Roozbeh Azami, Jenna Osborn, Kausik Sarkar, Todd Molden, Amanda Brooks, Yongki Choi, and Sanku Mallik. Jessica Pullan performed experiments, analyzed data and wrote manuscript. Kaitlin Dailey, Lina Alhalhooly, Roozbeh Azami, and Jenna Osborn performed experiment and assisted in experimental design. Kausik Sarkar, Todd Molden, Amanda Brooks, Yongki Choi, and Sanku Mallik reviewed the manuscript and assisted in experimental design.

be isolated from a multitude of sources to include serum, milk and urine.[3,4] However, the collection of exosomes from human sources can be difficult and costly, which necessitates an alternative source. [3,5] Bovine milk exosomes, which can be isolated at a high concentration, have not shown significant problems with immune response or off target effects *in vivo*, increasing their value in nanoparticle development.[2,3] Raw bovine milk has been used in previous studies that used exosomes as drug delivery vehicles; however, sourcing raw bovine milk in more urban areas can be difficult.[2] Conversely, pasteurized bovine milk is easily obtained in any environment and has the potential to become a main source of exosomes. The research outlined in this manuscript explores the impact of pasteurization on the durability of isolated exosomes as well as their use as an ultrasound contrasting agent.

Ultrasound is an almost universally available diagnostic tool across the socio-economic spectra within the United States.[6] While ultrasound can be used to visualize a wide variety of health conditions, low resolution and lack of contrast can make it more difficult to confirm findings; this is where ultrasound contrasting agents become critical.[2,7,8] Ultrasound contrasting agents with echogenic properties have shown benefits as a way to improve the diagnostic capabilities of ultrasound in the clinic. [2] Despite their efficacy at improving the sensitivity of ultrasound diagnostics, the specificity may be compromised due to both the lack of contrast targeting and rapid clearance.[9,10] For years dogma has suggested that only large, synthetic nanoparticles have echogenic properties, making them able to be used as an ultrasound contrast agent; however, our work has demonstrated that exosomes can also have this property. Our recently published manuscript on echogenic exosomes has opened the door for the use of exosomes as a contrasting agent.[2] Importantly, exosomes have the ability to by-pass some of the drawbacks of synthetic nanoparticles and up to this point have been largely unexplored. [2,11,12]

Development of the exosome's echogenic process has opened doors to examine how the process may affect its molecular cargo. Since echogenicity is a recently discovered property of exosomes, this paper explores the further characterization of echogenic exosomes. Due to this unique and novel development we have decided to further characterize and compare raw bovine milk exosomes and pasteurized bovine milk exosomes during and after the echogenic process. Freeze-thaw cycles, which are essential to create echogenic particles, have been known to affect biological macromolecules in various ways. It was important to examine the effect of the chemical modification of echogenicity in order to determine if there are changes to exosomes innate beneficial features. The further characterization includes transmission electron microscopy to examine the lipid bilayer, CD63 flow cytometry and RT-PCR for miRNA. Pasteurized, commercially available bovine milk exosomes were isolated and underwent the same echogenic process as raw exosomes with the same subsequent analysis and characterization process.

Materials and Methods

Exosome Isolation

Exosome isolation was followed as previously reported.[1] Raw bovine milk was collected from the North Dakota State University Dairy Farm in 1 L quantities. If the raw bovine milk was not used the same day of pickup, it was stored at 4C for up to 4 days. Due to the fat content of the milk, serial centrifugation was used to isolate exosomes. Raw bovine milk was placed in six 50 mL centrifuge tubes with 45 mL in each and spun for 20 min a 3,500g in a VWR Clinical 200 Centrifuge. Following the initial 20-minute spin, white fat deposits formed on the wall of the centrifuge tubes and the milk was passed through a cheesecloth to remove fat. A Beckman Coulter Optima XPN-80 Ultracentrifuge was used with a SW 41 Ti rotor for the remainder of centrifugation steps. After being passed through the cheesecloth, the milk was collected and

placed with equal weight into six 13.2 mL thin wall, Ultra-Clear tubes (Beckman Coulter, CA, USA.). Tubes were spun at 12,950g at 4C for 30 minutes. The milk was removed from the tubes and was filtered through cheesecloth to remove more fat. Once the milk was filtered, it was placed in 4 new ultracentrifuge tubes and spun at 98,500g for 70 minutes at 4C. Three layers then formed in each tube and the middle layer was collected. The middle layer was then placed in two fresh ultracentrifuge tubes and spun at 135,030g for 1 hour and 45 min at 4C. Subsequently, the liquid was removed from the ultracentrifuge tubes, taking care not to disturb the pellet. The pellet was then resuspended in 1 mL of phosphate buffer solution (1X Dulbecco's PBS, VWR). Both tubes of PBS suspended exosomes were combined leaving a clear film at the bottom of the tube. A 0.45 um filter was pre-wet using PBS. Then the exosomes were passed through the filter into an Eppendorf tube. The first three drops of PBS in the syringe filter were discarded after the exosomes were filtered through using a 1 mL syringe using two separate filters. To ensure all exosomes were retrieved from the filter, more PBS was passed through the filter until the first three drops come out and the remainder was discarded. Dynamic light scattering (ZS90, Malvern Panalytical, Westborough, MA) was performed to hydrodynamic diameters of the exosomes. Parafilm was placed around the outside of the Eppendorf tube and was kept at -80ºC until used. Pasteurized whole milk (local grocery store) was isolated through the same method as described above.

Exosome Tracking Analysis

The size distribution and concentration of exosomes were determined by nanoparticle tracking analysis (NTA) using the NanoSight NS300 system (Malvern Panalytical Ltd, UK). The exosome samples were diluted to 1000-fold in PBS for NTA measurements. The samples were infused with the syringe pump at constant speed of 20 into the microfluidic flow cell equipped

with a 532 nm laser and a high sensitivity scientific CMOS camera. At least three videos per sample were recorded with the camera level of 11 - 13 for 30 s at 25°C. All data were analyzed using NTA software (version 3.4) with a detection threshold of 5.

Echogenic Exosome Atomic Force Microscopy

Imaging was performed as we have previously reported.[1,2] The imaging samples were prepared by placing 10 μL of each solution on silicon substrates (University Wafer) for 10 minutes in a sealed compartment to prevent evaporation at room temperature. The samples were then washed with de-ionized water (Millipore) and dried under liquid nitrogen. The imaging measurements were performed using a commercial atomic force microscope (NT-MDT NTEGRA AFM). The samples were imaged under ambient conditions in semi-contact mode using an AFM tip with a resonant frequency of 190 kHz (Budget sensors).

Echogenic Exosomes High-Resolution Transmission Electron Microscopy (HRTEM) Imaging

Imaging was performed as we have previously reported.[1] A drop of the sample was placed on a 300-mesh formvar-carbon coated copper TEM grid (Electron Microscopy Sciences, Hatfield, Pennsylvania, USA) for 2 min and wicked off. Phosphotungstic acid 0.1%, pH adjusted to 7-8, was dropped onto the grid and allowed to stand for 2 minutes and then wicked off. After the grids were dry, images were obtained using a JEOL JEM-2100 LaB6 transmission electron microscope (JEOL USA, Peabody, Massachusetts) running at 200 kV.

Ultrasound of Pasteurized Echogenic Exosomes

Echogenic Exosomes were imaged as we previously reported.[2] Echogenic exosomes were reconstituted in BSA-HEPES solution or HEPES. The BSA-HEPES solution was made using 2.5 g of BSA in 500 mL of 10 mM HEPES buffer at pH 7.4. Concentration of 35 mg/mL echogenic

exosomes in BSA-HEPES on Vevo 3100 Imaging System (Fujifilm Visual Sonics, Toronto, ON, Canada) was used. Transducer head with 21 MHz frequency was utilized.

Flow Cytometry for Exosomes CD63

Isolated bovine milk exosomes suspended in 500 uL of PBS. Echogenic modified exosomes were resuspended in buffer and spun for 1 hour prior to primary antibody. CD63 Monoclonal Antibody (CC25, Invitrogen, USA) and allowed to rock at room temperature for 30 min. Exosomes were then washed with PBS three times to remove primary antibody by spinning at 10,000 RPM for 10min. Goat anti-Mouse IgG Antibody (GtxMu-003-FFITC, ImmunoReagents, Raleigh, NC) as then added and allowed to rock at room temperature for 30 min. After 30 minutes, secondary antibody was removed and exosomes washed three times with PBS through centrifugation at 10,000 RPM for 10 min. Exosomes resuspended in 500 uL of PBS and flow performed. Data was obtained using BD Accuri C6 Flow Cytometer and 20,000 events were captured for each sample.

RT PCR for miRNA

Protocol was taken from previously reported literature for bovine milk exosomes.[5] Total RNA was extracted from exosomes using TRIzol Reagent method (Invitrogen, Carlsbad, CA). Briefly exosome samples were lysed using TRIzol. RNA was precipitated then washed and solubilized. RNA yield was determined using absorbance (Take3, Biotek Epoch, Software Version 2.06.10, BopSPX, Netherlands). RNA was then stored at -80C until cDNA was generated. cDNA was generated using an miScript Reverse Transcription Kit (miScript II RT Kit, Qiagen). Protocol was followed for using miScript HiSpec Buffer with concentration of RNA to be 4 ng/uL. Generated cDNA was then subjected to quantitative (q)PCR on a QuantStudio 3 System (Applied Biosystems, Foster City, CA) using an miScript SYBR Green

PCR Kit and miScript Primer Assay (Qiagen) according to the manufacturer's instructions. The following real-time PCR protocol was used: initial activation of HotStarTaq DNA Polymerase (from miScript kit; 95°C, 15 min); 50 cycles of denaturation (94°C, 15 s), annealing (55°C, 30 s), and extension (70°C, 34 s); and melting curve analysis. The miScript Primer Assay (Qiagen) used for the target miRNA is miR320 (MS00013433). The data were analyzed using QuantStudio Design and Analysis Software version 1.5.1 (Applied Biosystems) with the fixed cycle threshold (Ct) setting.

Results and Discussion

Pasteurized Echogenic Exosomes

To expand the source of exosomes, exosomes from pasteurized, commercially available, bovine milk underwent the echogenic process after isolation. Particle counting determined the difference in exosome concentration between raw bovine milk[2] and pasteurized bovine milk isolations (**Figure 3.1**) at each step in the echogenic process. Exosomes were made echogenic through a freeze-thaw process as previously described.[2] Initially, the functionality of pasteurized, echogenic exosomes was assessed by exposing them to ultrasound (**Figure 3.2**). In line with results of raw milk echogenic exosomes, echogenic exosomes reconstituted in BSA-HEPES buffer alone showed increased signal compared to HEPES alone. When compared to our previously published intensity quantifications[2], we found that the raw echogenic exosomes exhibited 4 times more signal when reconstituted in BSA-HEPES compared to pasteurized echogenic exosomes. Raw echogenic exosomes exhibited 1.6 times more signal when reconstituted in HEPES compared to pasteurized echogenic exosomes.

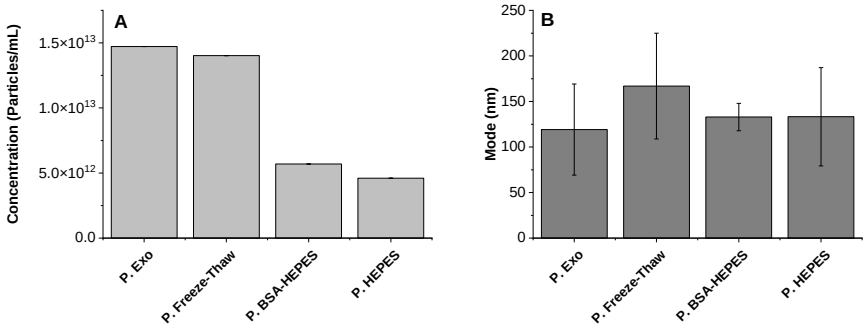

Figure 3.1. A. Pasteurized exosomes concentration at before process (P. Exo), after freeze-thaw (P. Freeze-Thaw), reconstituted in BSA-HEPES (P. BSA-HEPES) and reconstituted in HEPES (P. HEPES). B. Pasteurized echogenic exosome size mode before the process, after freeze-thaw, and reconstituted in BSA-HEPES and HEPES alone. N = 3

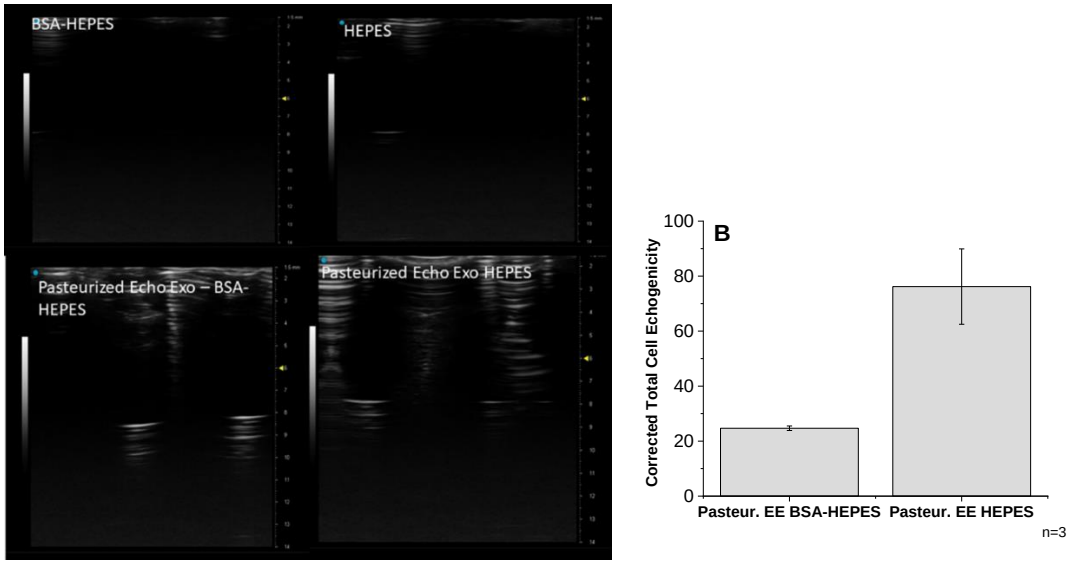

Figure 3.2. Pasteurized Echogenic Exosomes visualization via ultrasound. A. Pasteurized echogenic exosomes visualized via ultrasound compared when echogenic exosomes were resuspended in BSA-HEPES or HEPES buffer. B. Ultrasound images were quantified looking at the corrected total echogenicity. N=3, p>0.001.

Lipid Bilayer Examination

Following conformation of echogenicity, the presence of lipid bilayer, surface proteins and miRNA was confirmed. HR-TEM was performed before and after the echogenic process on exosomes resuspended in either BSA-HEPES or HEPES alone for both raw bovine milk

exosomes (**Figure 3.3**) and pasteurized bovine milk (**Figure 3.4**) exosomes. HR-TEM of raw bovine milk exosomes indicated the lipid bilayer was still intact but appeared to be distorted by air pockets when reconstituted in BSA-HEPES but not in HEPES alone (**Figure 3.3)**. HR-TEM imaging of pasteurized bovine milk exosomes displayed an intact lipid bilayer and did not show the same texturing on the exosome surface as the raw bovine milk exosomes (**Figure 3.3**). This could be a result of the pasteurization and homogenization processes.[13] Previous studies have not been performed to examine how the pasteurization and homogenization processes affect the exosomes. AFM was performed on the pasteurized echogenic exosomes to confirm HR-TEM findings and allow comparison of raw bovine milk echogenic exosomes (**Figure 3.3**). These findings confirmed the HR-TEM results and showed similar characteristics to raw bovine milk echogenic exosomes.

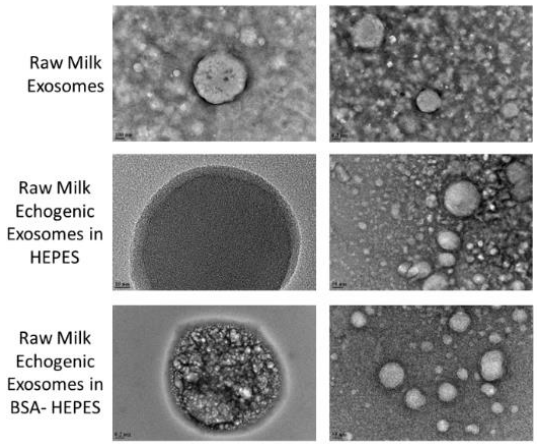

Figure 3.3. HR-TERM of raw bovine milk echogenic exosomes. Top row examines raw bovine milk exosomes. Middle row shows images of raw bovine milk echogenic exosomes resuspended in HEPES. Bottom row shows images of raw bovine milk echogenic exosomes resuspended in BSA-HEPES.

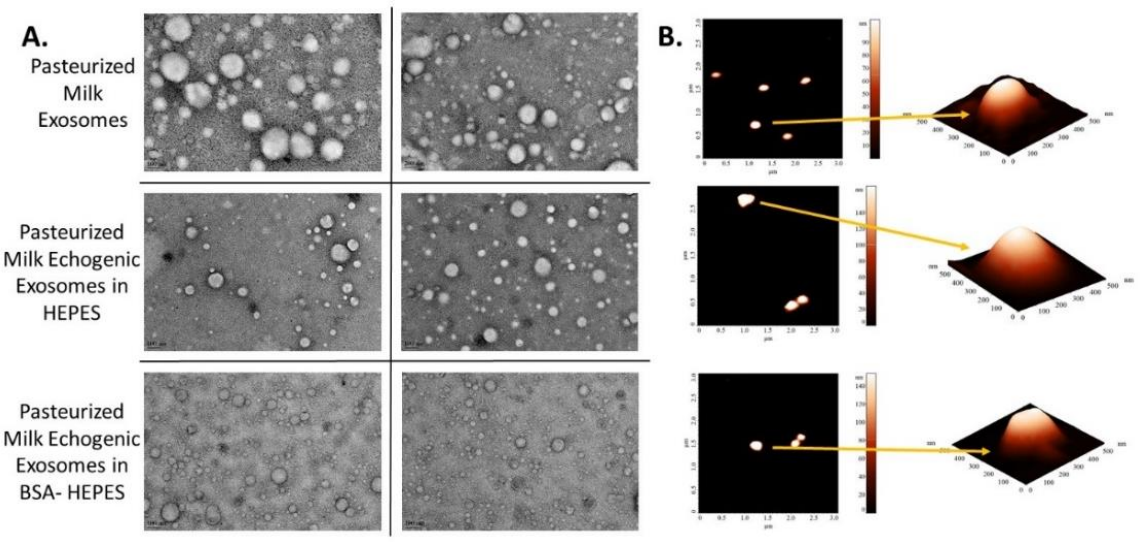

Figure 3.4. HR-TEM and AFM of pasteurized milk echogenic exosomes. A. HR-TEM of pasteurized bovine milk exosomes. Top row shows unmodified pasteurized bovine milk echogenic exosomes. Middle row shows pasteurized bovine milk echogenic exosomes resuspended in HEPES. Bottom row shows pasteurized bovine milk echogenic exosomes resuspended in BSA-HEPES. B. AFM imaging of pasteurized bovine milk exosomes. Top row shows unmodified pasteurized bovine milk echogenic exosomes. Middle row shows pasteurized bovine milk echogenic exosomes resuspended in HEPES. Bottom row shows pasteurized bovine milk echogenic exosomes resuspended in BSA-HEPES.

Surface Protein Structural Integrity

The next biological macromolecule examined was surface proteins. These surface proteins are critical for the innate clearance and targeting properties of exosomes. If the echogenic process made these proteins unable to be functional, many of the benefits of exosomes could be lost. Fortunately, surface proteins were examined through flow cytometry (**Figure 3.6**), examining the intact surface protein for CD63. Both processes indicated the continued presence and functionality of CD63 to bind to antibody. Raw bovine milk echogenic exosomes indicated increased levels of CD63 present compared to pasteurized bovine milk echogenic exosomes, which could be a result of the pasteurization and homogenization processes.

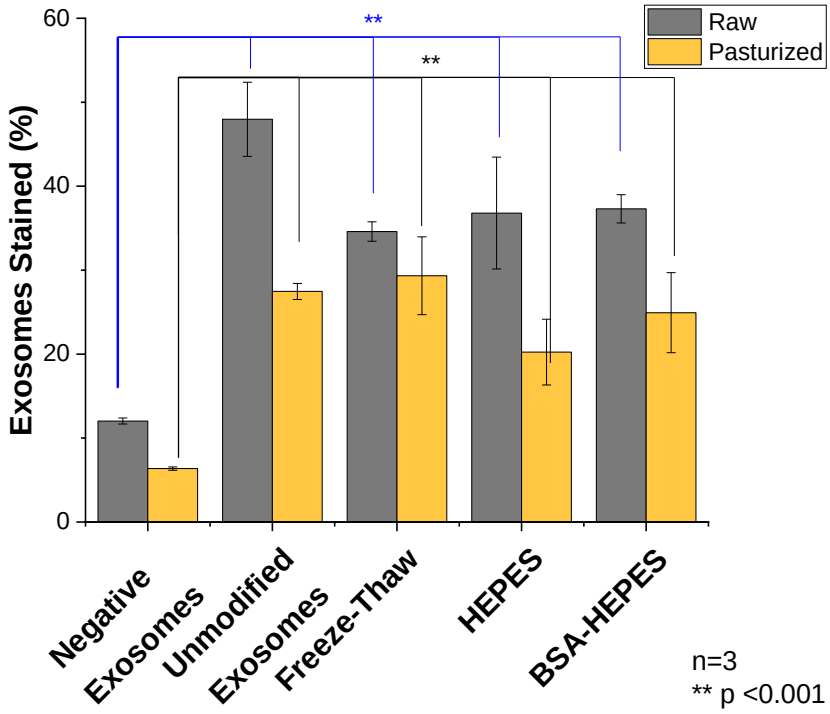

Figure 3.5. Flow cytometry for CD63 presence on exosomes. Compared raw and pasteurized exosomes before, before drying and after drying for echogenic protocol. Raw exosomes showed higher percentage of staining for CD63 compared to pasteurized exosomes for all conditions. Left bars are raw bovine milk exosomes, right bars are pasteurized bovine milk exosomes. N=3.

Presence of Nucleic Acids

RT-PCR was performed to assess the presence of miRNA, a critical biomacromolecule in cellular signaling. As miRNA has been well characterized in exosomes from a variety of sources, this was chosen for our studies.[5] miRNA 320 was found in both raw bovine milk, echogenic exosomes and pasteurized bovine milk, echogenic exosomes under all conditions: freeze-thaw, reconstituted in HEPES and reconstituted in BSA-HEPES. This indicates that neither the pasteurization process nor the echogenic process destroyed the nucleic acids present. Surprisingly, preliminary results indicated that pasteurized bovine milk exosomes have higher miR320 than raw bovine milk exosomes; however, further exploration is necessary.

Conclusions

While the scientific community has given up the thought that nanoparticles will answer every question in drug delivery and diagnostics, biological nanoparticles may still hold some of the original process due to their ability to circumvent the obstacles that plague their synthetic cousins.. Exosomes have the durability, versatility and extended half-life that synthetic nanoparticles often lack. Overall, the echogenic process does not appear to affect the lipid bilayer, surface proteins, or nucleic acids innately present on/in exosomes. These findings open the door to targeted contrasting. Additionally, the pasteurization and homogenization processes do not seem to affect the ability of the exosomes to undergo the echogenic process and reflect the sound waves of ultrasound imaging. These preliminary results open doors to further development of echogenic exosomes as an ultrasensitive ultrasound contrast agent as well as the development of alternative exosome sources to ensure that bovine milk is not the only source available.

Acknowledgments

This research was supported by NIH grant 1 R01GM 114080 to S.M. and K.S. JO and KS would like to acknowledge the ARCS MWC Chapter, The McNichols Family Foundation, and The Myers family for their support.

Conflicts of Interest

The authors declare no conflict of interest. The funders had no role in the design of this publication; in the collection, analyses, or interpretation of data; in the writing of the manuscript, or in the decision to publish the results.

References

1 Pullan, JE, Chemeiti P, Confeld M, Feng L, Froberg J, Choi Y, et al. Hypoxia Responsive Lipid Incorporation Into Bovine Milk Exosomes. Biomedical Science Instrumentation 2018;54:.

2 Osborn J, E. Pullan J, Froberg J, Shreffler J, N. Gange K, Molden T, et al. Echogenic exosomes as ultrasound contrast agents. Nanoscale Advances 2020. https://doi.org/10.1039/D0NA00339E.
3 Munagala R, Aqil F, Jeyabalan J, Gupta RC. Bovine milk-derived exosomes for drug delivery. Cancer Lett 2016;371:48–61. https://doi.org/10.1016/j.canlet.2015.10.020.
4 Corrado C, Raimondo S, Chiesi A, Ciccia F, De Leo G, Alessandro R. Exosomes as Intercellular Signaling Organelles Involved in Health and Disease: Basic Science and Clinical Applications. Int J Mol Sci 2013;14:5338–66. https://doi.org/10.3390/ijms14035338.
5 Izumi H, Tsuda M, Sato Y, Kosaka N, Ochiya T, Iwamoto H, et al. Bovine milk exosomes contain microRNA and mRNA and are taken up by human macrophages. Journal of Dairy Science 2015;98:2920–33. https://doi.org/10.3168/jds.2014-9076.
6 Sahlani L, Thompson L, Vira A, Panchal AR. Bedside ultrasound procedures: musculoskeletal and non-musculoskeletal. Eur J Trauma Emerg Surg 2016;42:127–38. https://doi.org/10.1007/s00068-015-0539-3.
7 Chong WK, Papadopoulou V, Dayton PA. Imaging with ultrasound contrast agents: current status and future. Abdom Radiol 2018;43:762–72. https://doi.org/10.1007/s00261-018-1516-1.
8 Hunt D, Romero J. Contrast-Enhanced Ultrasound. Magnetic Resonance Imaging Clinics of North America 2017;25:725–36. https://doi.org/10.1016/j.mric.2017.06.004.
9 Paul S, Nahire R, Mallik S, Sarkar K. Encapsulated microbubbles and echogenic liposomes for contrast ultrasound imaging and targeted drug delivery. Comput Mech 2014;53:413–35. https://doi.org/10.1007/s00466-013-0962-4.
10 Calliada F, Campani R, Bottinelli O, Bozzini A, Sommaruga MG. Ultrasound contrast agents: basic principles. Eur J Radiol 1998;27 Suppl 2:S157-160. https://doi.org/10.1016/s0720-048x(98)00057-6.
11 Liufu C, Li Y, Tu J, Zhang H, Yu J, Wang Y, et al. Echogenic PEGylated PEI-Loaded Microbubble As Efficient Gene Delivery System. Int J Nanomedicine 2019;14:8923–41. https://doi.org/10.2147/IJN.S217338.
12 Kulkarni P, Haldar MK, Karandish F, Confeld M, Hossain R, Borowicz P, et al. Tissue-Penetrating, Hypoxia-Responsive Echogenic Polymersomes For Drug Delivery To Solid Tumors. Chemistry 2018. https://doi.org/10.1002/chem.201802229.
13 Li Y, Joyner HS, Carter BG, Drake MA. Effects of fat content, pasteurization method, homogenization pressure, and storage time on the mechanical and sensory properties of bovine milk. Journal of Dairy Science 2018;101:2941–55. https://doi.org/10.3168/jds.2017-13568.

CHAPTER 4: MODIFIED BOVINE MILK EXOSOMES FOR DELIVERY OF DOXORUBICIN TO TRIPLE-NEGATIVE BREAST CANCER[4]

Abstract

Biological nanoparticles, such as exosomes, offer a new approach to drug delivery due to their innate ability to transport biomolecules. Exosomes are derived from cells and an integral component of cellular communication. However, the cellular cargo of human-derived exosomes could negatively impact their use as a safe drug carrier. Additionally, exosomes have the intrinsic, yet enigmatic, targeting characteristics of complex cellular communication. Hence, harnessing the natural transport abilities of exosomes for drug delivery requires predictably targeting these biological nanoparticles. This manuscript describes the use of two chemical modifications, incorporating aa neuropilin receptor agonist peptide (iRGD) and integrating a hypoxia-responsive lipid, for targeting and release of an encapsulated drug from bovine milk exosomes to triple-negative breast cancer cells. Triple-negative breast cancer is a very aggressive and deadly form of malignancy with limited treatment options. Incorporation of both the iRGD peptide and hypoxia-responsive lipid into the lipid bilayer of bovine milk exosomes and encapsulation of the anticancer drug, doxorubicin, created the peptide targeted, hypoxia-responsive bovine milk exosomes, iDHRX. Initial studies confirmed the presence of iRGD peptide and the exosomes' ability to target the αvβ3 integrin, overexpressed on triple-negative .9;[pi\,breast cancer cell surface. These modified exosomes were stable under normoxic

[4] The material in this chapter was co-authored by Jessica E Pullan, Kaitlin M Dailey, Sangeeta Bhallamudi, Li Feng, Lina Alhalhooly, James Froberg, Jenna M Osborn, Kausik Sarkar, Todd Molden, Sathish Venkatachalem, Yongki Choi, Amanda E Brooks, Sanku Mallik. Jessica Pullan performed the experimental design, experimentation, data anylsis and writing of the manuscript. Kaitlin M Dailey, Sangeeta Bhallamudi, Li Feng, Lina Alhalhooly, James Froberg, and Jenna M Osborn contributed to experimentation and experimental design. Todd Molden provided the milk. Kausik Sarkar, Sathish Venkatachalem, Yongki Choi, Amanda E Brooks, and Sanku Mallik provided contributions to experimental design, manuscript writing and revising.

conditions, but fragmented in the reducing microenvironment created by 10 mM glutathione. *In vitro* cellular internalization studies in monolayer and 3D spheroids of triple-negative breast cancer cells confirmed the cell-killing ability of iDHRX. Cell viability of 50% was reached at 10 µM iDHRX in the 3D spheroid model in 4 different triple-negative breast cancer cell lines tested. Overall, tumor penetrating, hypoxia-responsive exosomes encapsulating doxorubicin would be an effective strategy in reducing triple-negative breast cancer cell survival.

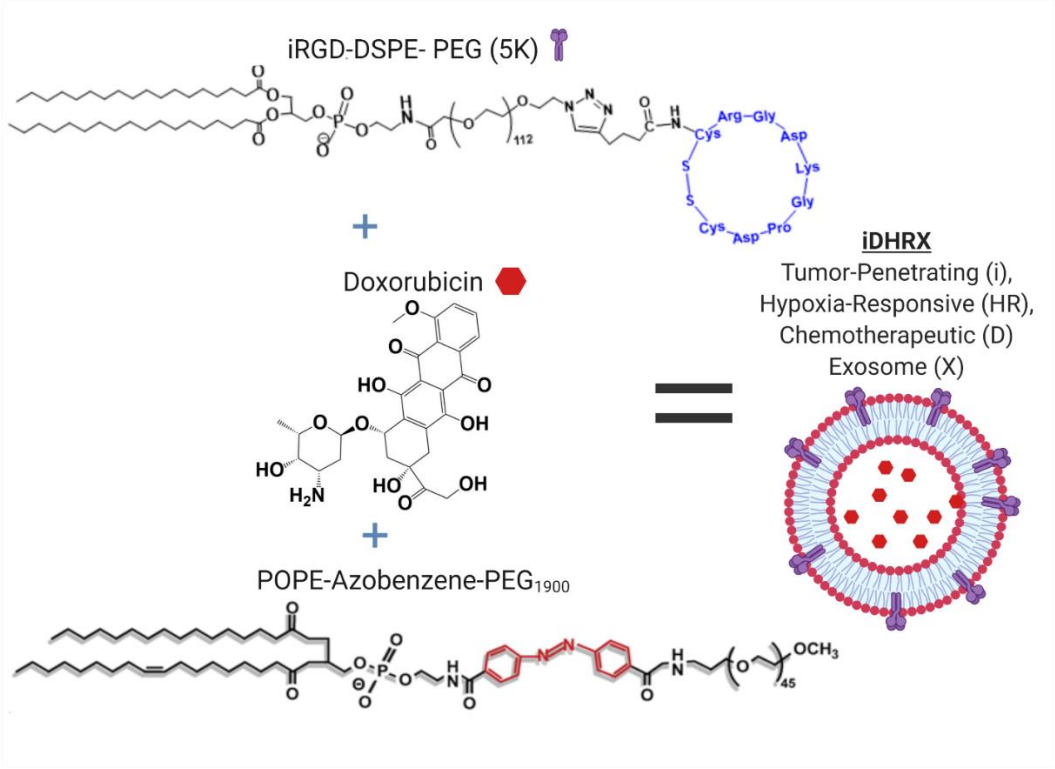

Figure 4.1. Graphical abstract showing the three modifications, iRGD-DSPE-PEG(5K), doxorubicin and POPE-Azobenzene-PEG(1.9K) to bovine milk exosomes that have been isolated through ultracentrifugation. These exosomes have been termed iHRX.

Introduction

With a 5-year overall survival rate of 90%, breast cancer appears to be a problem of the past. However, triple-negative breast cancer (TNBC) has significantly higher reoccurrence and mortality rates.[1] TNBC cells lack estrogen receptors, progesterone receptors, and human

epidermal growth factor receptor 2 (HER2) receptors, limiting current treatment strategies' effectiveness.[2,3] Out of the over 1,151,000 patients in the U.S. diagnosed with breast cancer, 10-15% will be TNBC. [4] Further compromising the efficacy of treatment, TNBC is often characterized by its aggressive, metastatic nature and frequent reoccurrence.[5,6] Metastatic cells often have genetic abnormalities, leading to refractory cancer.[7,8] Finding a strategy that is either unaffected by these changes or can account for them is necessary to prevent metastatic sites from growing unabated. One such strategy is targeting the unique aspects of the tumor microenvironment.

Solid tumors of TNBC have a unique cellular microenvironment that drug delivery systems can exploit. At a diameter greater than 100-180 μm, a solid tumor forms a dense cellular environment that continues to evolve as the tumor grows.[9] These local environment changes leads to unusual fluid flow within the tumor, lack of sufficient oxygen and nutrient exchange, and compromised therapeutic efficacy of anticancer drugs beyond the diffusion limit of the normal tissue margins.[10,11] Some of the unique characteristics of the tumor microenvironment include densely-packed cells, abnormal angiogenesis, increased acidity, acute hypoxia (< 2% oxygen), and upregulation of several markers, such as hypoxia-inducible factors (HIFs), carbonic anhydrases, neuropilin-1 receptor, $\alpha_v\beta_3$ integrin, etc.[12–22] Hypoxia[23] has been utilized with some success in drug delivery;[24,25] however, penetration of the carriers into solid tumors to reach the hypoxic niches is still a challenge. Combining a hypoxia sensing strategy to precisely release the drug payload only to the previously inaccessible "inter-tumor" with an integrated tumor penetrating peptide, which targets tumor-altered biomolecule expression, may provide a therapeutic drug level to the deepest recesses of the tumor while protecting healthy host tissue.

Such an elegant design is possible by using exosomes. This biologically-driven approach will lead to decreased off-target effects and more effective pharmaceutical delivery. [26–29]

Despite important pre-clinical and clinical data and a limited number of FDA-approved nanoparticle-based products, late-stage clinical trial failures continue to plague the field.[29] Some of these issues include toxicity and immune clearance.[29] Exosomes may circumvent these hurdles due to their biological nature.[30] Exosomes are nanosized (30-150 nm), extracellular vesicles secreted from cells (**Figure 4.2**)[30] for cellular communication.[31,32] The innate ability to transport biomolecules for communication makes exosomes uniquely suited as drug carriers. Exosomes provide many drug delivery options and diagnostics, and can be isolated from multiple bodily fluids across species, including bovine milk.[30] However, their cargo could communicate an unintended, even metastatic[33,34] message, posing a significant barrier for clinical translation. In contrast, the non-human exosomes are safer and more readily available.[33,34] Raw bovine milk is an attractive source of exosomes due to availability, low immunogenicity, and lack of human molecular cargo, and consequently, without unintended cellular communications.[30,35]

While bovine milk exosomes may be safer and readily available, their development as a drug delivery system is hindered by the inability of exosomes (regardless of their source) to target and penetrate a tumor and deliver their drug payload. In the current study, bovine milk exosomes were chemically modified to target the altered microenvironment of TNBC, penetrate, and deliver the encapsulated chemotherapeutic drug to three-dimensional (3D) tumor spheroids. Hypoxia- responsive lipid and a tumor penetrating peptide were incorporated into the lipid bilayer of the exosomes. The hypoxia-responsive lipid was designed to be reductively cleaved by in the hypoxic niches of a solid tumor, allowing for a burst release of the encapsulated drug. We

incorporated the reported neuropilin-1 receptor (NRP-1) agonist iRGD peptide on the exosomes for targeting and tumor penetration. The TNBC cells, especially under hypoxia, overexpress NRP-1 and the $\alpha_v\beta_3$ integrin on the surface.[24,26–28,36–43] Hence, the modified bovine milk exosomes with both the hypoxia-responsive lipid and the iRGD tumor targeting and penetrating peptide should result in significant cell death in an *in vitro* 3D spheroid model of TNBC.

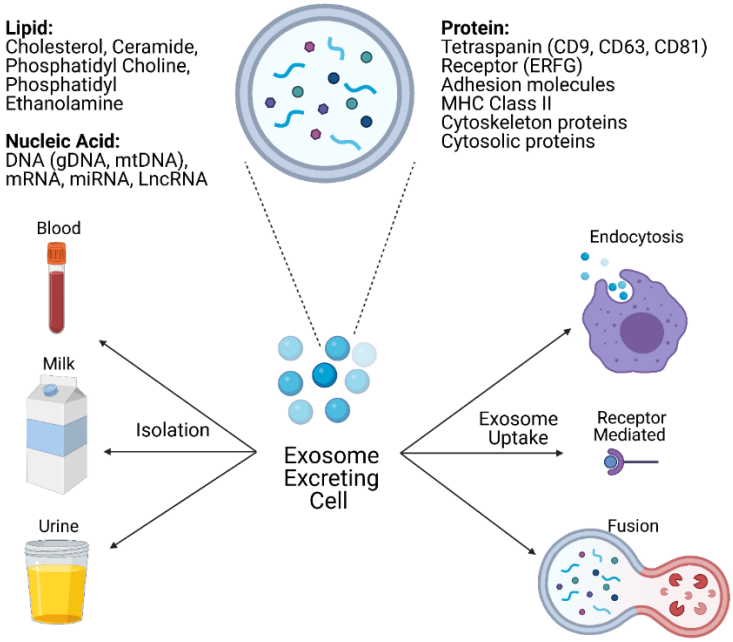

Figure 4.2. Exosomal secretion, structure, and uptake. Cell-secreted exosomes transport biomolecules throughout the body to receptor cells, where uptake occurs through three main mechanisms, a. fusion b. receptor-ligand interaction c. endocytosis. Exosomal structure consists of lipids, proteins, and nucleic acids from secreting cells and vary based on cellular origin.

Materials and Methods

Exosome Isolation

The procedure for exosome isolation was the same as previously reported.[44] Raw bovine milk was collected from the North Dakota State University Dairy Farm. We observed that the raw milk coule be stored at 4 ^{o}C for four days without impacting the isolation of exosomes. Serial centrifugation was used to isolate exosomes. Briefly, raw bovine milk was initially

centrifuged for 20 minutes at 3,500 g (VWR Clinical 200 Centrifuge). To remove the white fat deposits collected on the sides of the centrifuge tubes, the milk was passed through a cheesecloth. The milk was collected and placed into a thin wall, Ultra-Clear tubes (Beckman Coulter) and centrifuged at 12,950 g at 4 °C for 30 minutes (Beckman Coulter Optima XPN-80 ultracentrifuge with a S.W. 41 Ti rotor). The milk was removed from the tubes and was again filtered through a cheesecloth to remove fat. The filtered milk was placed in new ultracentrifuge tubes and spun at 98,500 g for 70 minutes at 4 °C. After ultra-centrifugation, three layers were evident in each tube. The middle whey layer was collected, transferred to two new tubes, and centrifuged at 135,030 g for 105 minutes at 4 °C. Subsequently, the supernatant was removed, taking care not to disturb the exosome pellet. The pellet was then resuspended in 1 mL of phosphate buffer saline (1X Dulbecco's PBS, VWR). A 0.2 μm filter was pre-wet using PBS, and the suspended exosomes were passed through the filter into an Eppendorf tube. The first three drops of PBS were discarded, and the remaining filtrate was collected. Notably, exosome recovery was maximized by dividing the PBS exosome suspension between two different syringe filters. Additionally, the exosome filtrate was washed with additional PBS and the first three drops were collected with the previous exosome filtrate. Dynamic light scattering (DLS) (ZS90, Malvern Panalytical) was performed to determine the purified exosomes' hdrodynamic diameters. Purified exosomes were kept at -80 °C until used.

Exosome Counting and Size Distribution by Tunable Resistive Pulse Sensing

All measurements were performed using qNano Gold (Izon Science) using a nanopore size NP150. The sample size and concentration were calibrated during each measurement using the manufacturer's calibration particles, carboxylated polystyrene beads, (CPC100, average diameter: 110 nm, concentration: 1.1 x 10^{13} particles/mL). Exosomes were diluted 100-500 times

for optimal counting using two different pressures of 4 and 8 mbar. At least 8 replicates were performed for each sample for each measurement.

Hypoxia Responsive Lipid Synthesis

We followed a synthetic protocol reported from our laboratory (**Figure 4.3**).[24,44] NMR (400 MHz Bruker Avance III HD) and ESI TOF Mass Spectroscopy were used to confirm the hypoxia responsive lipid structure (Supporting Information, **Figures A4 and A5**).

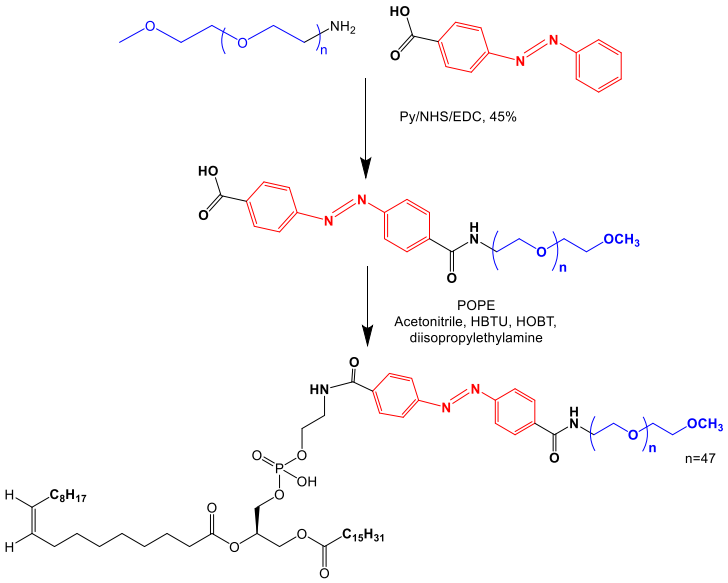

Figure 4.3. Synthetic scheme of hypoxia-responsive lipid, POPE-Azobenzene-PEG_{1600}.

Hypoxia-Responsive Lipid Incorporation into Exosomes

Incorporation of the hypoxia-responsive lipid was performed according to our previously reported protocol.[44] Exosomes were removed from the –80°C freezer and thawed. A 5 mg/mL solution of the hypoxia-responsive lipid in PBS was sonicated for 30 minutes to ensure complete dissolution. Hypoxia responsive lipid (80 µL) and purified exosomes (120 µL) were gently mixed and subsequently incubated at 37°C for one hour. After incubation, 100 µL PBS was added to create a homogeneous mixture. The liquid was placed into a centrifugal fliter (Nanosep Centrifugal Devices; MWCO: 100,000; Pall Corporation) and centrifuged at 9,400 g for 10

minutes to remove any unincorporated lipid. The liquid on top of the filter was used to resuspend any exosomes. All of the liquid (containing the exosomes) was removed, placed in an Eppendorf tube, and stored at –80°C until use.

Estimation of Hypoxia-Responsive Lipid Concentration in Exosomes

The amount of hypoxia-responsive lipid incorporated into the exosomes was estimated based on the presence of the PEG_{1600} using a PEGylated Protein ELISA (Enzo Life Sciences) according to the manufacturer's protocol. A series of dilutions (1.75 to 225 ng/mL) was performed to establish a standard curve. The optimum mixing ratio of hypoxia-responsive lipid to exosome for efficient incorporation was determined. Initial lipid solutions used include 1 mg/mL and 5 mg/mL, with ratios of lipid solution to exosomes of 1:1, 1:2, 1:4 and 3:4.

iRGD-DSPE-PEG_{5000} Synthesis

DSPE-PEG_{5000}-N_3 (NanOCS) was reacted with the alkyne (hexynoic acid) moiety of a synthesized iRGD peptide using click chemistry (1:2 molar ratio peptide to polymer) (**Figure 4.4**). The copper complex was prepared by mixing copper(II) sulfate with N,N,N′,N′,N″-pentamethyl diethylenetriamine (PMDETA) for 2 hours. An ascorbic acid solution (1.4 μmol) was prepared in distilled water. The reaction mixture was then stirred for 72 hours at room temperature. Subsequently, the solution was transferred to a 3.5-5 kDa dialysis bag and dialyzed against water for 72 hours to remove PMDETA, ascorbic acid, as well as unreacted iRGD peptide. The product was lyophilized and analyzed by CD spectroscopy (J-815 CD Spectrometer, Jasco) with 64 scans and at 4°C.

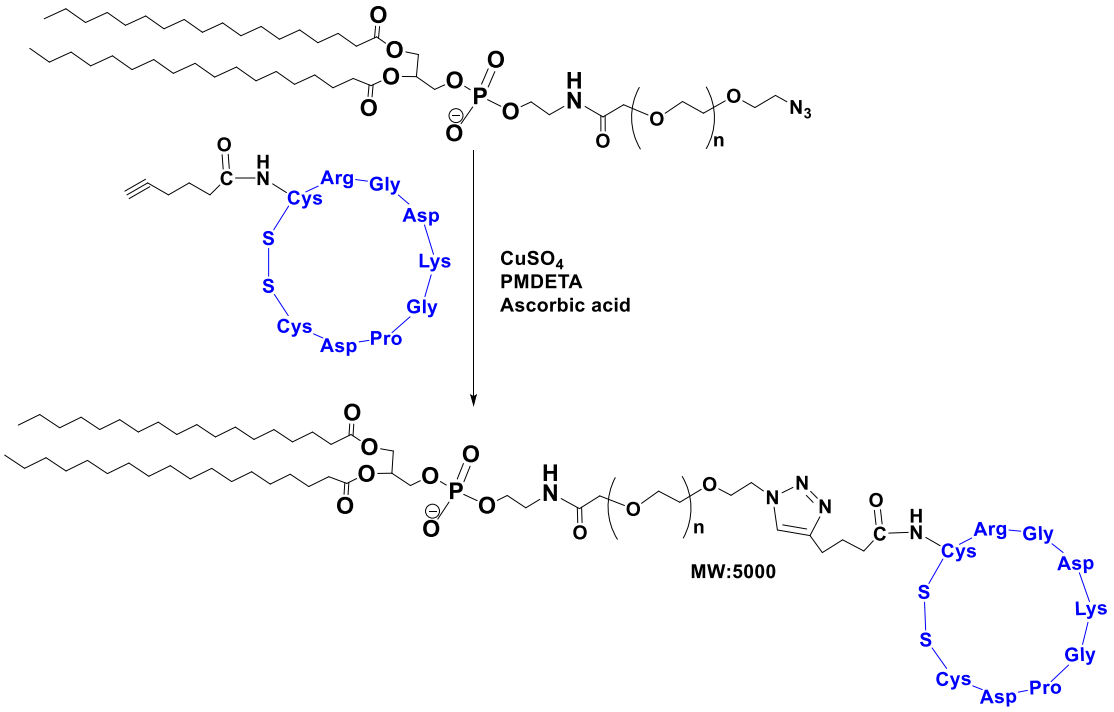

Figure 4.4. Synthesis of iRGD-DSPE-PEG$_{5000}$.

iRGD-DSPE-PEG$_{5000}$ Incorporation in Exosomes

Incorporation of iRGD-DPSE-PEG$_{5000}$ in the exosomes was performed according to our previously reported protocol.[44] A 5 mg/mL solution of the iRGD-DSPE-PEG$_{5000}$ in PBS was prepared and sonicated for 1 hour to ensure complete dissolution. iRGD-DSPE-PEG$_{5000}$ solution (80 µL) and hypoxia-responsive exosomes (120 µL) were gently mixed and incubated at 37 °C for one hour. After incubation, 100 µL PBS was added and the solution was ultra-filtered using a centrifugal filter (Nanosep Centrifugal Devices with 100,000 cut-off membrane, Pall Corporation) at 9,400 g for 10 minutes to remove any unincorporated peptide conjugate. The liquid on top was used to resuspend any exosomes on the filter, the liquid was removed, placed in an Eppendorf tube, and stored at –80 °C until use.

Encapsulation of Doxorubicin in Exosomes

Doxorubicin hydrochloride (Advanced ChemBlocks) was encapsulated into either modified or unmodified exosomes using electroporation (40 V, 125 μF and 750 Ω). After electroporation, exosomes were placed at 37 °C for 1 hour. Hypoxia-responsive, iRGD targeting exosomes (iHRX) were centrifuged at 9,400 g for 10 minutes in a centrifugal filter (Nanosep Centrifugal Devices with 100,000 cut-off membrane, Pall Corporation) to remove the free drug. Encapsulation efficiency was determined by UV-Vis Spectrophotometry (SpectraMax M5, Molecular Devices) for doxorubicin (480 nm).

Atomic Force Microscopy (AFM)

Samples for AFM were prepared by placing 10 μL of each solution (control or exosomes) on silicon substrates (University Wafer) for 10 minutes in a sealed chamber to prevent evaporation at room temperature. The samples were then washed with de-ionized water (Millipore) and dried under liquid nitrogen. Imaging measurements were performed using a commercial atomic force microscope (NT-MDT NTEGRA AFM). Samples were imaged under ambient conditions in semi-contact mode using an AFM tip with a resonant frequency of 190 kHz (Budget sensors).

High-Resolution Transmission Electron Microscopy (HRTEM) Imaging

A drop of the sample (control or exosome containing) was placed on a 300-mesh formvar-carbon coated copper TEM grid (Electron Microscopy Sciences, Hatfield, Pennsylvania, USA) for 1 minute and wicked off. Phosphotungstic acid 0.1%, pH adjusted to 7-8, was dropped onto the grid, allowed to stand for 2 minutes, and then wicked off. After the grids were dry, images were obtained using a JEOL JEM-2100 LaB6 transmission electron microscope (JEOL

USA, Peabody, Massachusetts) running at 200 kV. Magnification reported is for images at size 3.25 x 4 inches.

Flow Cytometry Analysis of CD63 in Exosomes

Freshly isolated bovine milk exosomes were suspended in 500 µL of PBS containing anti-CD63 monoclonal antibody (1:500 dilution, CC25, Invitrogen) and allowed to rock at room temperature for 30 minutes to facilitate interaction. Exosomes were then washed with PBS three times to remove the unbound antibody, centrifuging at 10,000 g for 10 minutes after each wash. Goat anti-mouse IgG antibody in PBS (1:1000 dilution, GtxMu-003-FFITC, ImmunoReagents) was then added and allowed to rock at room temperature for 30 minutes. Subsequently, the secondary antibody was removed, and the exosomes were again washed three times with PBS to remove the unbound secondary antibody. Exosomes were resuspended in 500 µL of PBS and flow cytometry was performed using BD Accuri C6 Flow Cytometer. Twenty thousand events were captured for each sample.

Incubation of HRX with Glutathione

A stock concentration (50 mM) of glutathione was prepared in phosphate-buffered saline (PBS, Corning). Four glutathione concentrations (reduces free acid, EMD Millipore) solution were prepared: 10 mM, 5 mM, 1 mM, and 50 µM. Concentrations were chosen to mimic the reducing environment within a tumor and commonly found in the blood.[45,46] A 10% dilution of hypoxia-responsive exosomes was added to each of the glutathione solutions. Dynamic light scattering (DLS) was used to monitor exosomes' size every 10 minutes for 2 hours. AFM imaging was also performed after 10 minutes and 2 hours of incubation, as described above.

Adhesion Assay with $\alpha_v\beta_3$ Integrin

To monitor exosomes' interactions, DSPE-PEG_{5000}-FITC (NANOCS) was incorporated into the exosomes lipid bilayer through the same method as described for iRGD-DSPE-PEG_{5000}. Groups tested for this study included integrin-coated cover slips treated with PBS (control), FITC labeled exosomes (control), and FITC tagged iHRX. Circular borosilicate glass covers slips (Fisher Scientific) was corona (air plasma) (Enercon Compak 2000 Corona Treater Model LM4045-06) treated with the wand passing over both sides of the cover slip four times. Treated cover slips were then placed in 6-well plates (Celltreat). Untreated coverslips were used as a control. After corona treatment, 100 µL of 10 µg/mL $\alpha_v\beta_3$ integrin (carrier-free, human recombinant protein, R&D Systems) or the carrier solution (PBS) was added to the cover slip and left at 4°C to evaporate to dryness. After 48 hours of drying, 100 µL of treatment (buffer or exosomes) was added to the integrin-treated slides. Cover slips were then placed at 4°C and the iRGD peptide was allowed to interact with the integrin for 48 hours while the water on the slides was evaporated to dryness. Slides were then washed with 200 µL PBS 3 times to remove unadhered treatment (control or exosomes). Coverslips were then read at a fluorescence excitation of 480 nm and emission of 500-700 nm with 2 nm steps. Finally, coverslips were placed on slides for fluorescence and brightfield imaging (Leica Fluorescence Microscope, 10x). At least three images were obtained for each coverslip. The fluorescence intensity was quantified using Fiji. Briefly, the image was separated into color channels, the area selected, and the corrected total cell fluorescence (CTCF) was determined using the internal density and the area and mean fluorescence. A one-way ANOVA was performed to determine statistical significance.

Cell Culture

MDA-MB-468 (triple-negative breast cancer lung metastasis, pleural effusion), MDA-MB-231 (triple-negative breast cancer lung metastasis pleural effusion), HCC 1806 (triple-negative, primary breast tumor) and HCC 1937 (triple-negative primary breast tumor) (TNBC) cell lines were purchased from American Type Culture Collection (ATCC). Cells were cultured in RPMI-1630 supplemented with 10% fetal bovine serum (Avantar Seradign). For normoxia, a humidified incubator containing 5% carbon dioxide, 21% oxygen, and 74% nitrogen at 37 ^{o}C was used. For hypoxia, a biospheroic C21 hypoxic chamber supplemented with 2% oxygen, 93% nitrogen, and 5% carbon dioxide was used. Media was changed every 48 hours and passage numbers were kept below 10 after receiving the cells from ATCC.

Western Blot of MDA-MB-468, MDA-MB-231, HCC 1937 and HCC 1806 Cell Lines for NRP1

All cells were lysed in Pierce RIPA buffer (Thermo Scientific) and protease inhibitor cocktail (Halt Proteases and Phosphatase Inhibitor Cocktails, Thermo Scientific) was added. A Bradford Assay (Micro BCA Protein Assay Kit, Thermo Scientific) was performed using the manufacturer's standard protocol on cell lysate to standardize the amount of protein from each cell line loaded on the gel. Cell lysate (20 µg) was run on a 4-12% SDS-PAGE (Bolt 4-12% Bis, Tris Mini Protein Gel, Invitrogen) and semi-dry transferred to nitrocellulose membrane (Biosciences). Membranes were blocked with 5% nonfat milk in TBS-Tween (0.01%, TBST) for 1 hour and incubated with recombinant anti-NRP1 antibody (ab81321, Abcam) or recombinant anti-GAPDH antibody (ab181602, Abcam) at 4 ^{o}C overnight while rocking. Membranes were washed three times in 0.01% TBS-Tween after the primary antibody was removed. Subsequently, the membranes were incubated with a secondary antibody, IRDye 680 LT goat

anti-Rabbit IgG (926-68021, Li-Cor), for 1 hour at room temperature while rocking. Finally, the membranes were washed three times in 0.01% TBST and imaged on an Odyssey CLx Imager (Li-Cor.) Spectra multicolor broad range protein ladder was used to confirm size (Thermo Scientific).

Flow Cytometry of MDA-MBA-468, MDA-MB-231, HCC 1937 and HCC 1806 Cell Lines for NRP1

The cultured cells were removed from the plate and suspended in 500 µL of PBS and recombinant anti-NRP1 primary antibody (ab81321, Abcam.) Primary antibody was allowed to interact at room temperature for 30 minutes. Cells were then washed with PBS three times to remove primary antibody via centrifuging at 1,200 g for 5 minutes. Goat anti-rabbit IgG H&L (FITC) antibody (ab6717, Abcam) was then added and allowed to rock at room temperature for 30 minutes. After 30 minutes, the secondary antibody was removed and the cells were washed three times with PBS. Cells were resuspended in 500 µL of PBS, and flow cytometry was performed using a BD Accuri C6 Flow Cytometer. Twenty thousand events were captured for each sample with three replicates for each cell line.

Western Blot of MDA-MBA-468, MDA-MB-231, HCC 1937 and HCC 1806 Cell Lines for α_v and β_3 Integrins

All cells were lysed in Pierce RIPA buffer supplemented with a protease inhibitor cocktail (Halt Proteases and Phosphatase Inhibitor Cocktails, Thermo Scientific) and micro BCA assay was performed as previously described. Cell lysate (20 µg) was run on 4-12% SDS-PAGE (Bolt 4-12% Bis, Tris Mini Protein Gel, Invitrogen) and semi-dry transferred to nitrocellulose membrane (Biosciences Louis, MO). Membranes were blocked with 5% nonfat milk in 0.01% TBS-Tween as previously described. They were then probed with recombinant integrin α_v

antibody (sc-376156, Santa Cruz Biotechnology), recombinant integrin β_3 antibody (4702, Cell Signaling) or recombinant anti-GAPDH antibody (ab181602, Abcam) at 4 ^{o}C overnight while rocking. Membranes were washed three times in 0.01% TBS-Tween after the primary antibody was removed. They were subsequently incubated with secondary antibody, IRDye 680 LT goat antirabbit IgG (926-68021, Li-Cor) or IRDye 800 LT goat anti-mouse IgG (926-32210, Li-Cor) for 1 hour at room temperature while rocking. Membranes were washed three times in 0.01% TBS-Tween and imaged on an Odyssey CLx Imager (Li-Cor). Spectra Multicolor Broad Range Protein Ladder was used to confirm size (Thermo Scientific).

Cellular Internalization

Ten thousand cells were seeded into Biotek 8-well glass plates. Once adhered, media was changed to serum-free RPMI-1640. Cell nucleus stain (Invitrogen ReadyProbes NucBlue Live Reagent) was applied for nuclear monitoring. Doxorubicin (20 μM) encapsulated in exosomes (iDHRX or DExo) was added to well plates, and imaged every 30 minutes for 24 h using the Lioheart FX (Biotek, USA) with DAPI with Texas Red filters. Texas Red fluorescence intensity was quantified using Fiji. The image was separated into color channels, the area selected, and the CTCF was determined using the internal density, area, and mean fluorescence.

Cytotoxicity

Monolayer Cultures: Ten thousand MDA-MB-231, MDA-MB-468, HCC 1806, or HCC 1937 cells were seeded into 8 wells of 96-well clear-bottom plates. The cells were incubated 24 hours to allow attachment before placing them in either a normal oxygen incubator (20% oxygen) or a hypoxia chamber (2% oxygen) for 24 hours. Cells were then treated with either iDHRX, exosomes, or free doxorubicin for 48 hours, the media was removed, and cells were washed three times to remove any remaining treatment. Subsequently, 20 μL of Alamar Blue

(10X, Invitrogen) and 180 µL of fresh medium were added. The absorbance was then measured at 570 nm and viability was calculated using **equation 1**.

$$\frac{(O2 \times A1)-(O1 \times A2)}{(O2 \times P1)-(O1 \times P2)} \; x\; 100 \qquad \text{(Equation 1)}$$

O1 = molar extinction coefficient (ε) of oxidized Alamar Blue at 570 nm (80,586)

O2 = ε of oxidized Alamar Blue at 600 nm (117,216)

A1 = absorbance of test wells at 570 nm

A2 = absorbance of test wells at 600 nm

P1 = absorbance of positive growth control well

P2 = absorbance of positive growth control well

Spheroid Cultures: Silicone molds were used to prepare spheroid scaffolds (Microtissues) using 2% agarose to create the "wells", following the manufacturer's protocol. Wells were seeded with 273,000 cells/190 µL to produce a spheroid with a diameter of at least 200-300 µm. The seeded scaffolds were incubated for 7 days, changing the RPMI-1640 with 10% FBS every 2 days. The scaffolds were then placed in either normoxic (20% oxygen) or hypoxic (2% oxygen) conditions for 24 h before respective treatments for 48 hours. Groups included no treatment, purified, unmodified exosomes encapsulating doxorubicin, free doxorubicin (1.25 µM), or iDHRX (5 µM, 7 µM, and 10 µM). After treatment, the scaffolds were washed with PBS before viability was analyzed by Celltiter-Glo 3D cell viability assay (Promega). Luminescence (SpectraMax, M5, Molecular Devices) was measured and viability was calculated according to the manufacturer's recommendations.

Penetration in Spheroid Cultures

The spheroids were allowed to grow for 7 days before to treatment. Treatment groups: control (no treatment), carboxyfluorescein, -iHRX, free doxorubicin, or carboxyfluorescein-iDHRX. After 7 days of growth, half of the spheroids were put in a hypoxic environment. After 24 hours, 1.25 µM free doxorubicin or 10 µM iDHRX was added. Spheroids were then imaged using fluorescence microscopy (20X, Leica Fluorescence Scope). A z-stack of each spheroid was constructed (from top to bottom) using steps of 5 µm. Each spheroid was visualized using both a Texas red filter to show the accumulation of doxorubicin and a FITC filter to show the exosome accumulation.

Results and Discussion

Characterization of Modified Exosomes

Exosomes were isolated from raw bovine milk. The diameter of the isolated exosomes was determined using dynamic light scattering (DLS), atomic force microscopy (AFM), and high-resolution transmission electron microscopy (HRTEM) (**Table 4.1**). As a rapid validation of the reproducibility of the isolation and modification processes, DLS was used to confirm that the size of each exosome batch was within the literature reports 30-150 nm (**Table 4.1**). To verify that the isolated extracellular vesicles are exosomes, flow cytometry for CD63 (a well-documented exosomal marker[30,35]) was performed (**Figure 4.5**). The larger diameter for the HRX is likely due to incorporating the hypoxia-responsive lipid and the iRGD-peptide conjugate with the PEG groups.

Table 4.1. Sizes of exosomes and hypoxia-responsive exosomes (HRX) by dynamic light scattering (DLS), atomic force microscopy (AFM), and high-resolution transmission microscopy (HRTEM).

	DLS Size (nm)	PDI	AFM (nm)	HRTEM (nm)
Isolated exosomes	52 ± 15	0.26 ± 0.08	60 ±10	40 ± 20
HRX	119 ± 24	0.23 ± 0.02	130 ±10	130 ± 20

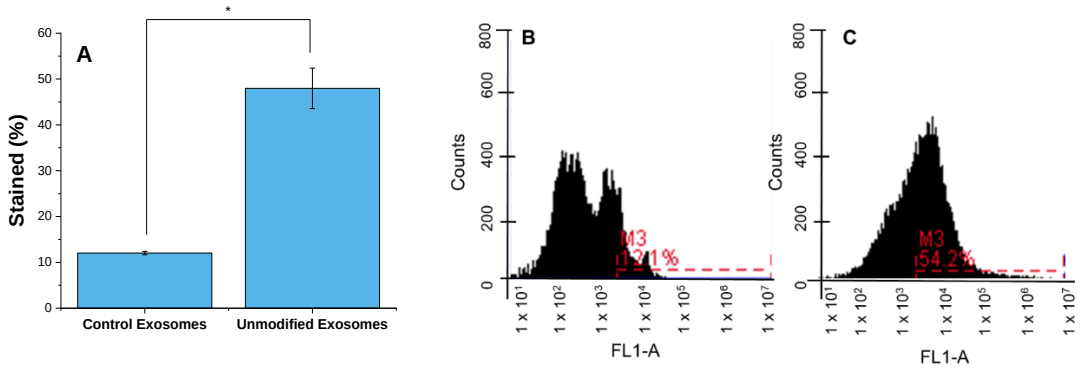

Figure 4.5. Flow Cytometry for CD63 of bovine milk exosomes. (A) Bar graph representing the difference in stained and unstained raw bovine milk exosomes. Control, unstained exosomes represents exosomes not exposed to the antibody; unmodified exosomes are exposed to the antibody but no further chemical modifications. Flow Cytometry plot of (B) raw unstained exosomes and (C) Raw stained. 20,000 hits were recorded. N = 3, $p < 0.001$ indicating significant difference between the two groups.

An accurate evaluation of their concentration was essential before modifying the isolated exosomes or using them for in vitro experiments with TNBC cells. Hence, exosome preparations were quantified using a tunable resistive pulse sensing instrument, giving an average of 1.1 x 10^{13} exosomes/mL. Purified exosomes were first modified to release encapsulated contents under reducing conditions. A synthesized hypoxia-responsive lipid (Figure 2) was incorporated into the exosome bilayer. The incorporation of the orange-red lipid into the bilayer was confirmed by UV-Vis spectroscopy. After optimization, a 100 µM solution of lipid (80 µL) and exosomes (120 µL approximately 1.3 x 10^{12} exosomes) provided the highest lipid incorporation (9.2 µM, 32% efficiency). The spherical structure and size of the exosomes were then confirmed by AFM (**Figure 4.5**), TEM (**Figure 4.6**), and DLS (**Table 4.1**). In addition to the hypoxia-responsive

lipid, an iRGD peptide (iRGD-DSPE-PEG_{5000}) was incorporated. Finally, doxorubicin, a chemotherapeutic, was encapsulated giving a completely modified exosome (iDHRX). Finally, doxorubicin, a chemotherapeutic, was encapsulated, giving a completely modified exosome (iDHRX). After incorporating the hypoxia-responsive lipid, iRGD-DSPE-PEG5000 modifications, and doxorubicin encapsulation, the exosomes were at a concentration of $5x10^{12}$ particles/mL **Figure 4.7**). The presence of iRGD-DSPE-PEG_{5000} on the HRX was confirmed through adhesion assay (**Figure 4.10**) and exosome structure through AFM. Doxorubicin encapsulation and efficiency [(65 ± 6)%, 90 μM].

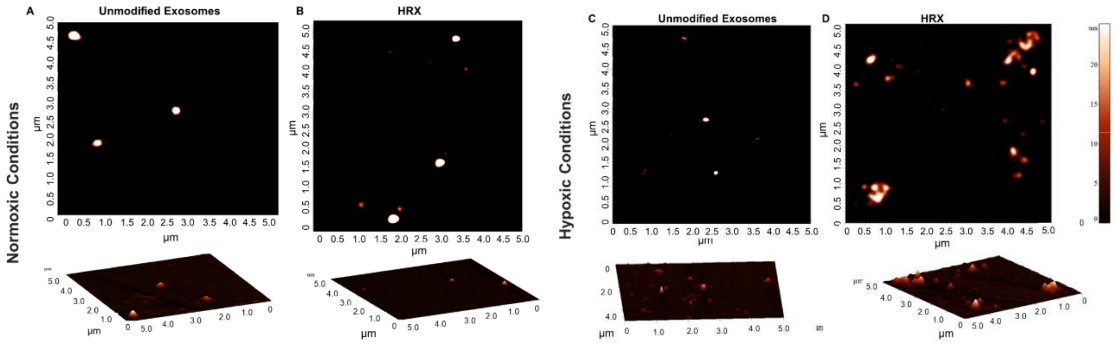

Figure 4.6. Atomic force microscopy images of unmodified exosomes and HRXs under normoxia and hypoxia. Fragments of the HRXs with of approximate size of 25 nm were observed in hypoxic conditions.

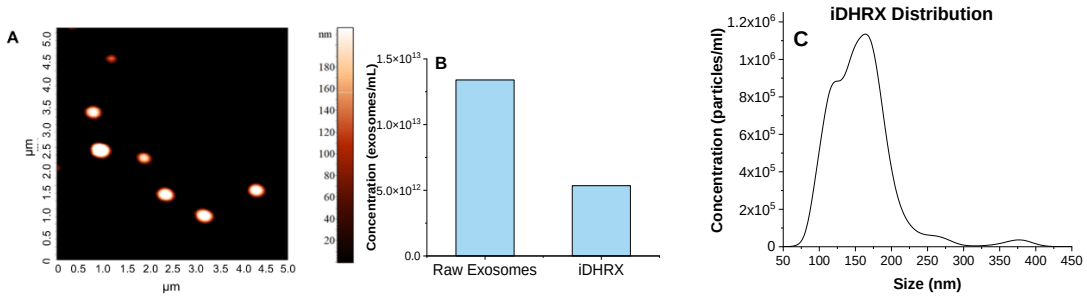

Figure 4.7. (**A**) AFM of iDHRX. The size range of exosomes 50 nm - 200 nm. (**B**) Particle counting for raw bovine milk exosomes and iDHRX. (**C**) The size distribution of iDHRX using qNano. The mode is 149 ± 7 nm and the mean is 167 ± 2 nm.

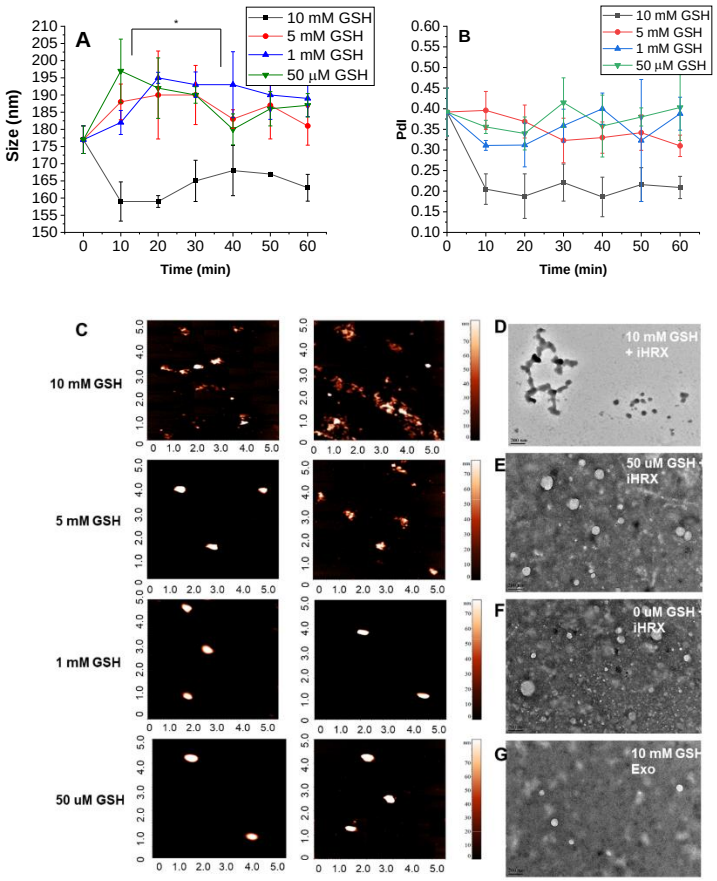

Figure 4.8. Size and shape of iHRX in the presence of glutathione. (A) Hydrodynamic diameters, (B) polydispersity indices, (C) AFM images, and (D) HR-TEM images of iHRX with glutathione as a function of time.

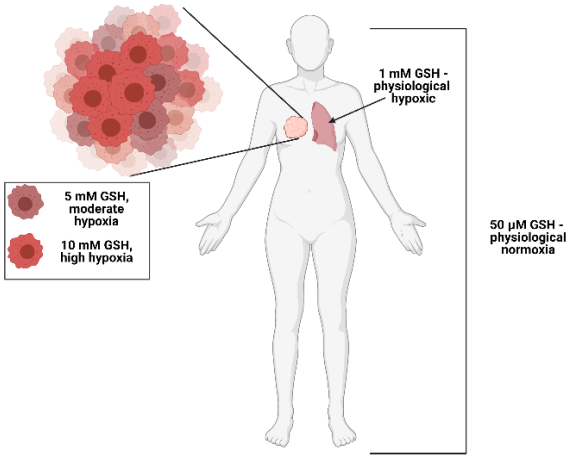

Figure 4.9. Glutathione (GSH) levels throughout the body. 50 uM GSH is physiological normoxia, 1 mM GSH is physiological hypoxia, 5 mM GSH is moderate hypoxia and 10 mM GSH is high hypoxia.

The reduction of the modified exosomes (iHRX) was determined using a glutathione concentration from 50 μM to 10 mM.45–47 With 10 mM glutathione, modified exosomes broke into fragments within 10 minutes of exposure. After 2 hours, exosomes exposed to 5 mM glutathione were fragmented. At concentrations less than 5 mM glutathione, HRX fragmentation was not observed. (**Figure 4.8**). Notably,10 mM glutathione is typically found within the center and most hypoxic niches of the tumors (**Figure 4.9**). The 5 mM glutathione is observed within the tumor's exterior margins during the transition to hypoxia and is significantly higher than other tissue within the body (1 mM to 50 μM).45–47 This fragmentation of exosomes at 10 mM glutathione with minimal fragmentation at 5 mM glutathione indicates that exosomes modified with a hypoxia-responsive lipid will only break under a reducing environment mimicking the hypoxic niches of solid tumors.

While incorporating the hypoxia-responsive lipid provides an efficient trigger to release the exosome-encapsulated payload, incorporation of iRGD peptide is essential for targeting, tumor penetration, and cellular internalization. A surface-adhesion assay was developed to confirm iRGD-DSPE-PEG5000 in the modified exosomes. The iRGD peptide interacts with αvβ3 integrin and NRP-1, both upregulated on cancer cells and facilitates targeting and penetration of the exosomes (**Figure 4.10**).[48–51] Hence, incorporating a single peptide, iRGD, can endow an exosome-based drug delivery system to both targets and penetrate. To visualize the iRGD peptide integrated into the exosomes' lipid bilayer, DSPE-PEG5000-FITC was incorporated into iHRX and exosomes. The surface of the slides were coated with the αvβ3 integrin allowing for iRGD peptide to bind, attaching to the surface. There was a significant increase (1.5-2 fold) in fluorescence intensity in CF-iHRX compared to the unmodified

exosomes (**Figure 4.11**). These results verified that the iRGD peptide was incorporated in the exosome bilayer.

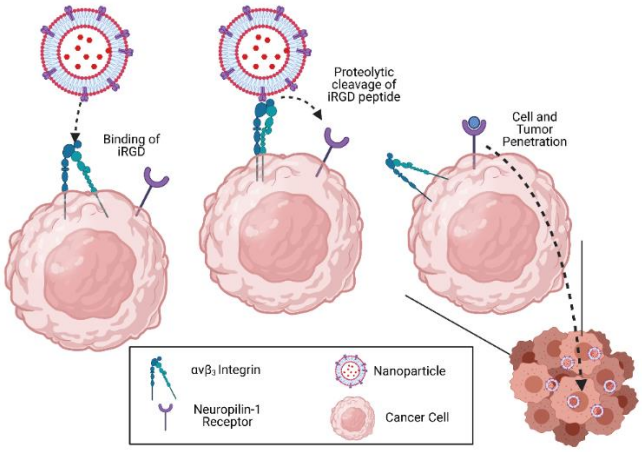

Figure 4.10. Mechanisms of iRGD peptide. iRGD peptide binds to αvβ3 integrin. Proteolytic cleavage occurs allowing for the transfer to the NRP-1 receptor which increases penetration into the solid tumor.

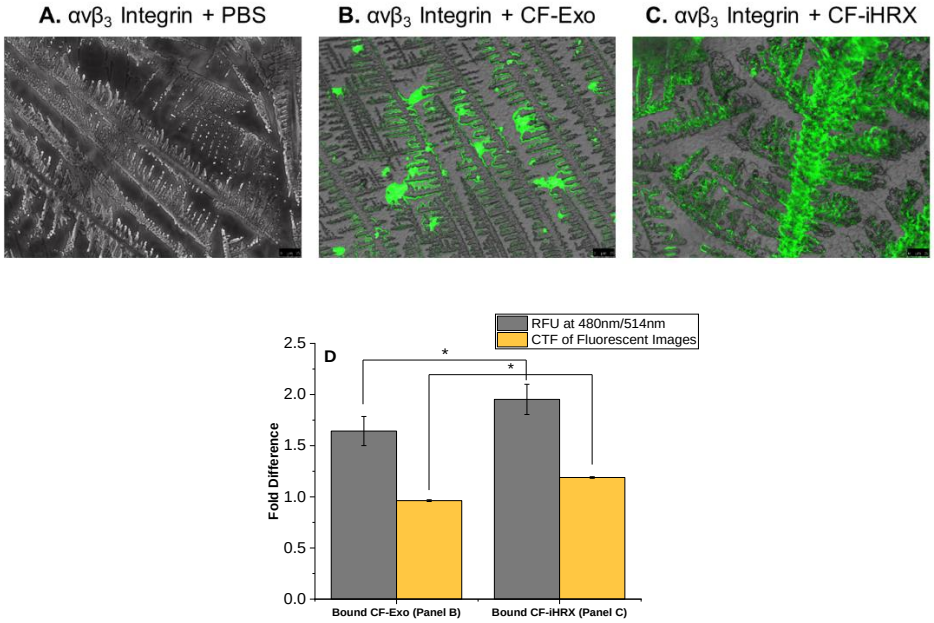

Figure 4.11. Adhesion assay of αvβ3 to iRGD peptide. Fluorescence images for (**A**) αvβ3 Integrin and PBS, (**B**) αvβ3 integrin and exosomes, and (**C**) αvβ3 integrin and iHRX. (**D**) Corrected total fluorescence and fluorescence signal show significant differences for both methods. N =12 and P-values <0.001

Cellular Studies

αvβ3 integrin expression in TNBC cells

The iRGD peptide first interacts with the αvβ3 integrin and then with NRP1 for the exosomes to penetrate the tumors.[40,42,49] The expressions of α_v and β_3 integrin subunits were confirmed on TNBC cell lines by western blotting. Expression levels for α_v integrin were consistent for HCC 1806 and HCC 1937 regardless of the amount of oxygen during cell culture. However, for MDA-MB-231 cells, α_v integrin expression was higher in normoxia than hypoxia; conversely, MDA-MB-468 cell lines showed higher αv expression levels in hypoxia compared to normoxia. The HCC 1806 and HCC 1937 cells showed increased expression of β_3 integrin in normoxic conditions, while MDA-MB-231 and MDA-MB-468 cell lines showed increased expression in hypoxic conditions. Overall, $\alpha_v\beta_3$ integrin is present on all cell lines, allowing the iRGD peptide on exosomes to interact (**Figure 4.12**)

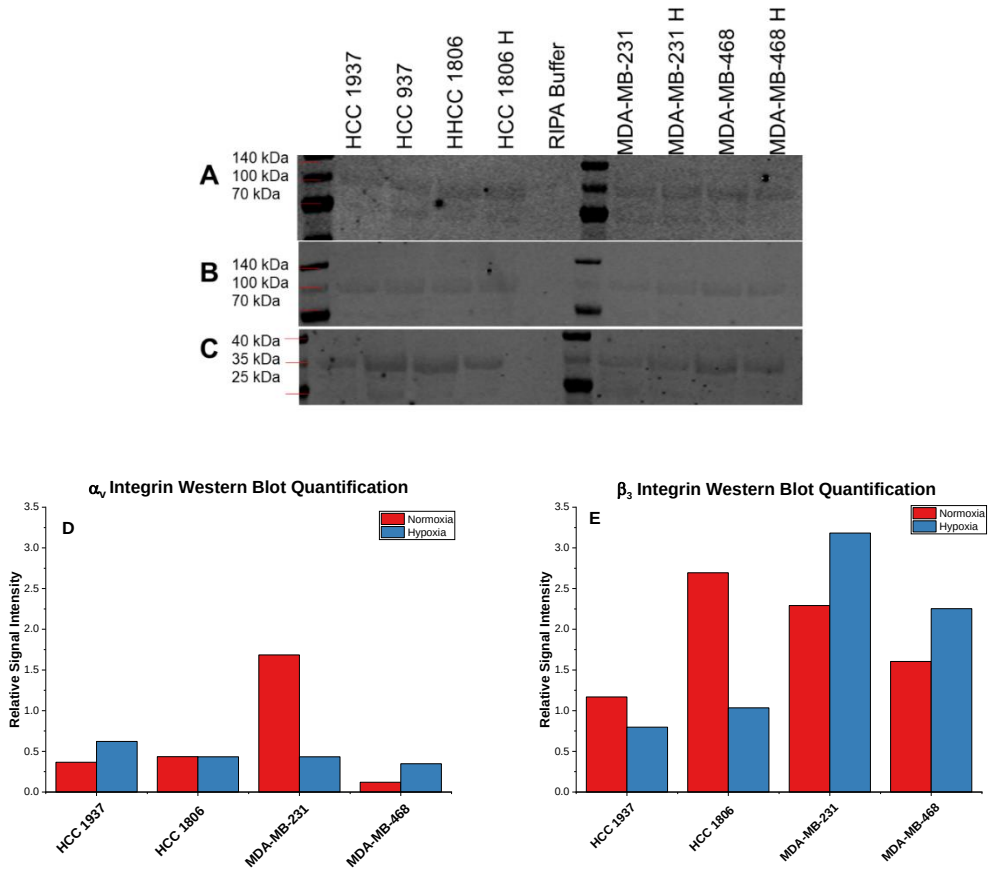

Figure 4.12. Western blot of integrin α_v and β_3 for cell lines HCC 1937, HCC 1806, MDA-MB-231, and MDA-MB-468 in normoxia and hypoxia. Western blots of (**A**) α_v integrin, (**B**) β_3 integrin, and (**C**) GAPDH. Quantification of (**C**) α_v integrin and (**D**) β_3 integrin compared to GAPDH.

NRP-1 expression in TNBC cells

Due to the crucial requirement of NRP1 expression for the penetration of nanoparticles, its expression in the cell lines was confirmed by flow cytometry and western blot analysis (**Figure 4.13**). Western blot analysis in hypoxia and normoxia showed different expression levels for all cell lines, except for MDA-MB-468. Flow cytometry indicated that MDA-MB-231 cells had increased NRP1 expression in hypoxic conditions, while HCC 1937 cells showed increased NRP1 expression in normoxic conditions. The NRP1 expression difference between normoxia

and hypoxia on the cells implies that certain cell lines may be more susceptible to iHRX drug delivery.

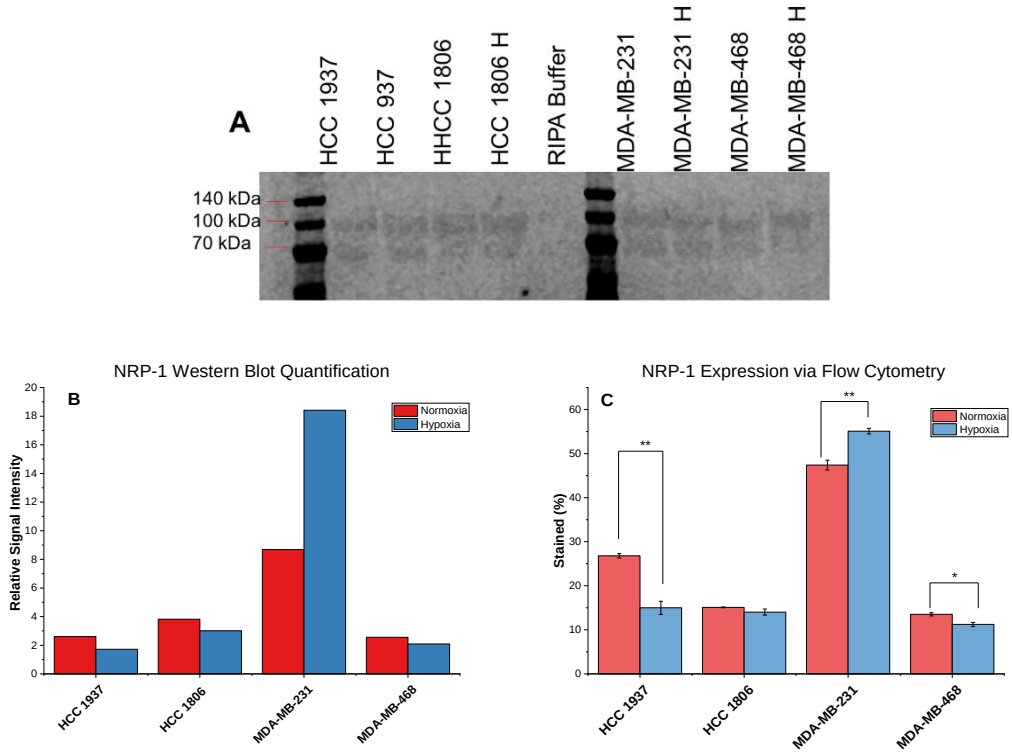

Figure 4.13. NRP1 expression for HCC 1937, HCC 1806, MDA-MB-231, and MDA-MB-468 cells in normoxia and hypoxia. (**A**) Western blot and (**B**) quantification (band intensity normalized to GAPDH) for each cell line. (**C**) NRP1 expression as determined by flow cytometry.

Normoixa Monolayer Cellular Internalization and Monolayer Cytotoxicity

Internalization of iRGD-exosomes (iDHRX) into monolayer MDA-MB-468, MDA-MB-231, HCC 1806, and HCC 1937 TNBC cells was monitored for 24 hours in normoxic conditions (**Figure 4.14**). iDHRX showed higher internalization after 2 hours compared to doxorubicin-encapsulated exosomes without the iRGD peptide (DExo). (**Figure 4.14**). Importantly, since doxorubicin levels were not visually detectable at 2 hours, DAPI levels, which indicate live cells, were compared as an indirect measurement of the effects of doxorubicin. (**Figure 4.14B**) Within the two hours after treating TNBC cells with doxorubicin in any form (free, encapsulated in

unmodified exosomes, or encapsulated in modified exosomes), the intensity of DAPI began to drop. Treating both HCC 1937 and MDA-MB-468s cells with iDHRX showed a quantifiable, significant difference in DAPI intensity. This difference could be attributed to the multiple uptake pathways of exosomes. For example, HCC 1937 cells have higher exosomal uptake compared to other cell lines regardless of NRP-1 and $\alpha_v\beta_3$ integrin expression levels in a 2D monolayer environment. [52–55] Labeling of the exosomes and higher magnification of individual cells would have increased resolution and may have allowed a more direct measurement of doxorubicin uptake, allowing a more mechanistic evaluation of cell line specific uptake. Regardless of the mechanism, exosomes, modified and unmodified, are being taken up by the cells and appear to be killing the cells within 2 hours, similar to free doxorubicin. Additional studies, such as evaluating DNA damage, looking for apoptotic bodies, or determining the level and function of topoisomerase II, to precisely measure exact levels of cell death at these early time points would assist in determining the mechanisms of cells death in the initial stages of internalization.[52]

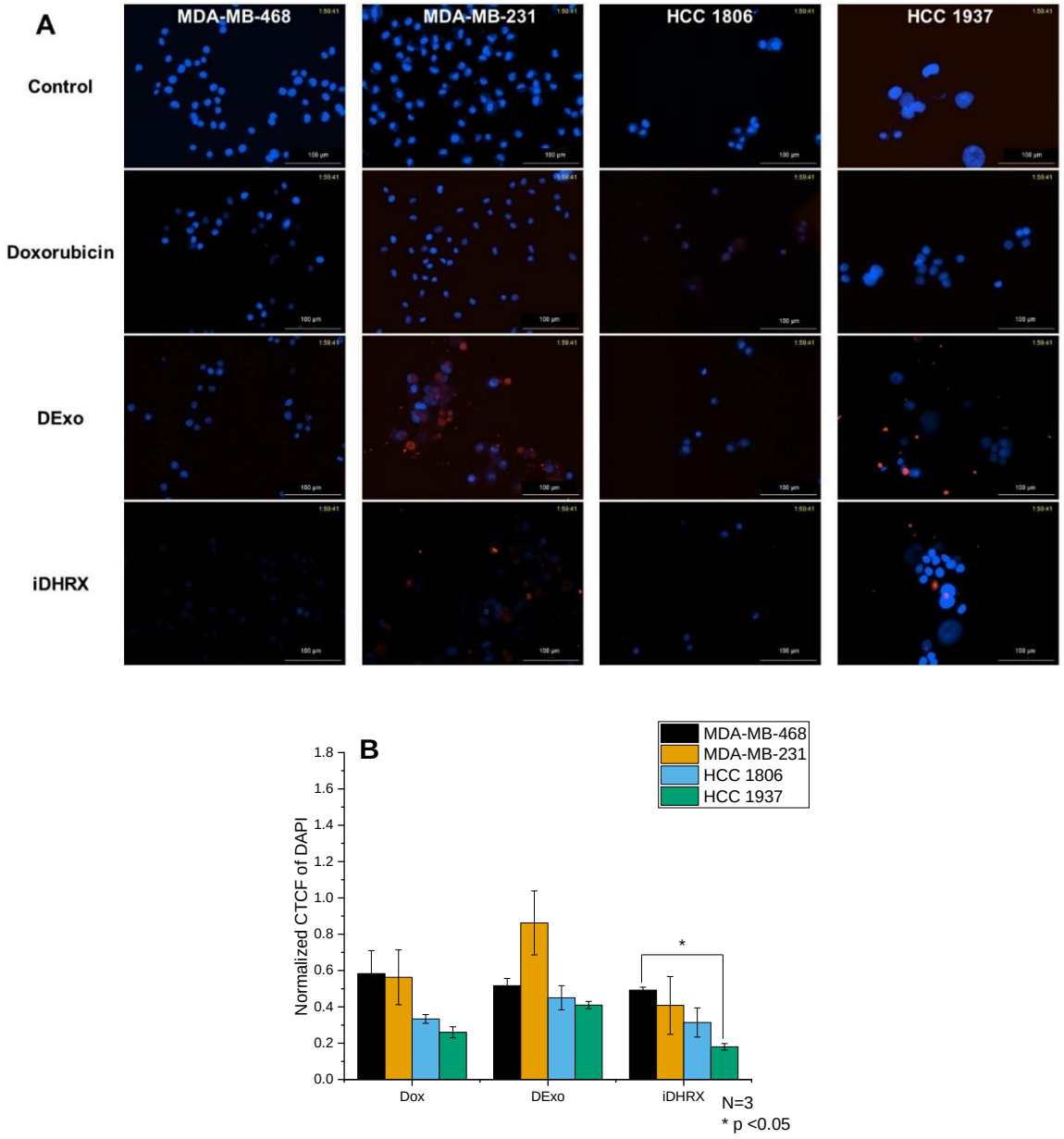

Figure 4.14. (**A**) Cellular Internalization for MDA-MB-468, MDA-MB-231, HCC 1806, and HCC 1937 at 2 hours. (**B**) Quantification of DAPI and normalized to the number of cells 2 hours after treatment with doxorubicin, indirectly indicating doxorubicin internalization. Notably, HCC 1937 cells and MDA-MB-468 cells show a statistically significant difference in DAPI intensity after 2 hours of treatment with iDHRX. N = 3, * $p<0.05$, ** $p<0.001$.

Monolayer cytotoxicity results for the four cell lines indicated significant ($p < 0.001$) cell death when treated with iDHRX compared to both unmodified exosomes and no treatment controls (**Figure 4.15**). Doxorubicin concentrations of 0.5 µM to 20 µM in iDHRX were tested

for MDA-MB-468, HCC 1806, and HCC 1937 cells. The lowest concentration of iDHRX to show significance amongst each cell line is reported. EC50 values (**Table 4.2**) were calculated for each cell line based on these cytotoxicity results. As expected, HCC 1937 cells had increased EC50 values compared to other cell lines tested.[53] The variability of the EC50 and effectiveness of treatment is likely due to genetic variability and protein expression (efflux pumps) on the cells. Additionally, the lack of tumor microenvironment and cellular interactions can also affect the effectiveness of treatment, indicating a need for 3D spheroid viability and penetration results.

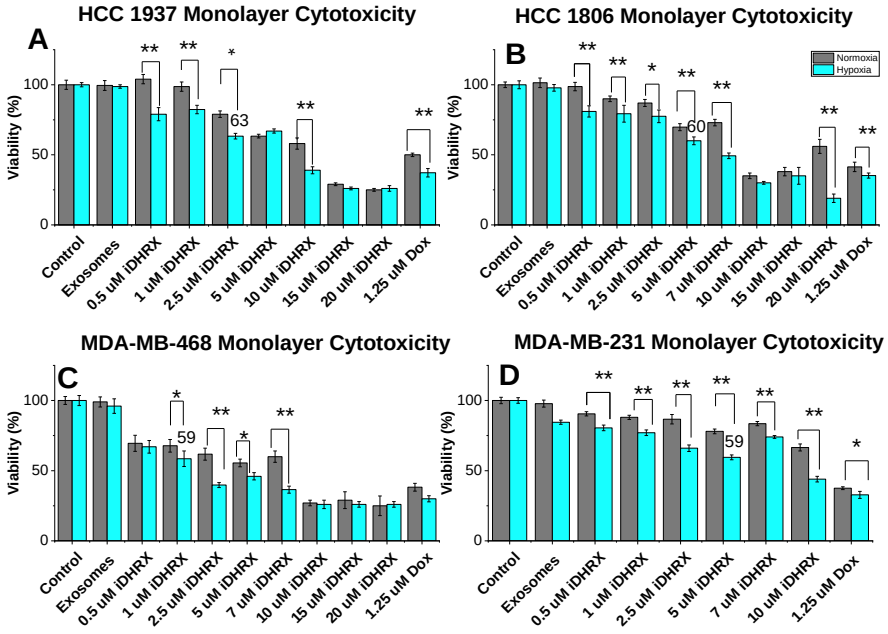

Figure 4.15. Monolayer Cytotoxicity for **A**. HCC 1937, **B**. HCC 1806, **C**. MDA-MB-468 and **D**. MDA-MB-231. 24 replicates were performed for each cell type. * $p<0.05$, ** $p<0.001$.

Table 4.2. Monolayer EC50 values for all cell lines in normoxia or hypoxia at concentrations of µM.

Cell Line	EC50 Value (µM)	Cell Line	EC50 Value (µM)
MDA-MB-468 Normoxia	6.1 ± 2.2	HCC 1806 Normoxia	6.7 ± 1.4
MDA-MB-468 Hypoxia	4.9 ± 0.3	HCC 1806 Hypoxia	6.9 ± 1.8
MDA-MB-231 Normoxia	5.2 ± 0.4	HCC 1937 Normoxia	9.0 ± 1.7
MDA-MB-231 Hypoxia	3.7± 0.7	HCC 1937 Hypoxia	6.3 ± 1.8

3D spheroid cytotoxicity and depth of penetration

A 3D spheroid cytotoxicity assay indicated less cell death than monolayer cultures (**Figure 4.16**). For spheroids, a hypoxic gradient begins to form at 200 µm, allowing external hypoxia conditions to serve as a control. [23,54,55] Consequently, the spheroids showed similar viability in both hypoxia and normoxia. MDA-MB cells showed more significant death at several dosages compared to HCC cells. HCC 1937 spheroids showed significant cell death at 10 µM iDHRX and 1.25 µM doxorubicin and showed the least effective treatment compared to other cell lines. This is likely due to the efflux pumps and doxorubicin resistance often found in the HCC 1937 cells. [53,56,57] EC50 values (**Table 4.3**) were calculated for spheroid cultures and indicated equivalent to slightly higher values to that of monolayer EC50 values.

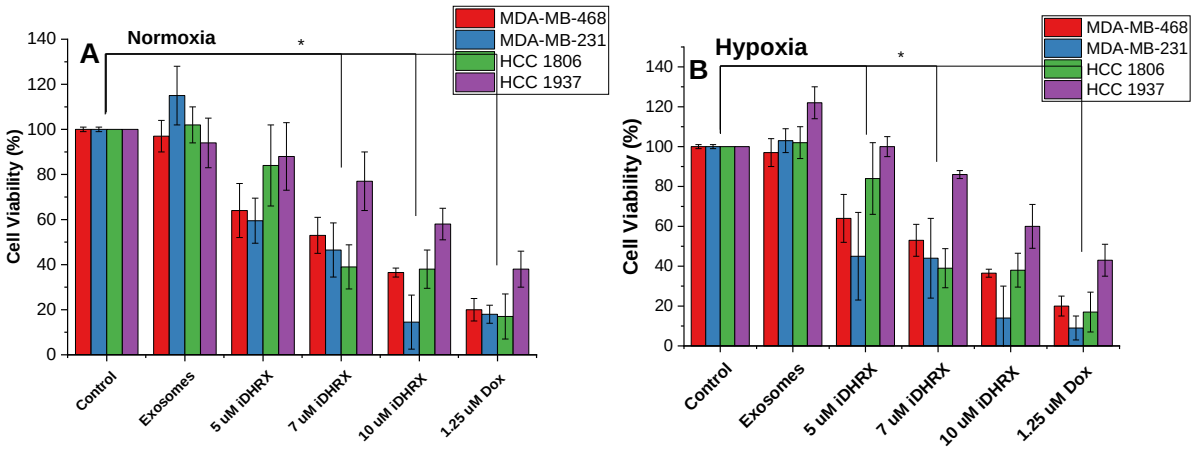

Figure 4.16. Spheroid viability for HCC 1806 (green), HCC 1937 (purple), MDA-MB-468 (red), and MDA-MB-231 (blue) triple-negative breast cancer cell lines. Each cell line was treated in a normoxic (**A**) and hypoxic (**B**) environment for 48 hours. N = 3 *p<0.05

Table 4.3. Spheroid EC50 values for all cell lines in normoxia or hypoxia at concentrations of μM.

Cell Line	EC50 Value (μM)	Cell Line	EC50 Value (μM)
MDA-MB-468 Normoxia	4.4 ± 0.8	HCC 1806 Normoxia	6.7 ± 2.6
MDA-MB-468 Hypoxia	5.9 ± 1.8	HCC 1806 Hypoxia	6.9 ± 0.7
MDA-MB-231 Normoxia	7.1 ± 3.1	HCC 1937 Normoxia	10.4 ± 2.6
MDA-MB-231 Hypoxia	8.2 ± 1.2	HCC 1937 Hypoxia	9.9 ±0.9

Analyses of the depth of penetration of iDHRX in the cultured spheroids were performed by confocal fluorescence microscopy. Visual comparisons were made for treatments with 1.25 μM free doxorubicin and 10 μM iDHRX at 30 minutes, 1 hour, 2 hours, 6 hours, and 24 hours. iDHRX reached the center of the 3D spheroids within 1 hour, while free doxorubicin does not reach the same levels until at least 2 hours. By 6 hours, the penetration levels become steady, indicating an equilibrium between the interior and exterior of the 3D spheroid has been reached for both free doxorubicin and iDHRX. (**Figure 4.17 and 4.18**) While the images and viability data display the beginning of an explination of exosome penetration and doxorubicin efficacy within spheroids there are some questions regarding the exact uptake mechanism of iDHRX that a continuous monitoring at higher magnification will answer but are currently unavailable.

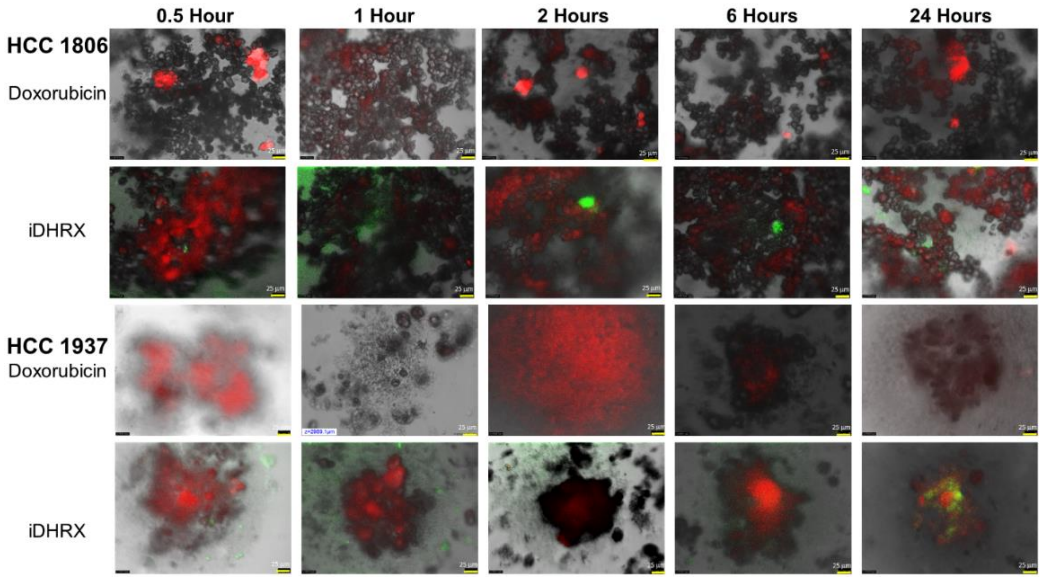

Figure 4.17. Penetration of doxorubicin and iDHRX in the spheroids of HCC 1806 and HCC 1937 cell spheroids. Doxorubicin was visualized using Texas red fluorescence filter. Exosomes were visualized using a FITC filter. Each image is taken at the focus depth, each slice is 5 µm thick. Scale bar is 25 µm.

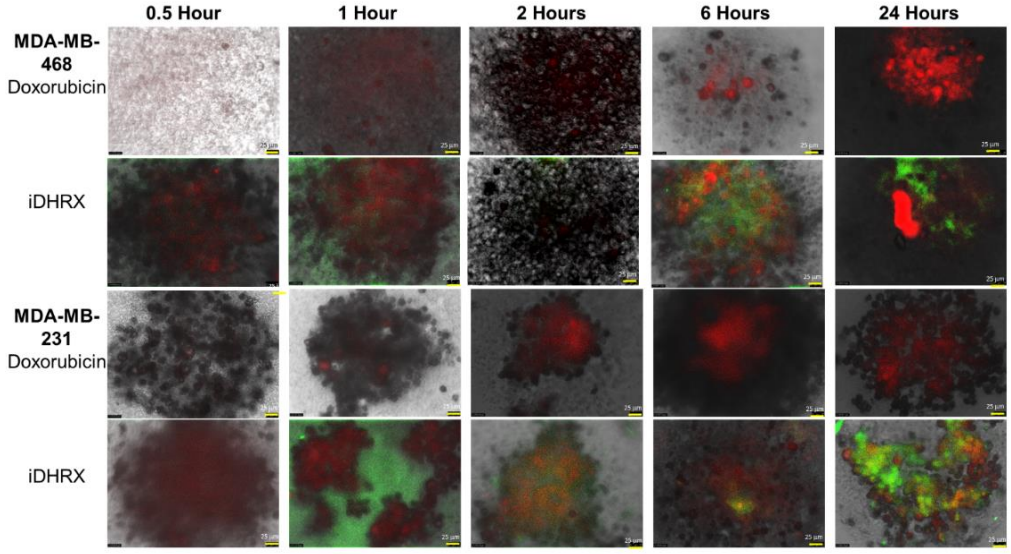

Figure 4.18. Penetration of doxorubicin and iDHRX in the spheroids MDA-MB-468 and MDA-MB-231 cell spheroids. Doxorubicin was visualized using Texas red fluorescence filter. Exosomes were visualized using a FITC filter. Each image is taken at the focus depth, each slice is 5 µm thick. Scale bar is 25µm.

Comparative analysis of primary versus metastasis site

A statistical analysis of all spheroids' iDHRX treatments in normoxia was performed. At 10 μM iDHRX treatment, cell viability was highest for HCC 1937 spheroids (58%) and lowest for MDA-MB-231 spheroids (14%, Figure 16). Overall, HCC 1937 cell spheroids showed increased viability than the others, possibly due to the doxorubicin resistance for this primary tumor-derived cell line.61 The MDA-MB-231 and MDA-MB-468 cells showed decreased cell viability, indicating they respond better to doxorubicin and the iDHRX treatment in an in vitro tumor microenvironment (**Figure 4.19**).

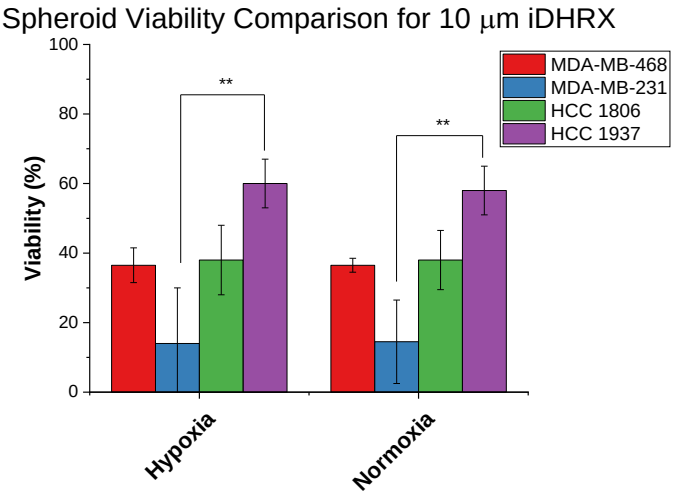

Figure 4.19. 3D Spheroid Cytotoxicity Comparison between metastatic and primary tumor sites for iDHRX in normoxia and hypoxia. N= 3 * p <0.05, ** p<0.001

Conclusions

Bovine milk exosomes have been successfully modified for active targeting to NRP-1 and hypoxia sensitivity, and a chemotherapeutic agent was then encapsulated. The hypoxia-responsive lipid and iRGD peptide modifications facilitated the delivery of doxorubicin to triple-negative breast cancer cells. The modified exosomes fragment in hypoxia (2% or less oxygen), causing the encapsulated doxorubicin to release. The iRGD peptide on the surface allowed the

exosomes to penetrate the spheroids of the breast cancer cells. The released doxorubicin showed significant cytotoxicity in monolayer and spheroid cultures of the four different triple-negative breast cancer cell lines.

Acknowledgements

HRTEM material is based upon work supported by the National Science Foundation under Grant No. 0821655. Any opinions, findings, and conclusions or recommendations expressed in this material are those of the author(s) and do not necessarily reflect the views of the National Science Foundation. All other work was based upon the support of National Institute of Heath under Grant No. 2RO1GM114040.

Author Contributions

S.M., VS, and K.S. acknowledge support from NIH (NIGMS) grant 2R01GM 114080. S.M. also acknowledges partial supports from NIH grant U54 GM12872 and NSF EPSCoR Track-1 Cooperative Agreement OIA #1946202. Any opinions, findings, and conclusions or recommendations expressed in this material are those of the author(s) and do not necessarily reflect the views of the NSF.

Conflicts of Interest

The authors declare no conflict of interest. The funders had no role in the design of this publication; in the collection, analyses, or interpretation of data; in the writing of the manuscript, or in the decision to publish the results.

References

1 Siegel, R. L.; Miller, K. D.; Jemal, A. Cancer Statistics, 2020. CA: A Cancer Journal for Clini-cians 2020, 70 (1), 7–30. https://doi.org/10.3322/caac.21590.

2 Goldman, E.; Zinger, A.; da Silva, D.; Yaari, Z.; Kajal, A.; Vardi-Oknin, D.; Goldfeder, M.; Schroeder, J. E.; Shainsky-Roitman, J.; Hershkovitz, D.; Schroeder, A. Nanoparticles Target Early-Stage Breast Cancer Metastasis in Vivo. Nanotechnology 2017, 28 (43), 43LT01. https://doi.org/10.1088/1361-6528/aa8a3d.

3 Jamdade, V. S.; Sethi, N.; Mundhe, N. A.; Ku-mar, P.; Lahkar, M.; Sinha, N. Therapeutic Targets of Triple-Negative Breast Cancer: A Review. Br J Pharmacol 2015, 172 (17), 4228–4237. https://doi.org/10.1111/bph.13211.
4 Triple-negative Breast Cancer | Details, Diag-nosis, and Signs https://www.cancer.org/cancer/breast-cancer/understanding-a-breast-cancer-diagnosis/types-of-breast-cancer/triple-negative.html (accessed Mar 18, 2021).
5 da Silva, J. L.; Cardoso Nunes, N. C.; Izetti, P.; de Mesquita, G. G.; de Melo, A. C. Triple Neg-ative Breast Cancer: A Thorough Review of Biomarkers. Critical Reviews in Oncolo-gy/Hematology 2020, 145, 102855. https://doi.org/10.1016/j.critrevonc.2019.102855.
6 Tzikas, A.-K.; Nemes, S.; Linderholm, B. K. A Comparison between Young and Old Patients with Triple-Negative Breast Cancer: Biology, Survival and Metastatic Patterns. Breast Can-cer Res Treat 2020, 182 (3), 643–654. https://doi.org/10.1007/s10549-020-05727-x.
7 Sharma, P. Biology and Management of Pa-tients With Triple-Negative Breast Cancer. Oncologist 2016, 21 (9), 1050–1062. https://doi.org/10.1634/theoncologist.2016-0067.
8 Lyons, T. G. Targeted Therapies for Triple-Negative Breast Cancer. Curr. Treat. Options in Oncol. 2019, 20 (11), 82. https://doi.org/10.1007/s11864-019-0682-x.
9 Joiner, M. C.; Kogel, A. J. van der. Basic Clini-cal Radiobiology; CRC Press, 2018.
10 Soltani, M.; Chen, P. Effect of Tumor Shape and Size on Drug Delivery to Solid Tumors. Journal of Biological Engineering 2012, 6 (1), 4. https://doi.org/10.1186/1754-1611-6-4.
11 Soltani, M.; Chen, P. Numerical Modeling of Fluid Flow in Solid Tumors. PLoS One 2011, 6 (6). https://doi.org/10.1371/journal.pone.0020344.
12 Kim, Y.; Stolarska, M. A.; Othmer, H. G. The Role of the Microenvironment in Tumor Growth and Invasion. Prog Biophys Mol Biol 2011, 106 (2), 353–379. https://doi.org/10.1016/j.pbiomolbio.2011.06.006.
13 Belli, C.; Trapani, D.; Viale, G.; D'Amico, P.; Duso, B. A.; Della Vigna, P.; Orsi, F.; Curigliano, G. Targeting the Microenviron-ment in Solid Tumors. Cancer Treatment Reviews 2018, 65, 22–32. https://doi.org/10.1016/j.ctrv.2018.02.004.
14 Bender, R. J.; Gabhann, F. M. Expression of VEGF and Semaphorin Genes Define Subgroups of Triple Negative Breast Cancer. PLOS ONE 2013, 8 (5), e61788. https://doi.org/10.1371/journal.pone.0061788.
15 Naik, A.; Al-Zeheimi, N.; Bakheit, C. S.; Al Ri-yami, M.; Al Jarrah, A.; Al Moundhri, M. S.; Al Habsi, Z.; Basheer, M.; Adham, S. A. Neuro-pilin-1 Associated Molecules in the Blood Dis-tinguish Poor Prognosis Breast Cancer: A Cross-Sectional Study. Sci Rep 2017, 7. https://doi.org/10.1038/s41598-017-03280-0.
16 Darvishi, B.; Boroumandieh, S.; Majidzadeh-A, K.; Salehi, M.; Jafari, F.; Farahmand, L. The Role of Activated Leukocyte Cell Adhesion Molecule (ALCAM) in Cancer Progression, In-vasion, Metastasis and Recurrence: A Novel Cancer Stem Cell Marker and Tumor-Specific Prognostic Marker. Experimental and Molecu-lar Pathology 2020, 104443. https://doi.org/10.1016/j.yexmp.2020.104443.
17 Mani, S. A.; Guo, W.; Liao, M.-J.; Eaton, E. Ng.; Ayyanan, A.; Zhou, A. Y.; Brooks, M.; Reinhard, F.; Zhang, C. C.; Shipitsin, M.; Campbell, L. L.; Polyak, K.; Brisken, C.; Yang, J.; Weinberg, R. A. The Epithelial-Mesenchymal Transition Generates Cells with Properties of Stem Cells. Cell 2008, 133 (4), 704–715. https://doi.org/10.1016/j.cell.2008.03.027.

18 Park, S.-Y.; Choi, J.-H.; Nam, J.-S. Targeting Cancer Stem Cells in Triple-Negative Breast Cancer. Cancers (Basel) 2019, 11 (7). https://doi.org/10.3390/cancers11070965.
19 Morel, A.-P.; Lièvre, M.; Thomas, C.; Hinkal, G.; Ansieau, S.; Puisieux, A. Generation of Breast Cancer Stem Cells through Epithelial-Mesenchymal Transition. PLoS One 2008, 3 (8). https://doi.org/10.1371/journal.pone.0002888.
20 Rahman, S. M.; Campbell, J. M.; Coates, R. N.; Render, K. M.; Byrne, C. E.; Martin, E. C.; Melvin, A. T. Evaluation of Intercellular Communication between Breast Cancer Cells and Adipose-Derived Stem Cells via Passive Diffusion in a Two-Layer Microfluidic Device. Lab Chip 2020. https://doi.org/10.1039/D0LC00142B.
21 Kong, D.; Hughes, C. J.; Ford, H. L. Cellular Plasticity in Breast Cancer Progression and Therapy. Front. Mol. Biosci. 2020, 7. https://doi.org/10.3389/fmolb.2020.00072.
22 Reynolds, D. S.; Tevis, K. M.; Blessing, W. A.; Colson, Y. L.; Zaman, M. H.; Grinstaff, M. W. Breast Cancer Spheroids Reveal a Differential Cancer Stem Cell Response to Chemothera-peutic Treatment. Scientific Reports 2017, 7 (1), 10382. https://doi.org/10.1038/s41598-017-10863-4.
23 McKeown, S. R. Defining Normoxia, Physoxia and Hypoxia in Tumours—Implications for Treatment Response. Br J Radiol 2014, 87 (1035). https://doi.org/10.1259/bjr.20130676.
24 Kulkarni, P.; Haldar, M. K.; Katti, P.; Dawes, C.; You, S.; Choi, Y.; Mallik, S. Hypoxia Re-sponsive, Tumor Penetrating Lipid Nanoparti-cles for Delivery of Chemotherapeutics to Pancreatic Cancer Cell Spheroids. Bioconjug Chem 2016, 27 (8), 1830–1838. https://doi.org/10.1021/acs.bioconjchem.6b00241.
25 Sharma, A.; Arambula, J. F.; Koo, S.; Kumar, R.; Singh, H.; Sessler, J. L.; Kim, J. S. Hypoxia-Targeted Drug Delivery. Chem. Soc. Rev. 2019, 48 (3), 771–813. https://doi.org/10.1039/C8CS00304A.
26 Sugahara, K. N.; Teesalu, T.; Karmali, P. P.; Kotamraju, V. R.; Agemy, L.; Girard, O. M.; Hanahan, D.; Mattrey, R. F.; Ruoslahti, E. Tis-sue-Penetrating Delivery of Compounds and Nanoparticles into Tumors. Cancer Cell 2009, 16 (6), 510–520. https://doi.org/10.1016/j.ccr.2009.10.013.
27 Zhang, Y.-R.; Lin, R.; Li, H.-J.; He, W.; Du, J.-Z.; Wang, J. Strategies to Improve Tumor Pene-tration of Nanomedicines through Nanoparti-cle Design. Wiley Interdisciplinary Reviews: Nanomedicine and Nanobiotechnology 2018, 0 (0), e1519. https://doi.org/10.1002/wnan.1519.
28 Kadonosono, T.; Yamano, A.; Goto, T.; Tsu-baki, T.; Niibori, M.; Kuchimaru, T.; Kizaka-Kondoh, S. Cell Penetrating Peptides Improve Tumor Delivery of Cargos through Neuropilin-1-Dependent Extravasation. Journal of Con-trolled Release 2015, 201, 14–21. https://doi.org/10.1016/j.jconrel.2015.01.011.
29 Pullan, J. E.; Shreffler, J. W.; Dailey, K. M.; Mallik, S.; Brooks, A. E. Overcoming Hurdles in Nanoparticle Clinical Translation: The In-fluence of Experimental Design and Surface Modification. International Journal of Molecu-lar Sciences 2019, 20 (23), 6056. https://doi.org/10.3390/ijms20236056.
30 Munagala, R.; Aqil, F.; Jeyabalan, J.; Gupta, R. C. Bovine Milk-Derived Exosomes for Drug Delivery. Cancer Lett 2016, 371 (1), 48–61. https://doi.org/10.1016/j.canlet.2015.10.020.

31 De Toro, J.; Herschlik, L.; Waldner, C.; Mongini, C. Emerging Roles of Exosomes in Normal and Pathological Conditions: New In-sights for Diagnosis and Therapeutic Applica-tions. Front. Immunol. 2015, 6. https://doi.org/10.3389/fimmu.2015.00203.
32 Corrado, C.; Raimondo, S.; Chiesi, A.; Ciccia, F.; De Leo, G.; Alessandro, R. Exosomes as In-tercellular Signaling Organelles Involved in Health and Disease: Basic Science and Clinical Applications. Int J Mol Sci 2013, 14 (3), 5338–5366. https://doi.org/10.3390/ijms14035338.
33 Azmi, A. S.; Bao, B.; Sarkar, F. H. Exosomes in Cancer Development, Metastasis and Drug Resistance: A Comprehensive Review. Cancer Metastasis Rev 2013, 32 (0). https://doi.org/10.1007/s10555-013-9441-9.
34 Becker, A.; Thakur, B. K.; Weiss, J. M.; Kim, H. S.; Peinado, H.; Lyden, D. Extracellular Vesi-cles in Cancer: Cell-to-Cell Mediators of Me-tastasis. Cancer Cell 2016, 30 (6), 836–848. https://doi.org/10.1016/j.ccell.2016.10.009.
35 Samuel, M.; Chisanga, D.; Liem, M.; Keerthikumar, S.; Anand, S.; Ang, C.-S.; Adda, C. G.; Versteegen, E.; Jois, M.; Mathivanan, S. Bovine Milk-Derived Exosomes from Colos-trum Are Enriched with Proteins Implicated in Immune Response and Growth. Scientific Re-ports 2017, 7 (1), 5933. https://doi.org/10.1038/s41598-017-06288-8.
36 Kang, T.; Gao, X.; Hu, Q.; Jiang, D.; Feng, X.; Zhang, X.; Song, Q.; Yao, L.; Huang, M.; Jiang, X.; Pang, Z.; Chen, H.; Chen, J. INGR-Modified PEG-PLGA Nanoparticles That Recognize Tu-mor Vasculature and Penetrate Gliomas. Bi-omaterials 2014, 35 (14), 4319–4332. https://doi.org/10.1016/j.biomaterials.2014.01.082.
37 Alberici, L.; Roth, L.; Sugahara, K. N.; Agemy, L.; Kotamraju, V. R.; Teesalu, T.; Bordignon, C.; Traversari, C.; Rizzardi, G.-P.; Ruoslahti, E. De Novo Design of a Tumor-Penetrating Pep-tide. Cancer Res 2013, 73 (2), 804–812. https://doi.org/10.1158/0008-5472.CAN-12-1668.
38 Sun, Q.; Ojha, T.; Kiessling, F.; Lammers, T.; Shi, Y. Enhancing Tumor Penetration of Na-nomedicines. Biomacromolecules 2017, 18 (5), 1449–1459. https://doi.org/10.1021/acs.biomac.7b00068.
39 Diaz Bessone, M. I.; Simón-Gracia, L.; Scodel-ler, P.; Ramirez, M. de los A.; Lago Huvelle, M. A.; Soler-Illia, G. J. A. A.; Simian, M. IRGD-Guided Tamoxifen Polymersomes Inhibit Es-trogen Receptor Transcriptional Activity and Decrease the Number of Breast Cancer Cells with Self-Renewing Capacity. J Nanobiotech-nology 2019, 17. https://doi.org/10.1186/s12951-019-0553-4.
40 Liu, X.; Jiang, J.; Ji, Y.; Lu, J.; Chan, R.; Meng, H. Targeted Drug Delivery Using IRGD Peptide for Solid Cancer Treatment. Mol. Syst. Des. Eng. 2017, 2 (4), 370–379. https://doi.org/10.1039/C7ME00050B.
41 Ma, L.; Chen, Q.; Ma, P.; Han, M. K.; Xu, Z.; Kang, Y.; Xiao, B.; Merlin, D. IRGD-Functionalized PEGylated Nanoparticles for Enhanced Colon Tumor Accumulation and Targeted Drug Delivery. Nanomedicine (Lond) 2017, 12 (16), 1991–2006. https://doi.org/10.2217/nnm-2017-0107.
42 Zuo, H. iRGD: A Promising Peptide for Cancer Imaging and a Potential Therapeutic Agent for Various Cancers https://www.hindawi.com/journals/jo/2019/9367845/ (accessed May 11, 2020). https://doi.org/10.1155/2019/9367845.
43 Kang, S.; Lee, S.; Park, S. IRGD Peptide as a Tumor-Penetrating Enhancer for Tumor-Targeted Drug Delivery. Polymers (Basel) 2020, 12 (9). https://doi.org/10.3390/polym12091906.

44 Pullan, J. E.; Chemeiti, P.; Confeld, M.; Feng, L.; Froberg, J.; Choi, Y.; Mallik, S. Hypoxia Re-sponsive Lipid Incorporation Into Bovine Milk Exosomes. Biomedical Science Instrumenta-tion 2018, 54 (1), 293–300.
45 Gamcsik, M. P.; Kasibhatla, M. S.; Teeter, S. D.; Colvin, O. M. Glutathione Levels in Human Tumors. Biomarkers 2012, 17 (8), 671–691. https://doi.org/10.3109/1354750X.2012.715672.
46 Tu, Y.; Peng, F.; White, P. B.; Wilson, D. A. Redox-Sensitive Stomatocyte Nanomotors: Destruction and Drug Release in the Presence of Glutathione. Angewandte Chemie Interna-tional Edition 2017, 56 (26), 7620–7624. https://doi.org/10.1002/anie.201703276.
47 Bansal, A.; Simon, M. C. Glutathione Metabo-lism in Cancer Progression and Treatment Re-sistance. J Cell Biol 2018, 217 (7), 2291–2298. https://doi.org/10.1083/jcb.201804161.
48 Ding, N.; Zou, Z.; Sha, H.; Su, S.; Qian, H.; Meng, F.; Chen, F.; Du, S.; Zhou, S.; Chen, H.; Zhang, L.; Yang, J.; Wei, J.; Liu, B. IRGD Syner-gizes with PD-1 Knockout Immunotherapy by Enhancing Lymphocyte Infiltration in Gastric Cancer. Nat Commun 2019, 10. https://doi.org/10.1038/s41467-019-09296-6.
49) Danhier, F.; Le Breton, A.; Préat, V. RGD-Based Strategies To Target Alpha(v) Beta(3) Integrin in Cancer Therapy and Diagnosis. Mol. Pharmaceutics 2012, 9 (11), 2961–2973. https://doi.org/10.1021/mp3002733.
50) Liu, Z.; Wang, F.; Chen, X. Integrin Avβ3-Targeted Cancer Therapy. Drug Dev Res 2008, 69 (6), 329–339. https://doi.org/10.1002/ddr.20265.
51) Sloan, E. K.; Pouliot, N.; Stanley, K. L.; Chia, J.; Moseley, J. M.; Hards, D. K.; Anderson, R. L. Tumor-Specific Expression of Avβ3 Integrin Promotes Spontaneous Metastasis of Breast Cancer to Bone. Breast Cancer Res 2006, 8 (2), R20. https://doi.org/10.1186/bcr1398.
52 Johnson-Arbor, K.; Dubey, R. Doxorubicin. In StatPearls; StatPearls Publishing: Treasure Is-land (FL), 2021.
53 Calcagno, A. M.; Fostel, J. M.; To, K. K. W.; Salcido, C. D.; Martin, S. E.; Chewning, K. J.; Wu, C.-P.; Varticovski, L.; Bates, S. E.; Caplen, N. J.; Ambudkar, S. V. Single-Step Doxorubi-cin-Selected Cancer Cells Overexpress the ABCG2 Drug Transporter through Epigenetic Changes. Br J Cancer 2008, 98 (9), 1515–1524. https://doi.org/10.1038/sj.bjc.6604334.
54 Zaidi, M.; Fu, F.; Cojocari, D.; McKee, T. D.; Wouters, B. G. Quantitative Visualization of Hypoxia and Proliferation Gradients Within Histological Tissue Sections. Front Bioeng Bio-technol 2019, 7. https://doi.org/10.3389/fbioe.2019.00397.
55 Walsh, J. C.; Lebedev, A.; Aten, E.; Madsen, K.; Marciano, L.; Kolb, H. C. The Clinical Im-portance of Assessing Tumor Hypoxia: Rela-tionship of Tumor Hypoxia to Prognosis and Therapeutic Opportunities. Antioxid Redox Signal 2014, 21 (10), 1516–1554. https://doi.org/10.1089/ars.2013.5378.
56 Tassone, P.; Tagliaferri, P.; Perricelli, A.; Blot-ta, S.; Quaresima, B.; Martelli, M. L.; Goel, A.; Barbieri, V.; Costanzo, F.; Boland, C. R.; Venu-ta, S. BRCA1 Expression Modulates Chemo-sensitivity of BRCA1-Defective HCC1937 Hu-man Breast Cancer Cells. Br J Cancer 2003, 88 (8), 1285–1291. https://doi.org/10.1038/sj.bjc.6600859.
57 Toyoda, Y.; Takada, T.; Suzuki, H. Inhibitors of Human ABCG2: From Technical Background to Recent Updates With Clinical Implications. Front. Pharmacol. 2019, 10. https://doi.org/10.3389/fphar.2019.00208.

58 Sarkadi, B.; Homolya, L.; Szakács, G.; Váradi, A. Human Multidrug Resistance ABCB and ABCG Transporters: Participation in a Chemo-immunity Defense System. Physiological Re-views 2006, 86 (4), 1179–1236. https://doi.org/10.1152/physrev.00037.2005.

CHAPTER 5: CONCLUSION

In light of a growing interest, the potential array of applications for exosomes is still being determined. Current applications in basic science, biomarker diagnostics, and drug delivery show potential and offer an alternative and promising way forward in nanoparticle-based research.[1–5] The goal of this research was to open a door into new application areas for further development and to test the limits of exosome modifications.

One of the heavily debated areas in the field is the best source of exosomes; however, this question cannot be answered without the downstream application in mind. For example, biomarker diagnostics must use patient derived exosomes but whether the ideal source is blood, urine or other bodily fluids is still under investigation.[3,6,7] Alternatively, drug delivery exosomes may have various sources, including cell culture derived and bovine derived, each with their own pros and cons.[1,8–10] The development and use of bovine milk derived exosomes is in its infancy with much still needing to be elucidated, particularly about their biodistribution and pharmacokinetic properties.[1] Nevertheless, this source of exosomes is one of the most promising with a high collection rate and easy access. This research explores the use and pushes the boundaries of bovine milk derived exosomes for use as an ultrasound contrast agent and a customizable drug delivery system.

While most ultrasound contrast agents are larger, in the micron range, the echogenic, bovine-derived exosomes first reported in this work are unique due to their size and biological origin.[11,12] The development of the techniques to make these biological nanoparticles echogenic opens the door for *in vivo* targeted diagnostics. In addition to this first in the field development, it was also shown that echogenic exosomes can be made with raw or pasteurized bovine milk, greatly enhancing the availability of this source. As an additional benefit of this work, the

characterization and equivalency of exosomes isolated from both raw and pasteurized milk demonstrated the heartiness of exosomes and their ability to protect their cargo under harsh conditions such as pasteurization, a significant advantage for future clinical translation, particularly in the context of oral drug delivery.

In the second application of exosome modifications a customizable, targeted system was explored as a nanoparticle cancer drug delivery vehicle. Cancer drug delivery using nanoparticles is heavily studied area but the technology continues to fall short of its promise, often due to late-stage failures of rapid clearance and low dosage.[13–16] The innate nature of exosomes decreases this rapid clearance.[17] With the addition of the iRGD targeting and penetrating peptide, the efficacy of the exosome drug delivery increases. This has been shown through positive *in vitro* results where the modified exosomes described in this dissertation provided increased cell death compared to controls. *In vivo* biodistribution and efficacy studies will ultimately show the potency of this as a cancer nanoparticle drug delivery method. One of the big benefits to the current study is not only the *in vitro* results, but also a comprehensive outline of the methods necessary for characterization. Extending our thinking about these methods and outcomes allows an insight into the ease of which other lipids, peptides or small molecules could be incorporation to bovine milk exosomes. While cancer drug delivery is important, the main goal of these modified exosomes was to show the effectiveness of the model system.

Despite the promise that the modified exosomes described in this work have, the potential limitations of this work cannot be ignored. Some of these limitations were simply derived from logistical limitations that require increasing the number of replicates to improve the statistical power and confirm some of the preliminary results presented here, such as the *in vivo* response to

echogenic exosomes. Monitoring the impact of echogenic exosomes on other internal organs is a necessary translational step. Monitoring the presence of echogenic exosomes in the liver and lungs would have been particularly beneficial. Alternatively, additional experimentation, which in this case was limited by equipment and exosome specific protocols, is necessary to reveal precise mechanisms of action. Examples of these limitations is outlined below. Based on the results seen in the TNBC depth of penetration and cytotoxicity studies, further examination into spheroid cytotoxicity data is needed to confirm the microenvironment of the spheroids is present and at the levels to cause breakage of the exosomes. Additionally, higher magnification of cellular internalization data, in normoxic and hypoxic conditions, would provide pivotal information regarding the mechanism of exosomal uptake for these cell lines and potential limitations for exosomal based chemotherapeutic delivery. In addition to these specific limitations, it is also important to note that this work was also impacted by the fundamental requirement for more rigorous controls across the entire field of exosomes; however, the work described in this dissertation pushes the field forward and incorporated additional exosome characterization not seen in much of the current literature. While there are some significant technical barriers to the use of exosomes as proposed in this work, alternative strategies have been described and developed to allow the continued development of exosomes due to their versatility, accessibility and translatability. The ability to incorporate a wide range of lipids within the bilayer of the exosome opens to door to many possibilities for future studies. In spite of these limitations, the results presented in this dissertation provide an important stepping stone to future work not only within modified bovine milk exosomes but also for the more global clinical translation of exosomes.

For both applications considered here, echogenic and cancer drug delivery, *in vivo* studies, more specifically biodistribution studies need to be performed in order to have a more accurate idea of not only how successful bovine milk exosomes may be, but also for an accurate assessment of the potential of clinical translation. The *in vivo* experimental design will be different due to the biological nature of exosomes compared to other nanoparticle systems. While differences in synthetic and biological based nanoparticles are the biggest draw for the use of exosomes, it simultaneously creates challenges in experimental design as typical methods cannot always be utilized, as was clearly demonstrated in the development of the iRGD adhesion assay. The first hurdle that will need to be overcome for an accurate evaluation of exosome biodistribution is *in vivo* visualization. The challenge will be in identifying a label that does not disrupt the primary function and benefit of the exosome. Several techniques have been explored but the field has not reached a consensus.[18] The ability to incorporate a FITC-lipid shows promise in biodistribution for iDHRX, such as described in this work. Ironically, a good option for monitoring the distribution of the echogenic exosomes remains unclear as it would require monitoring multiple locations simultaneously via ultrasound. These complications will make i*n vivo* studies difficult but remain a necessary step for the advancement of exosomes as either an ultrasound contrast agent or a chemotherapeutic drug delivery vehicle. Nevertheless, overall, chemically modified bovine milk exosomes have great potential in the world of pharmaceutical development.

References

1 Munagala R, Aqil F, Jeyabalan J, Gupta RC. Bovine milk-derived exosomes for drug delivery. Cancer Lett 2016;371:48–61. https://doi.org/10.1016/j.canlet.2015.10.020.

2 Pullan JE, Confeld MI, Osborn JK, Kim J, Sarkar K, Mallik S. Exosomes as Drug Carriers for Cancer Therapy. Mol Pharmaceutics 2019;16:1789–98. https://doi.org/10.1021/acs.molpharmaceut.9b00104.

3 Duijvesz D, Burnum-Johnson KE, Gritsenko MA, Hoogland AM, Berg MSV den, Willemsen R, et al. Proteomic Profiling of Exosomes Leads to the Identification of Novel Biomarkers for Prostate Cancer. PLOS ONE 2013;8:e82589. https://doi.org/10.1371/journal.pone.0082589.
4 Makler A, Asghar W. Exosomal biomarkers for cancer diagnosis and patient monitoring. Expert Review of Molecular Diagnostics 2020;0:1–14. https://doi.org/10.1080/14737159.2020.1731308.
5 Vlassov AV, Magdaleno S, Setterquist R, Conrad R. Exosomes: Current knowledge of their composition, biological functions, and diagnostic and therapeutic potentials. Biochimica et Biophysica Acta (BBA) - General Subjects 2012;1820:940–8. https://doi.org/10.1016/j.bbagen.2012.03.017.
6 Fernando MR, Jiang C, Krzyzanowski GD, Ryan WL. New evidence that a large proportion of human blood plasma cell-free DNA is localized in exosomes. PLoS One 2017;12:. https://doi.org/10.1371/journal.pone.0183915.
7 Nilsson J, Skog J, Nordstrand A, Baranov V, Mincheva-Nilsson L, Breakefield XO, et al. Prostate cancer-derived urine exosomes: a novel approach to biomarkers for prostate cancer. Br J Cancer 2009;100:1603–7. https://doi.org/10.1038/sj.bjc.6605058.
8 Antimisiaris SG, Mourtas S, Marazioti A. Exosomes and Exosome-Inspired Vesicles for Targeted Drug Delivery. Pharmaceutics 2018;10:. https://doi.org/10.3390/pharmaceutics10040218.
9 Batrakova EV, Kim MS. Using exosomes, naturally-equipped nanocarriers, for drug delivery. J Control Release 2015;219:396–405. https://doi.org/10.1016/j.jconrel.2015.07.030.
10 Bunggulawa EJ, Wang W, Yin T, Wang N, Durkan C, Wang Y, et al. Recent advancements in the use of exosomes as drug delivery systems. Journal of Nanobiotechnology 2018;16:81. https://doi.org/10.1186/s12951-018-0403-9.
11 Osborn J, E. Pullan J, Froberg J, Shreffler J, N. Gange K, Molden T, et al. Echogenic exosomes as ultrasound contrast agents. Nanoscale Advances 2020. https://doi.org/10.1039/D0NA00339E.
12 Chong WK, Papadopoulou V, Dayton PA. Imaging with ultrasound contrast agents: current status and future. Abdom Radiol 2018;43:762–72. https://doi.org/10.1007/s00261-018-1516-1.
13 Ishida T, Harashima H, Kiwada H. Liposome Clearance. Bioscience Reports 2002;22:197–224. https://doi.org/10.1023/A:1020134521778.
14 Kai MP, Brighton HE, Fromen CA, Shen TW, Luft JC, Luft YE, et al. Tumor Presence Induces Global Immune Changes and Enhances Nanoparticle Clearance. ACS Nano 2016;10:861–70. https://doi.org/10.1021/acsnano.5b05999.
15 Waegeneers N, Brasseur A, Van Doren E, Van der Heyden S, Serreyn P-J, Pussemier L, et al. Short-term biodistribution and clearance of intravenously administered silica nanoparticles. Toxicol Rep 2018;5:632–8. https://doi.org/10.1016/j.toxrep.2018.05.004.
16 Pullan JE, Shreffler JW, Dailey KM, Mallik S, Brooks AE. Overcoming Hurdles in Nanoparticle Clinical Translation: The Influence of Experimental Design and Surface Modification. International Journal of Molecular Sciences 2019;20:6056. https://doi.org/10.3390/ijms20236056.
17 Yamashita T, Takahashi Y, Nishikawa M, Takakura Y. Effect of exosome isolation methods on physicochemical properties of exosomes and clearance of exosomes from the

blood circulation. European Journal of Pharmaceutics and Biopharmaceutics 2016;98:1–8. https://doi.org/10.1016/j.ejpb.2015.10.017.

18 Yi YW, Lee JH, Kim S-Y, Pack C-G, Ha DH, Park SR, et al. Advances in Analysis of Biodistribution of Exosomes by Molecular Imaging. Int J Mol Sci 2020;21:. https://doi.org/10.3390/ijms21020665.

APPENDIX

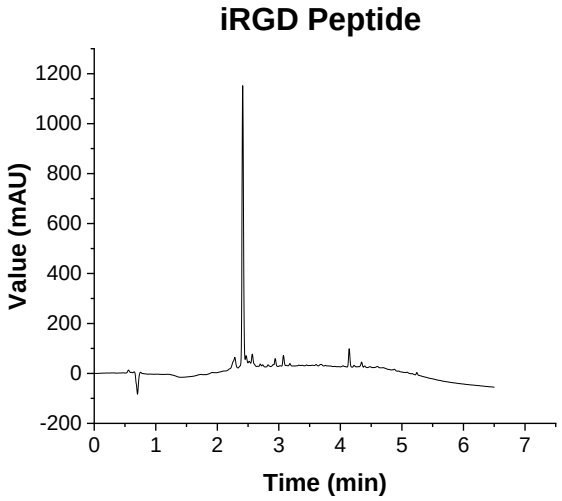

Figure A1. C18 Reverse-phase HPLC for iRGD peptide.

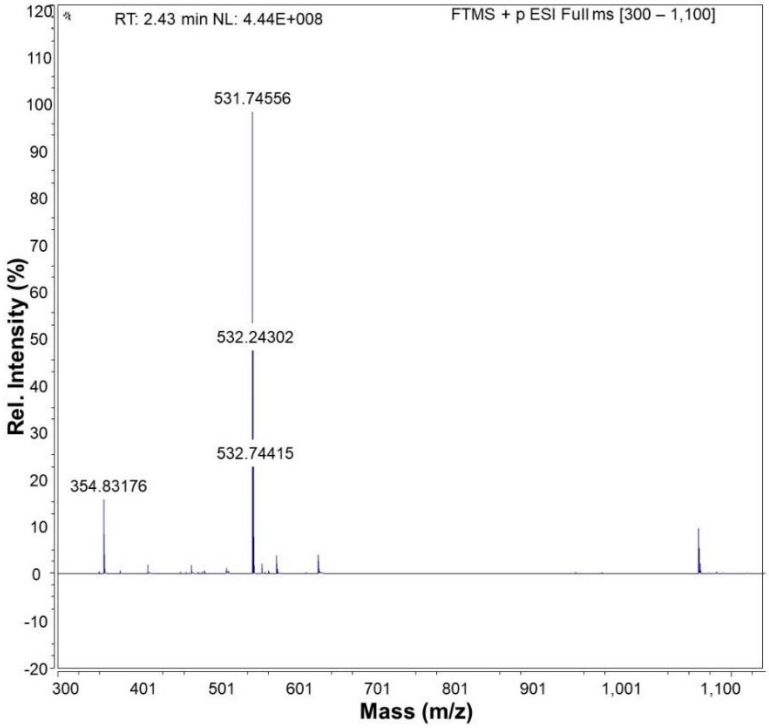

Figure A2. ESI Mass Spectroscopy of iRGD peptide.

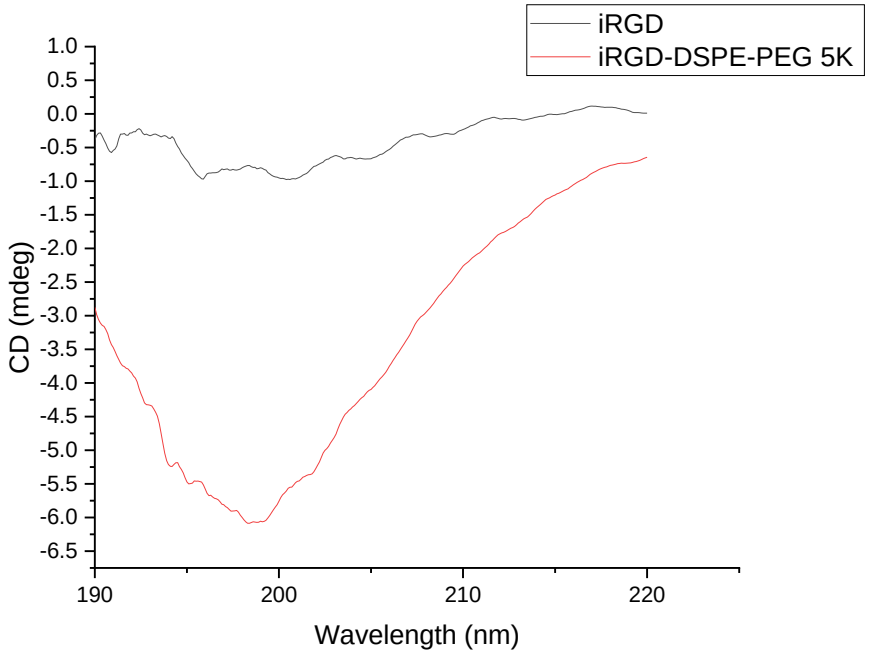

Figure A3. Circular dichroism (CD) spectrum of the synthesized cyclic iRGD peptide and its cognate with DSPE-PEG5000 lipid.

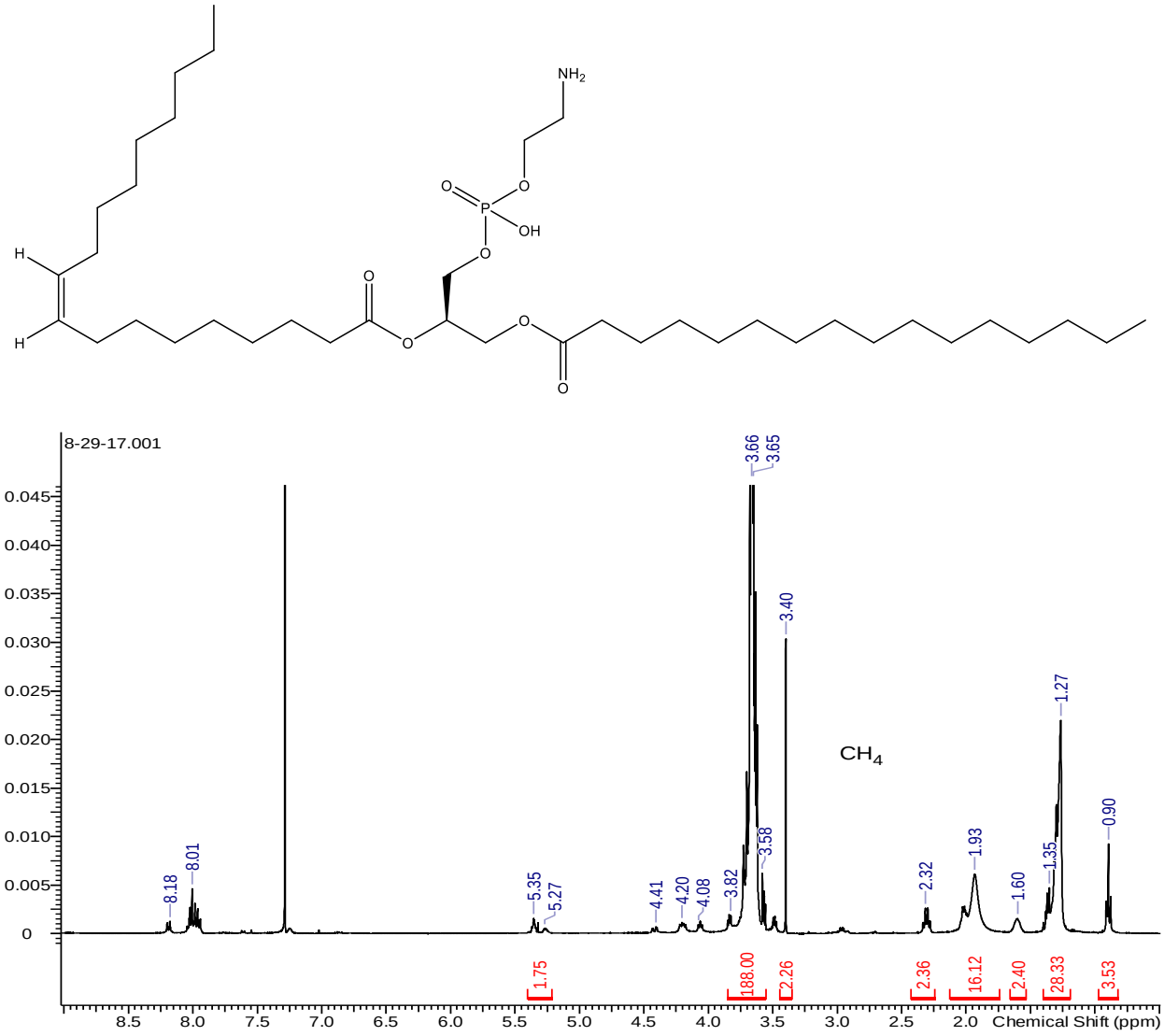

Figure A4. 1H NMR (400 MHz, chloroform-d) spectrum of hypoxia-responsive lipid PEG-Azobenzene-POPE

δ ppm: 7.55-8.23(CH=CH- CH, m, 8 H), 5.35-5.27(CH2-CH=CH-CH2, m, 2 H), 4-4.5 (-CH-CH2-O, m, 4 H), 3.66 ((CH2-CH2-O), t, 4 H), 3.40 ((CH3-O), s, 3 H), 2.32 ((CH2-C=O), m, 4 H), 2.16 (CH2-CH=CH- CH2, m, 4 H), 1.26 ((- CH2-CH2), m, 44 H), 0.9 ((CH3- CH2), t, 6 H)

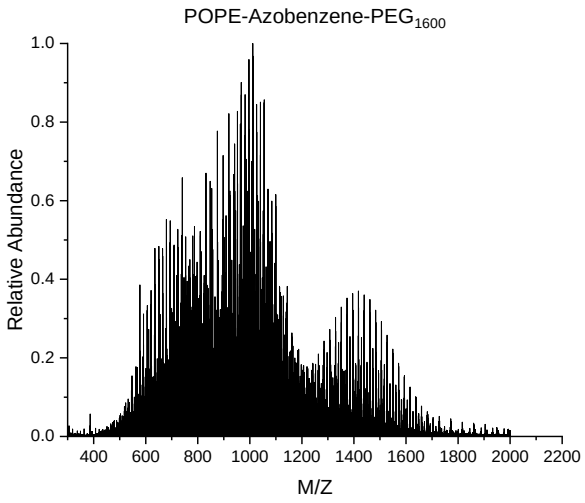

Figure A5. TOF ESI spectrum of hypoxia responsive lipid.

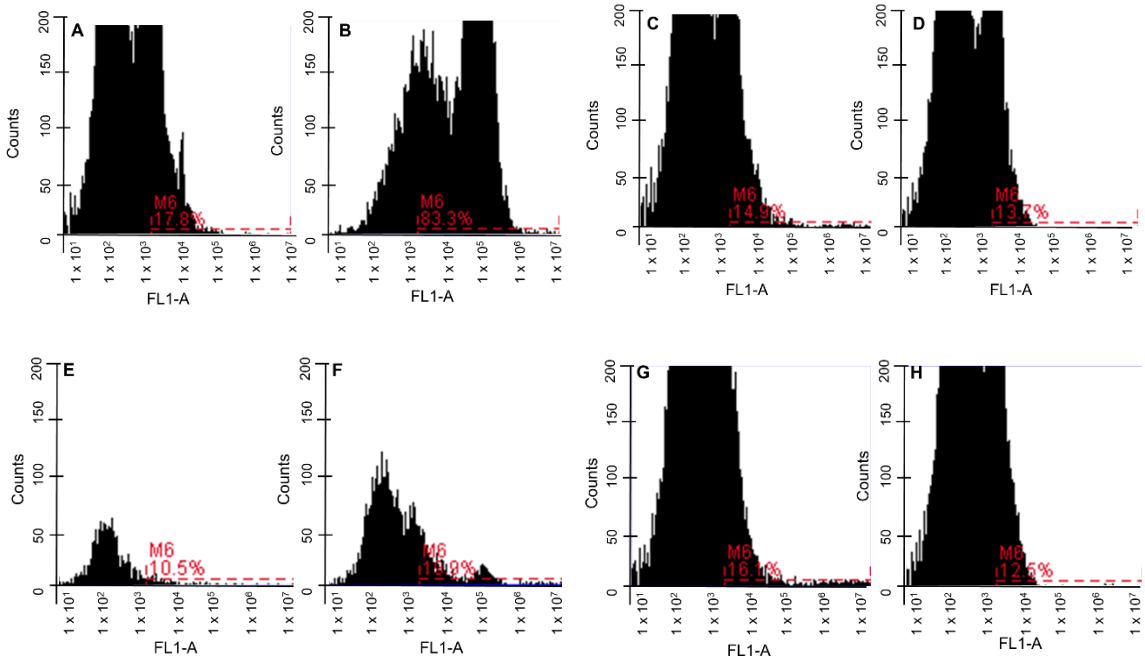

Figure A6. Flow cytometry of NRP-1. **A**. MDA-MB-231 Normoxia **B.** MDA-MB-231 Hypoxia **C**. MDA-MB-468 Normoxia **D**. MDA-MB-468 Hypoxia **E**. HCC 1806 Normoxia **F**. HCC 1806 Hypoxia **G**. HCC 1937 Normoxia **H.** HCC 1937 Hypoxia